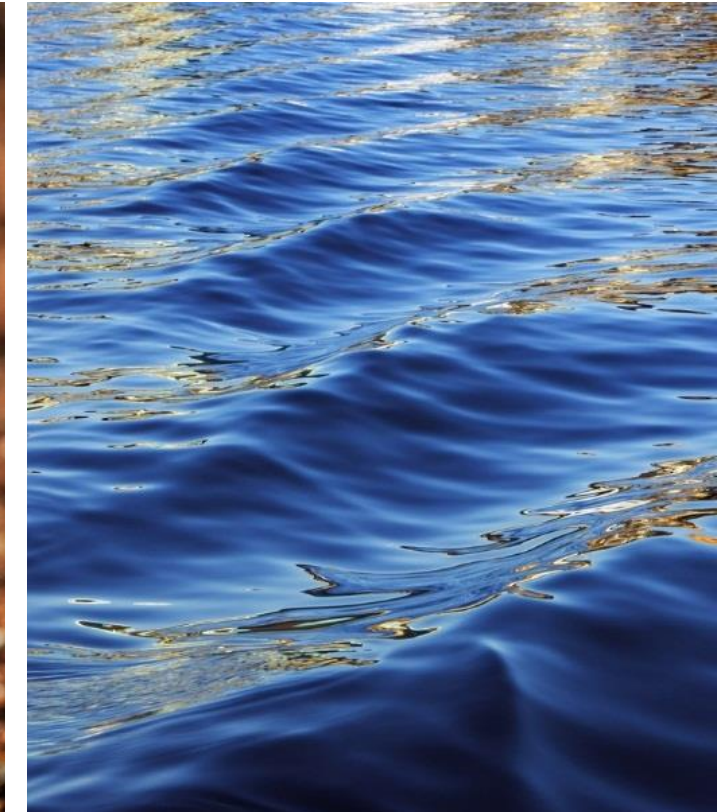




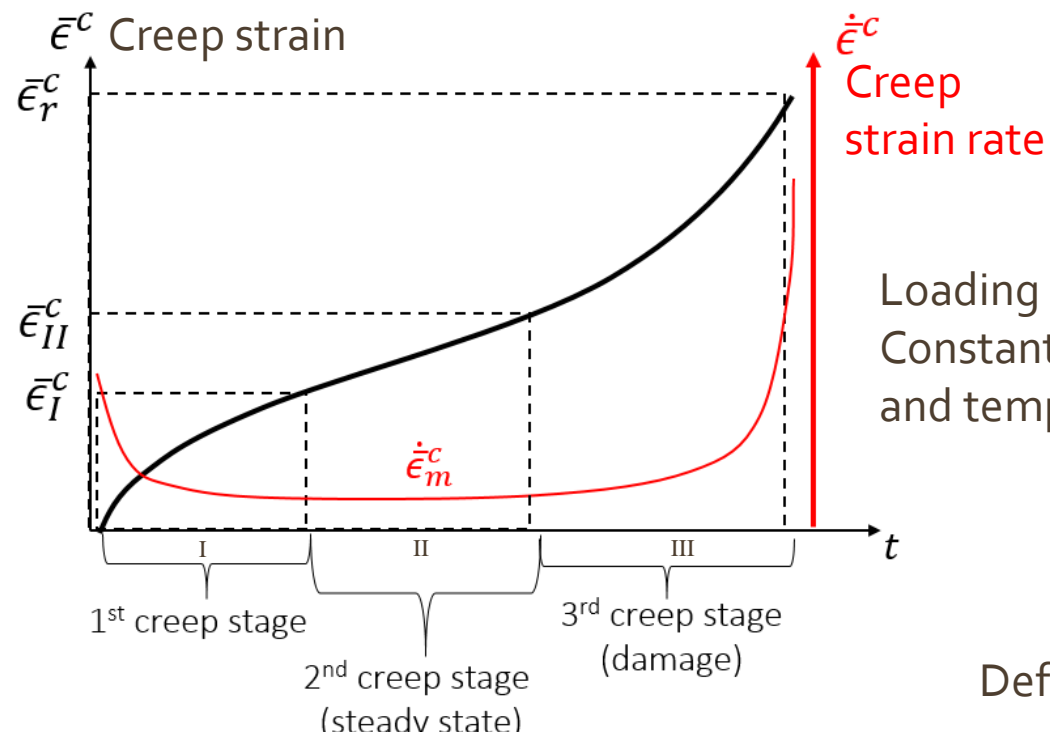
A creep survey: from creep mechanisms to macroscopic and microscopic models

AM Habraken,
G. Bryndza, F. Chen, L. Duchêne, A. Mertens,
C. Rojas, J. Tchuindjang



Toward sustainability
A good design reduces energy consumption, saves raw material

What is creep?



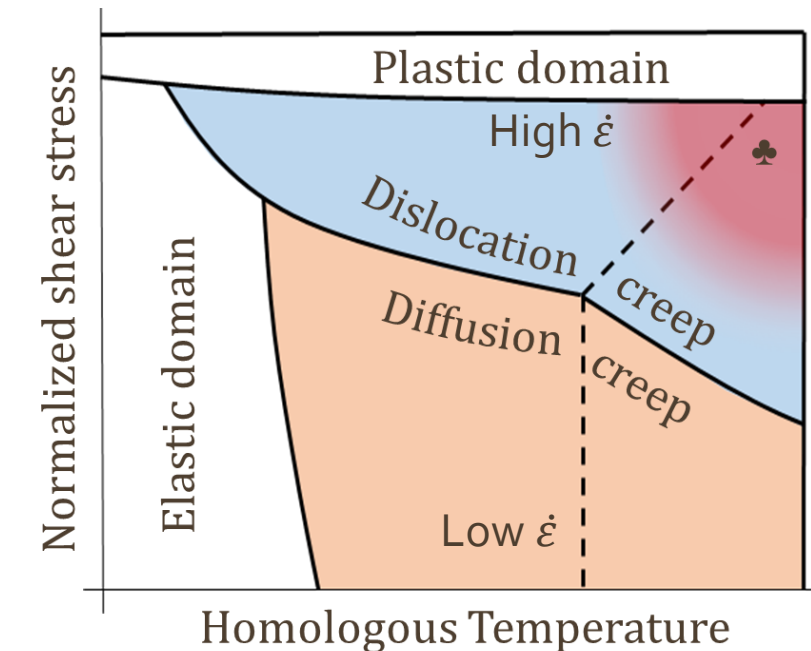
Typical creep curves

Schematic Deformation Mechanism Map
4 Regions

Loading =
Constant stress
and temperature

Deformation Mechanism Map

Deformation-Mechanism Maps, The Plasticity and Creep of Metals and Ceramics, by Harold J Frost, Dartmouth College, USA, and Michael F Ashby, Cambridge University, UK
<https://defmech.engineering.dartmouth.edu/>



♣: Dynamic recrystallization (DRX)

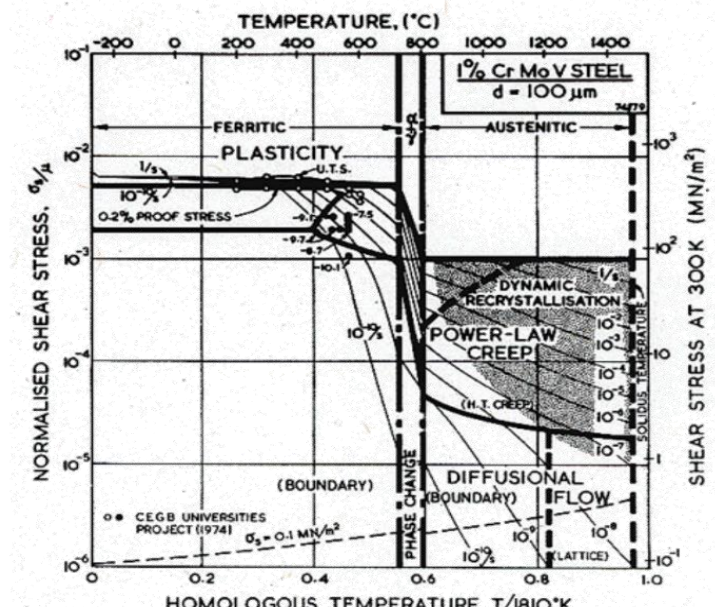


Fig. 8.7. A 1% Cr-Mo-V steel, of grain size 100 μm, showing data.

Why is creep studied ?

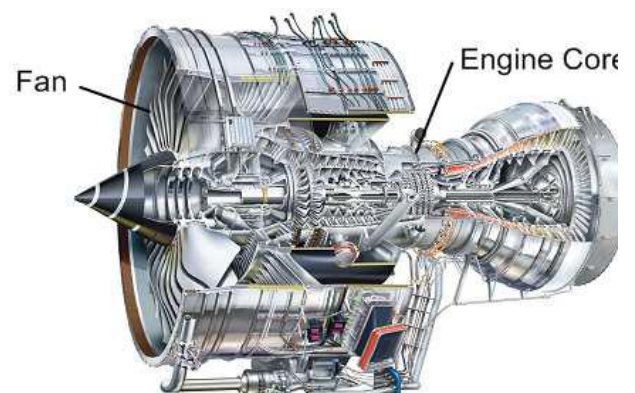
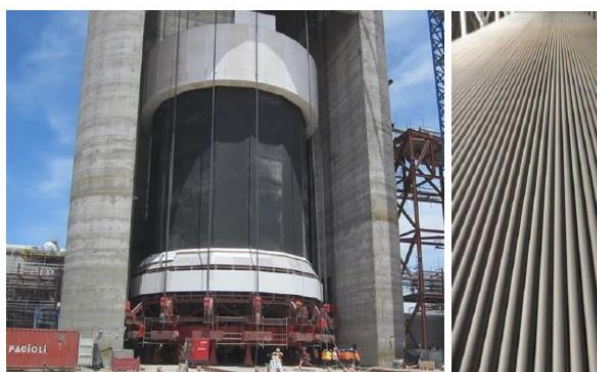


PETROCHEMICAL industry

- Many sectors have creep issues



- Modeling creep
 - Correct design of parts
 - Optimal industrial maintenance and investment plan
 - Reduce product development time (validation tests)
- Understanding creep mechanism → Optimal design of alloy composition, heat treatments



Contents

- Introduction
- **Phenomenological approaches**
 - Scalars
 - Larson Miller etc...
 - Curves and constitutive laws FE
 - Norton
 - Graham Wales
- **Micro physical based approaches**
 - The basis
 - Incoloy 718 application
- **Fatigue-Creep, Dwell effect and FE Morch constitutive macro law**
- **Nitriding effect**
- **AID4Greenest EU project ...**

Contents

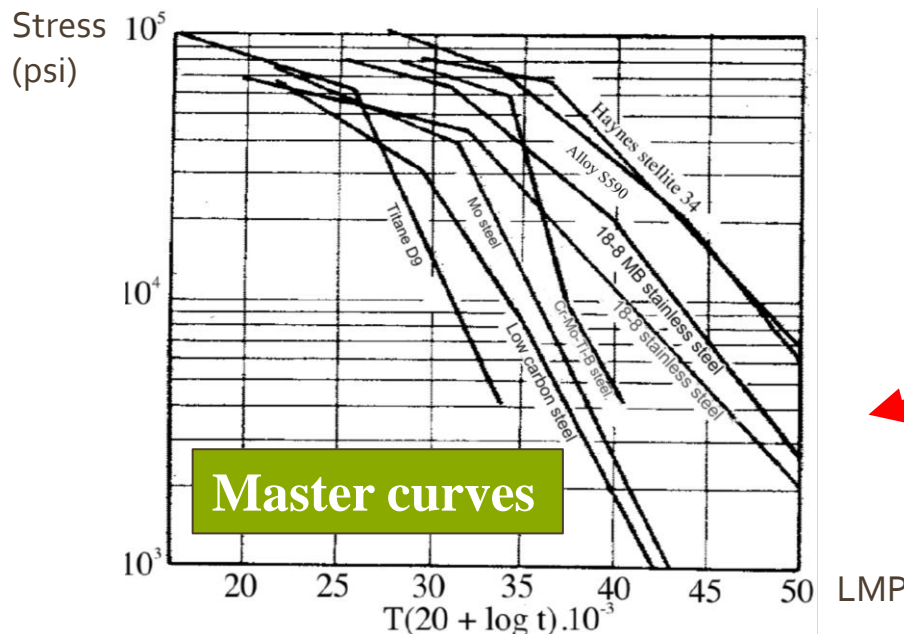
- Introduction
- **Phenomenological approaches**
 - Scalars
 - Larson Miller etc...
 - Curves and constitutive laws FE
 - Norton
 - Graham Wales
- **Micro physical based approach**
 - The basis
 - Incoloy 718 application
- **Fatigue-Creep, Dwell effect and FE Morch constitutive macro law**
- **Nitriding effect**
- **AID4Greenest EU project ...**

About master curves, Larsen-Miller Parameter LMP

Stationary creep (power law):

$$\dot{\varepsilon} = B\sigma^n e^{-\frac{\Delta H}{kT}}$$

B and n are material constants
 ΔH is activation energy
 n is normally between 3 and 8



Master curves

FR Larson, J. Miller, Transactions of the ASME (1954)

GE Dieter, "Mechanical Metallurgy," McGraw-Hill Book Company (1988)

Larson and Miller formulation:

$$\dot{\varepsilon} = Ae^{-\frac{\Delta H}{kT}}$$

A is a constant
 ΔH is activation energy

$$\ln\left(\frac{\dot{\varepsilon}}{t}\right) = \ln(Ae^{-\frac{\Delta H}{kT}})$$

$$\ln(t) = \ln\left(\frac{\dot{\varepsilon}}{A}\right) + \frac{\Delta H}{kT}$$

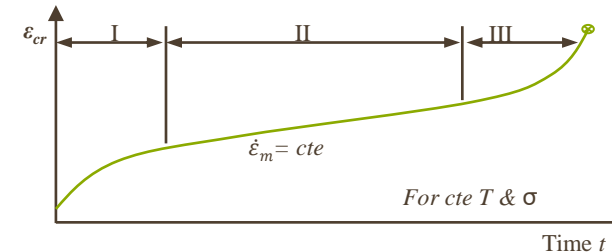
Rupture stress is plotted as
 a function of a parameter ($x=t_R$ or $\dot{\varepsilon}_m$)
 $T(\ln(x) + C_1)$
 As $\dot{\varepsilon}_m \cdot t_r = cte$
 Monkman-Grant*

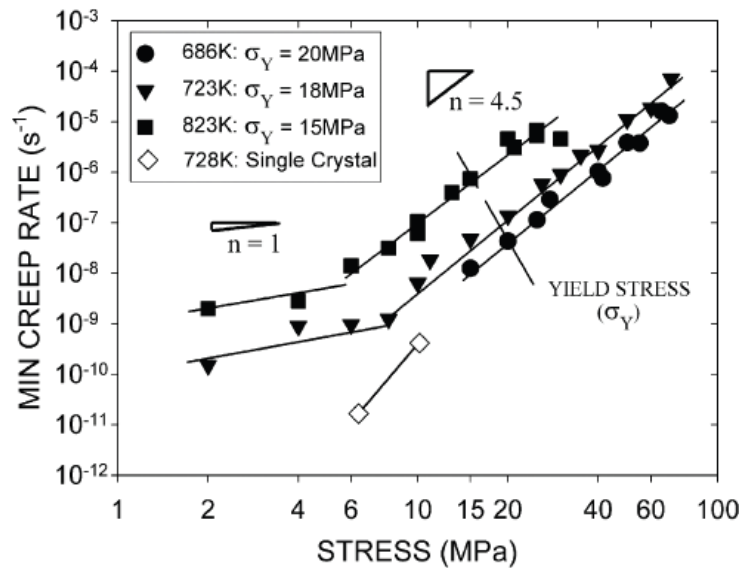
$$Const = T(\ln(t) + C_1)$$

For most of the alloys $35 < C_1 < 60$

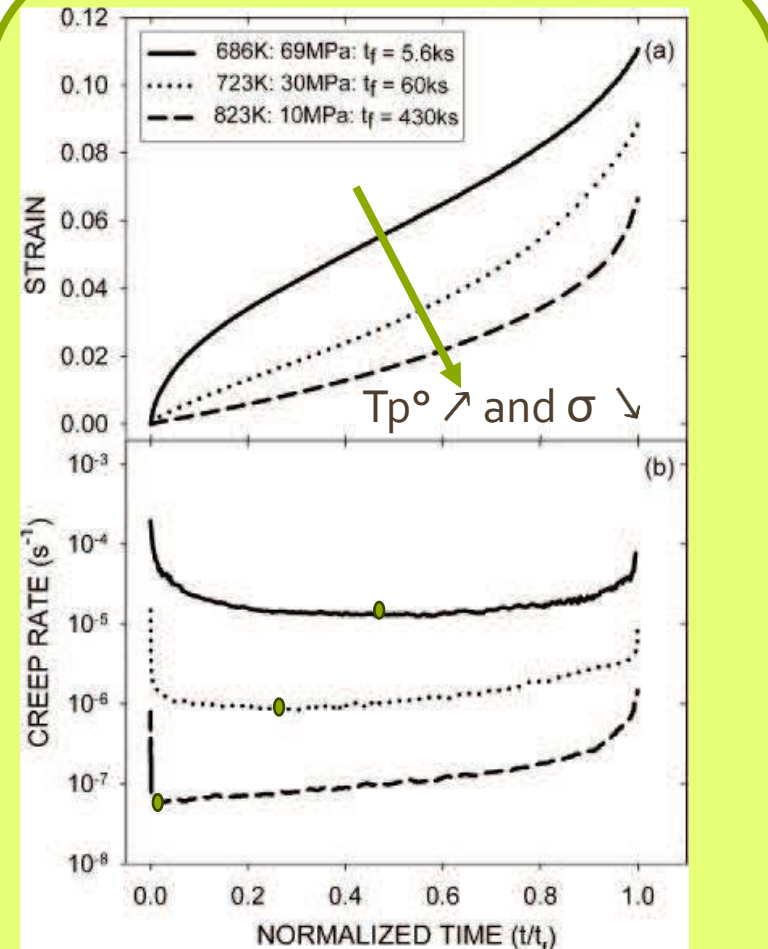
Link σ to T and t_R or $\dot{\varepsilon}_m$

OK for microstructure = cte !





$\neq n$ with "no" physical meaning



Experimental creep observations
If $T_p^\circ \uparrow$ and $\sigma \downarrow$
Creep state II $\dot{\epsilon}_m^c \downarrow$ earlier

From power-law analysis
there is no indication that creep
behavior changes in the higher
stress regime.

LMP does not point the
correct position of
mechanism change
 \rightarrow diffusion \rightarrow dislocation

No effect of yield stress

No info on creep curves

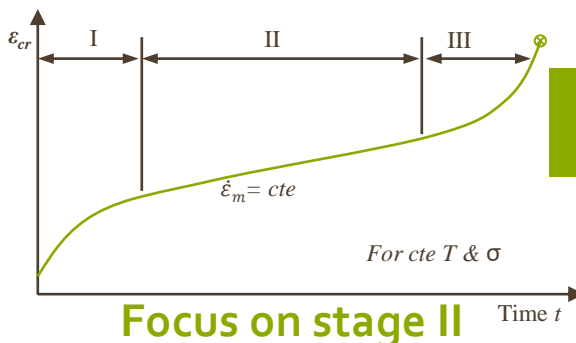
$(\sigma = \text{cte} \ T = \text{cte})$

$\varepsilon = f(\sigma, T, t)$



Wilshire introduced the use of σ/σ_Y
And focuses on stage I and III

Issues of LMP approach and exponential function (Norton)



$Q_c n$: single constants for different creep regions,
physical meaning is lost

+ A constant \rightarrow no effect of yield stress on creep behavior

In experiments : each mechanisms has its kinetic



Wilshire equations (focus on stage I and III)

Based on relative stress $= \sigma / \sigma_{UTS}$

$\rightarrow Q_c^*$ related to different physical mechanism depending on creep region

\neq equations \neq mechanisms $\rightarrow t_r$ or $\dot{\epsilon}_m^c$

$\dot{\epsilon}_m \cdot t_r = \text{cte}$ Monkman-Grant

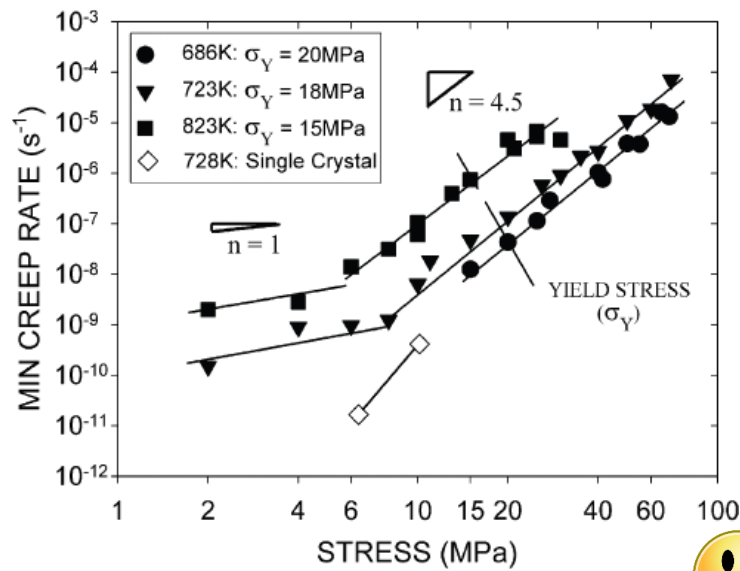
allows to pass from 1->2

$$\left\{ \begin{array}{l} \sigma / \sigma_{UTS} = \exp \left\{ -k_i [t_r \exp (-Q_c^*/RT)]^u \right\} \\ \sigma / \sigma_{UTS} = \exp \left\{ -k_v [\dot{\epsilon}_m \exp (-Q_c^*/RT)]^v \right\} \end{array} \right. \quad \begin{array}{l} (1) \\ (2) \end{array}$$

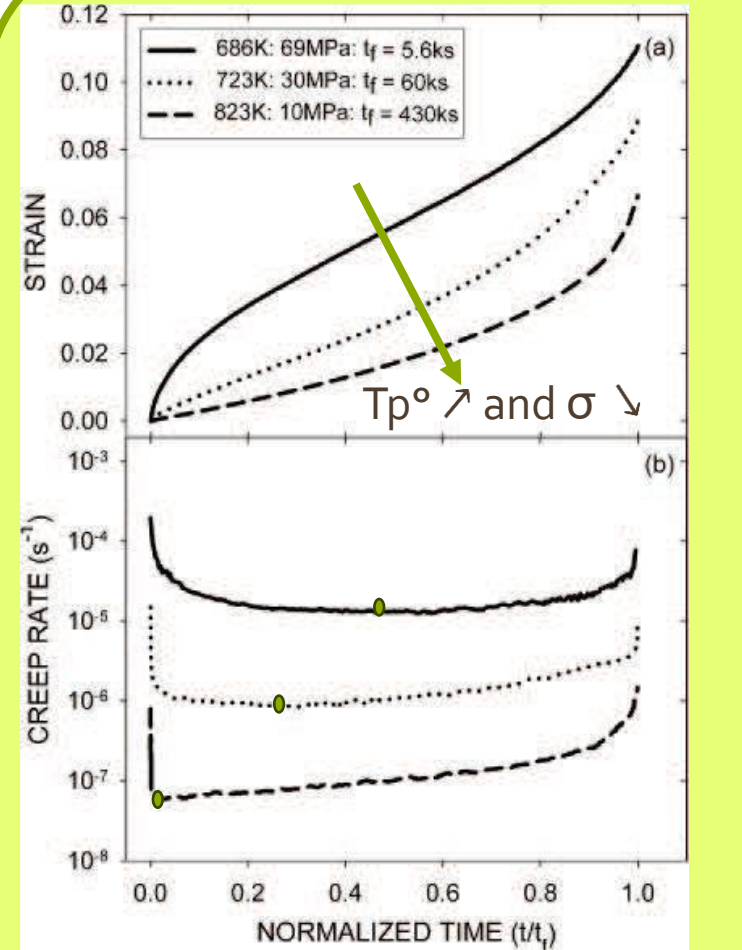
Whole curve
parameters k_w , w = functions of strain



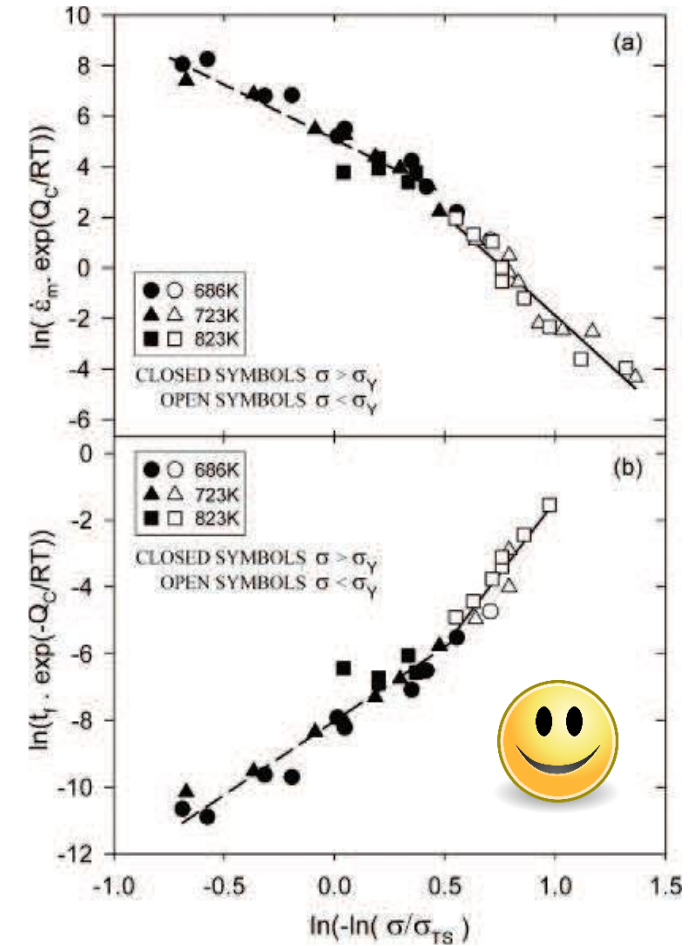
$$\sigma / \sigma_{UTS} = \exp \left\{ -k_w [t_\epsilon \cdot \exp (-Q_c^*/RT)]^w \right\}$$



Norton approach $\rightarrow \neq n$



Experimental creep observations
If $T_p^\circ \uparrow$ and $\sigma \downarrow$
Creep state II \downarrow
earlier



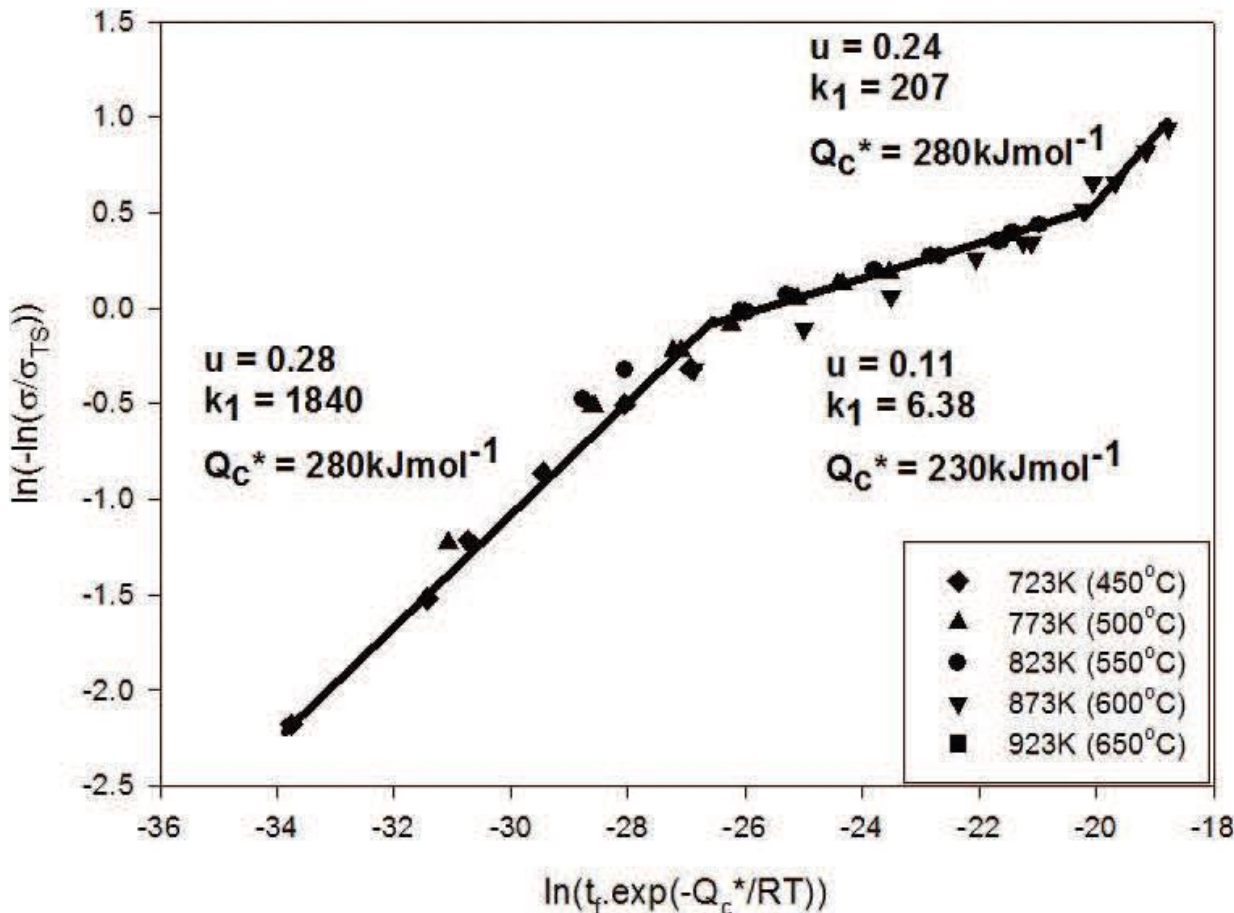
Wilshire equations

$Q_c^* = \text{cte} = \text{grain boundary diffusion}$
 $k_i, u, v \neq \text{for } \sigma < \sigma_y \text{ and } \sigma > \sigma_y$

$$\sigma/\sigma_{UTS} = \exp \left\{ -k_u [t_f \cdot \exp(-Q_c^*/RT)]^u \right\}$$

$$\sigma/\sigma_{UTS} = \exp \left\{ -k_v [\dot{\varepsilon}_m \exp(-Q_c^*/RT)]^v \right\}$$

Issues of Wilshire approach



Wilshire equations

Q_c^* , k_i , u , $v \neq$ multiple ctes

3 Different mechanisms

For 2.25 CR - 1Mo

- High T and long t : bainite degradation \rightarrow ferrite
- Low σ : mainly GB effect
- High σ : increase of dislocation density

$$\sigma/\sigma_{UTS} = \exp \left\{ -k_u [t_f \cdot \exp (-Q_c^*/RT)]^u \right\}$$

$$\sigma/\sigma_{UTS} = \exp \left\{ -k_v [\dot{\varepsilon}_m \exp (-Q_c^*/RT)]^v \right\}$$



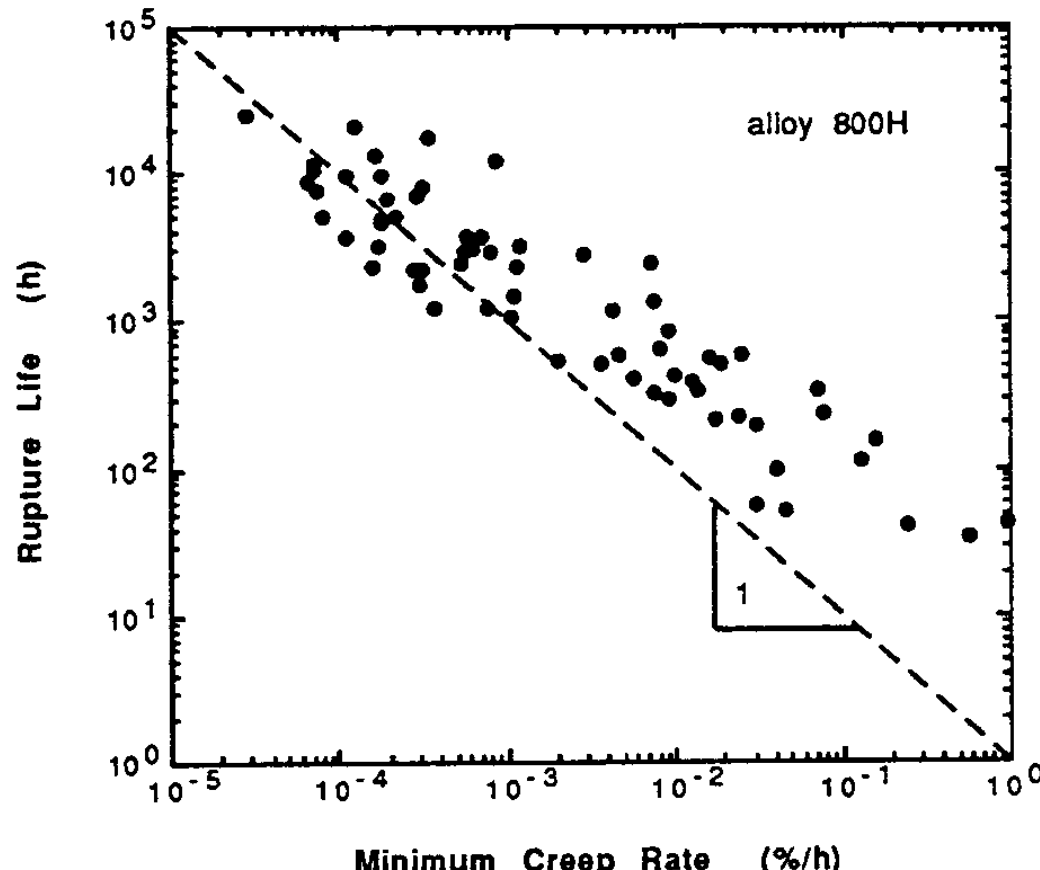
Needs many data

Just scalars t_f or $\dot{\varepsilon}_m$ identified

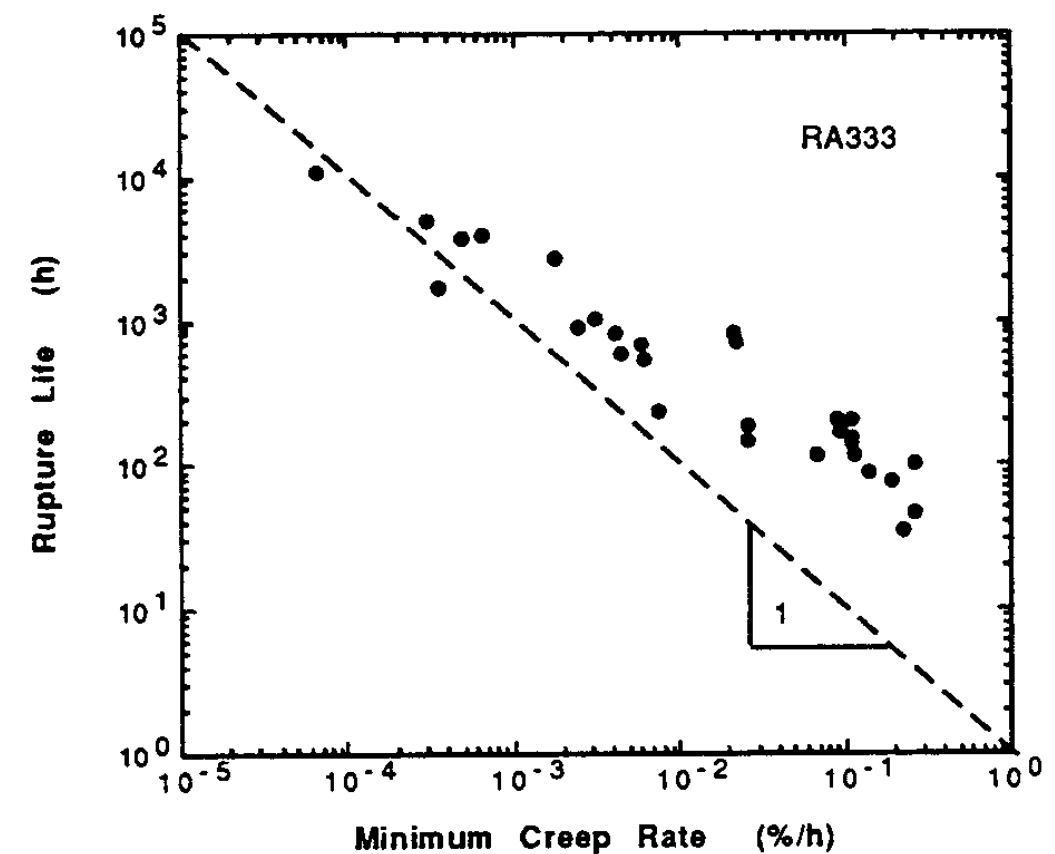
Strong effect of microstructure evolution

Need to chose correct functions
integrating all information
for FE simulations to model creep
under variable T , σ and long t

Issue in Monkman-Grant assumption of $\dot{\epsilon}_m \cdot t_r = cte$



Austenitic Incoloy alloy (Fe-Ni-Cr)



Ni-Cr alloy with solid solution strengthening

Issues in Design of piping and support components in high-temperature fluidized bed combustor systems

Machine learning to predict t_r

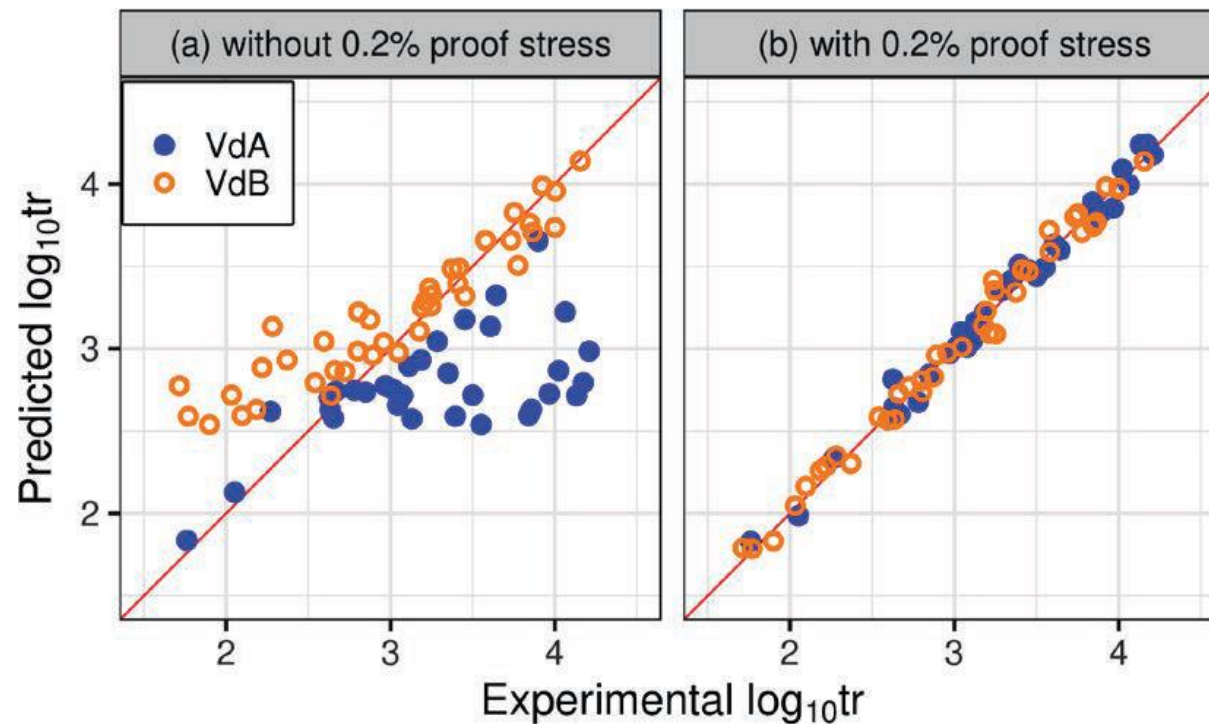
Data base used : 27 compositions (ferritic heat resistant steel) a total of 212 creep curves
from carbon steel to low-alloy and high-alloy steels (Fe+ Pe, Fe+Pe+Ba, Ma+Ba) , 0 to 9%Cr

Input: composition, test condition (T, σ) + yield stress σ_y (to express process manufacturing difference)

Output: $\log_{10} t_r$

Validation with or
without yield stress
included in the
training

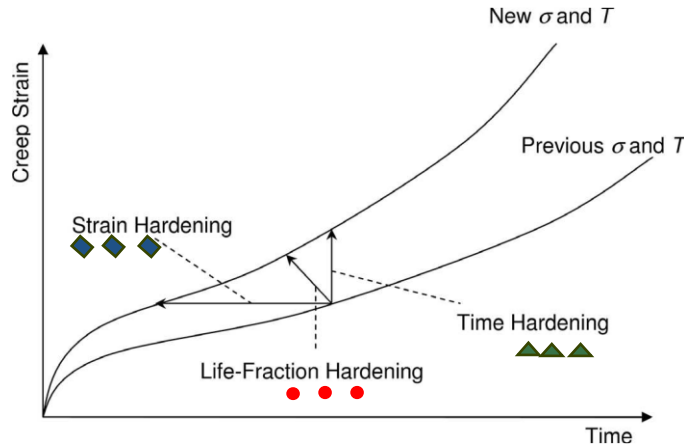
similar results in
Nakamura et al.
Materials Today Com 2023,
With σ_y replaced by Hv



Model developed
on a single family
Fe+ Pe,
Fe+Pe+Ba,
Ma+Ba had
no higher accuracy than
the global model on the
whole data set

Accuracy of
support vector regression (SVR) > random forest (RF) or gradient tree boosting (GTB) methods

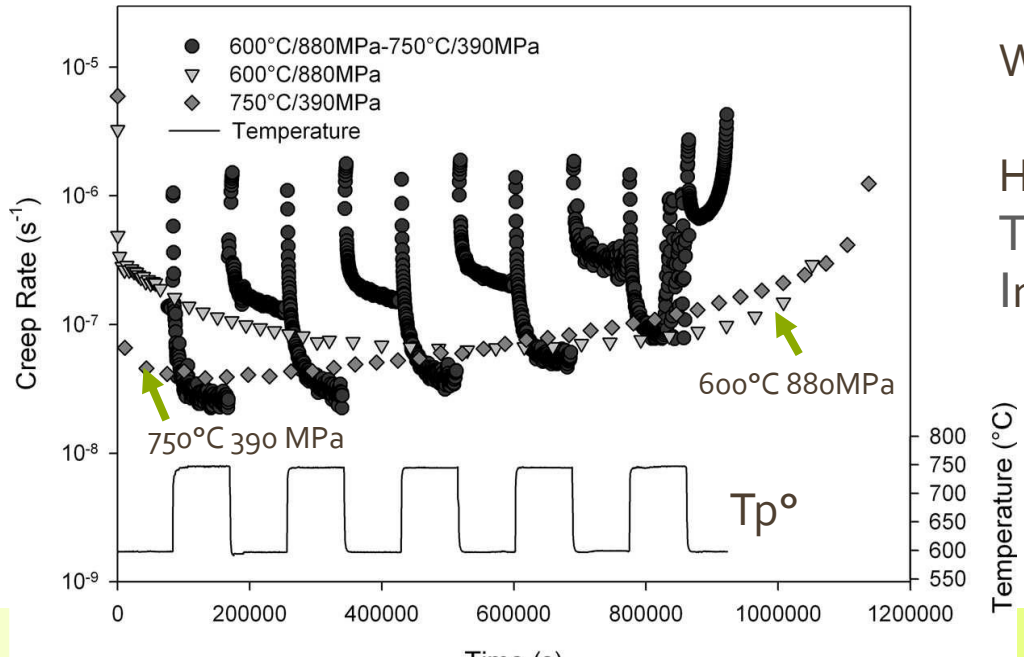
Extrapolationfrom these “scalars” toward FE



1. Define a **constitutive law** with internal variables
1. Use of them to jump between 1D reference curves $\varepsilon = f(\sigma, T, t)$
(1 curve for $\sigma = \text{cte}$ $T = \text{cte}$)

→ The use of state variables is better than horizontal or vertical shift

Experiments Creep under TP° and stress jump

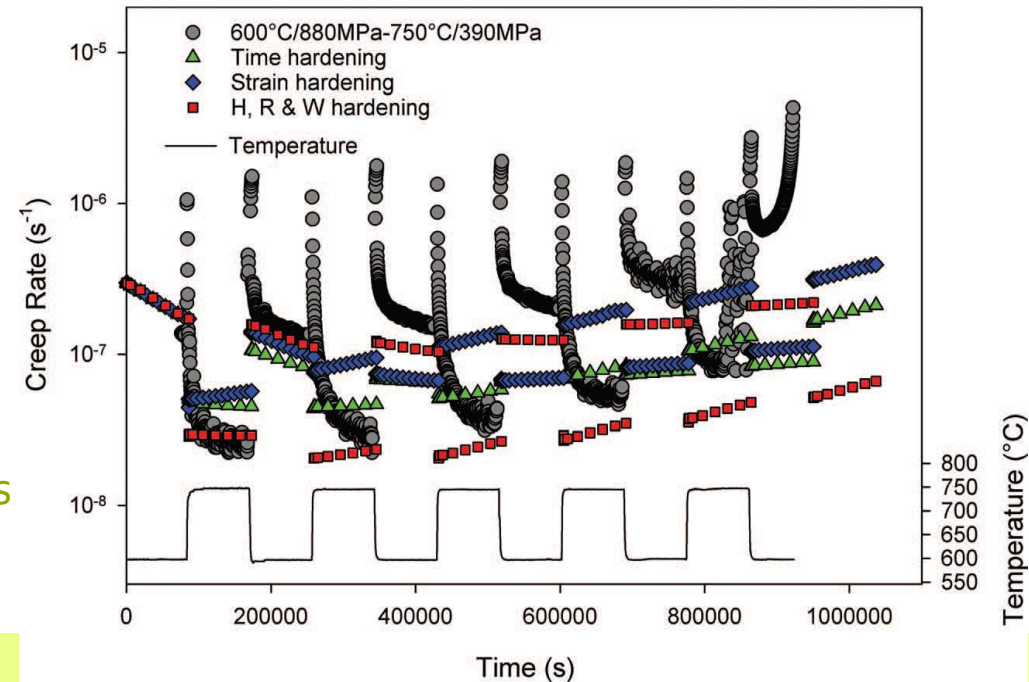


Waspaloy

Harrison et al. in
Tanski · 2018
IntechOpen

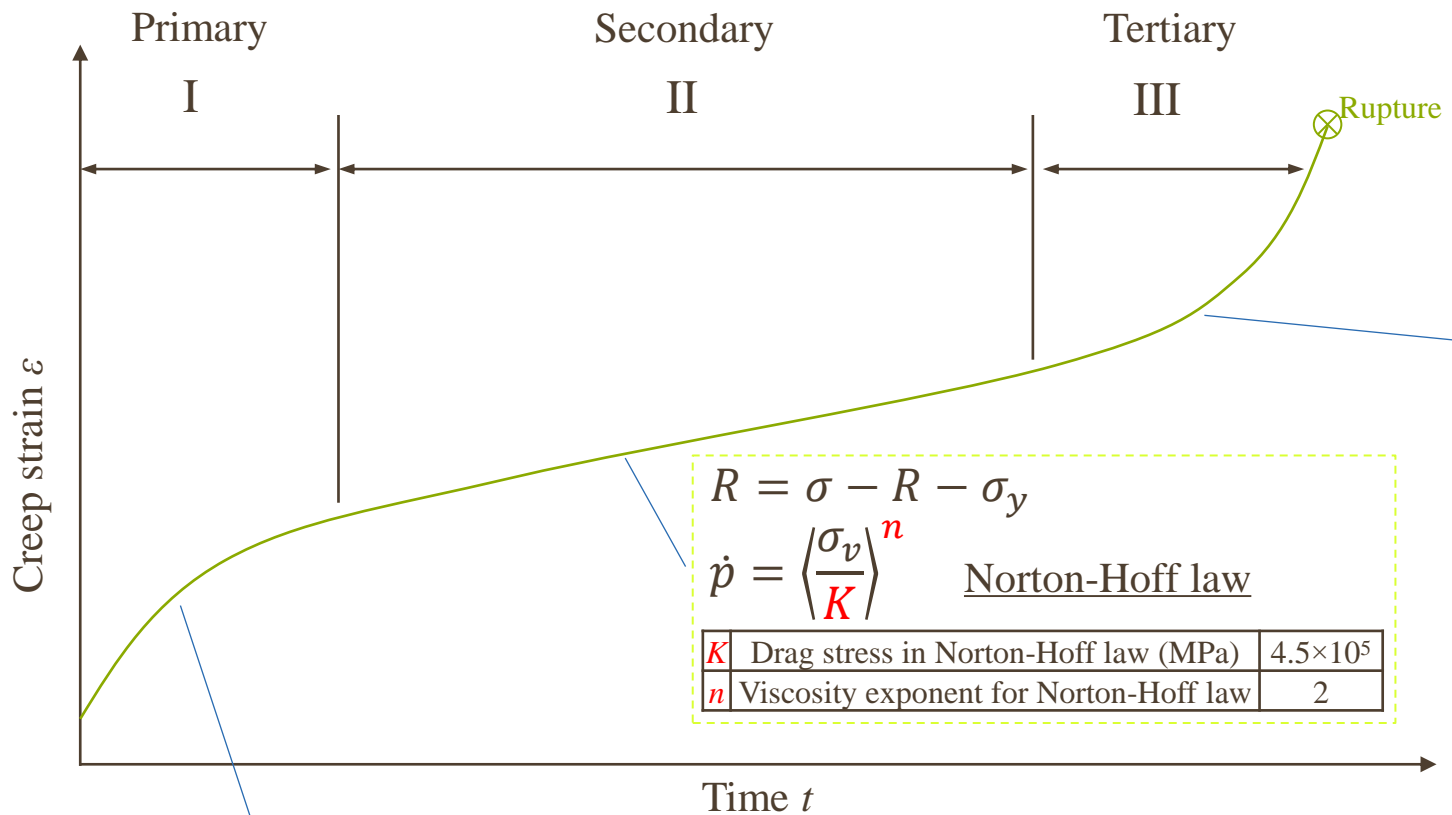
Model
predictions
still far ..

Model Prediction (Experiment in grey)



Elasto-visco-plastic creep damage model

Helene Morch [Uliege Ph.D. 2022 Walloon Region project], Norton type + damage



Isotropic hardening

$$R = Q(1 - e^{-bp})$$

b	Rate of isotropic hardening	104
Q	Total isotropic saturation size of the yield surface	100

OPTIM
+ Manual identification

Elasticity

T	Temperature (C°)	550
E	Young's modulus (MPa)	1.7×10^5
v	Poisson's Ratio	0.3

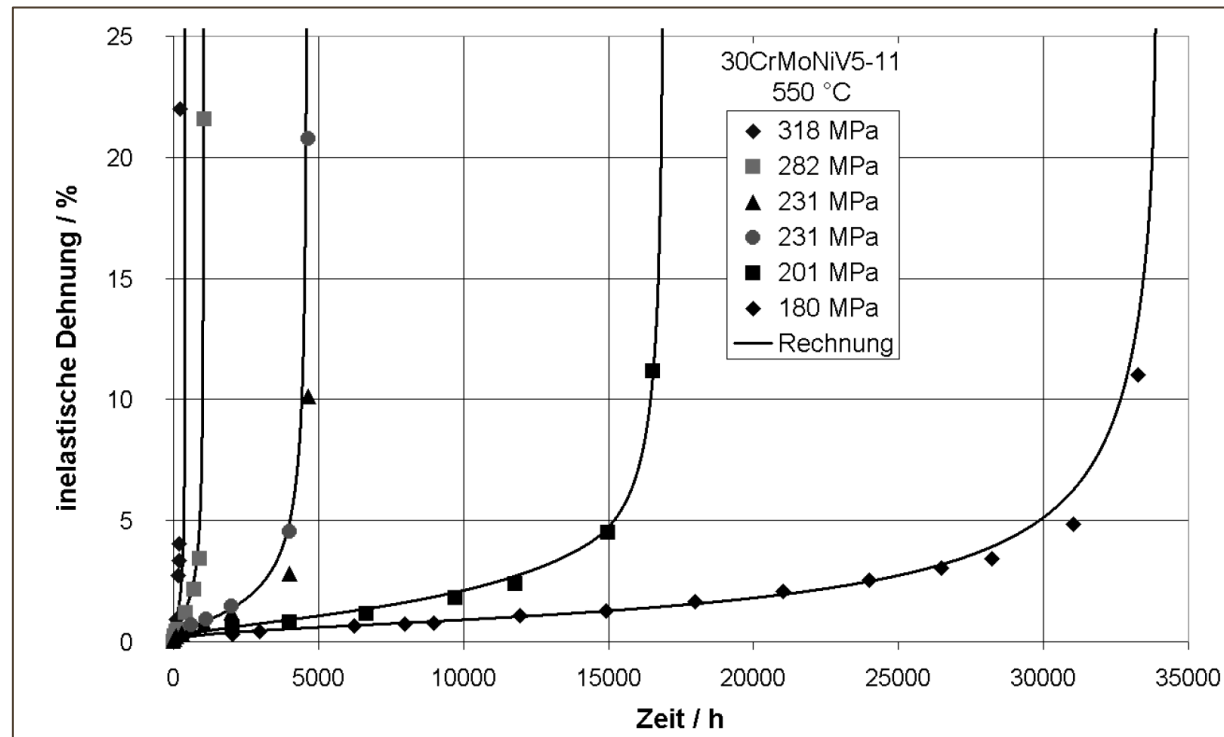
Damage: Rabotnov-Kachanov equation:

$$\dot{D}_c = k_3 \left(\frac{Y(\sigma^d * k_4)}{S_c} \right)^{s_c} \frac{1}{(1 - D)^k}$$

h	Mico-defects closure parameter	0.2
D_{crit}	Critical damage value (<1)	0.99
τ	Specific time for the appearance of creep	1×10^5
k_3	Global safety coefficient on creep damage	1
k_4	Safety coefficient applied to stress level on creep damage	1
S_c	Creep damage parameter	38.00
s_c	Creep damage exponent	3.50
k_c	Kachanov creep damage exponent	4.00

Law identified for 30CrMoNiV5-11

Used Creep curves from literature for 30CrMoNiV5-11



Schemmel J. Beschreibung des Verformungs-, 2003.

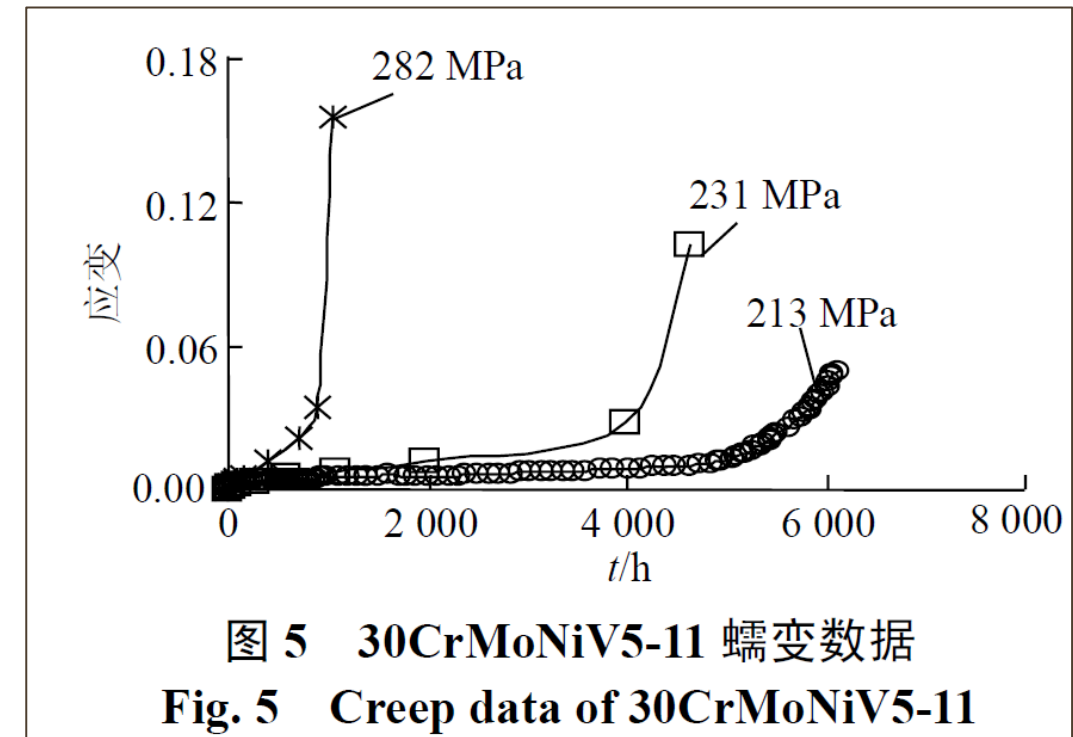
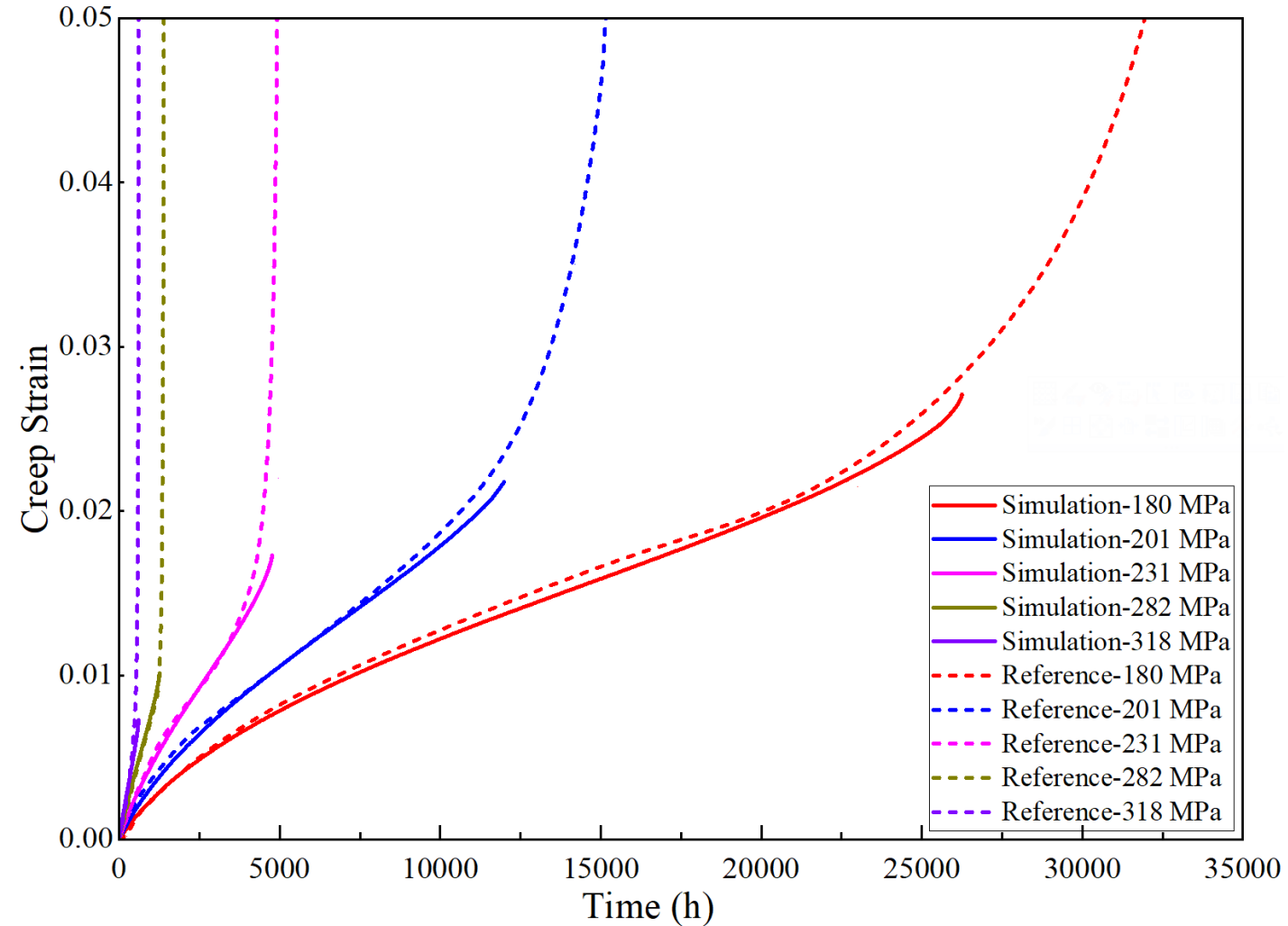
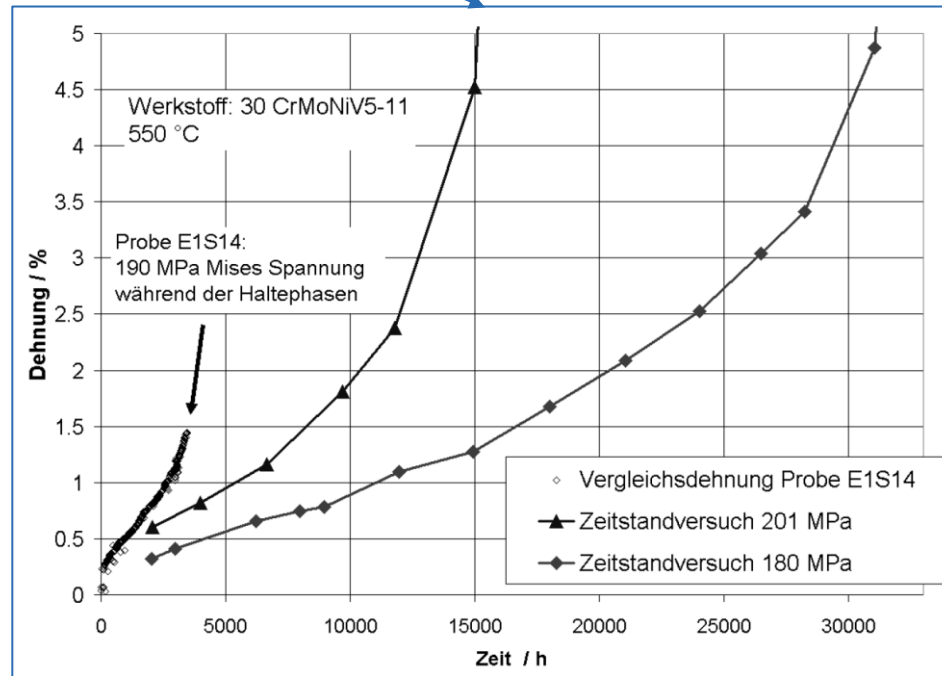
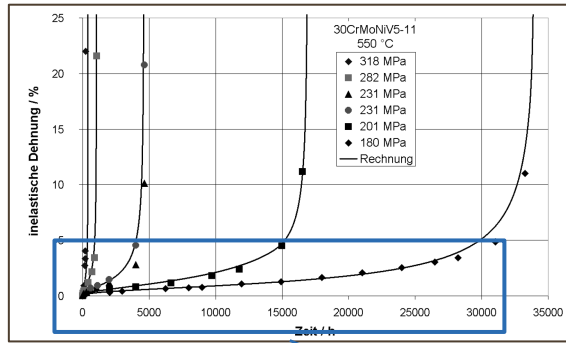


图 5 30CrMoNiV5-11 蠕变数据
Fig. 5 Creep data of 30CrMoNiV5-11

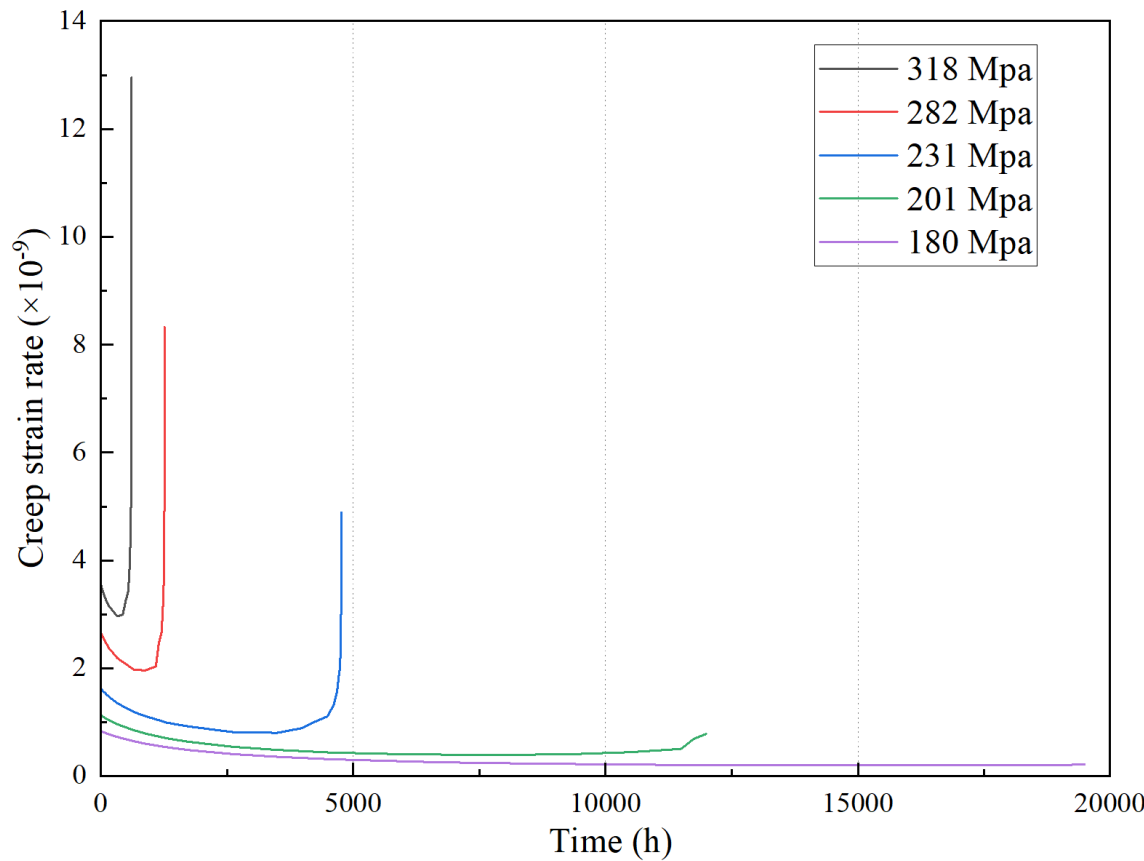
徐鸿,倪永中,王树东. 中国电机工程学报,2009,29(32):88-91.

Single element test (performed by ULiege Lagamine)



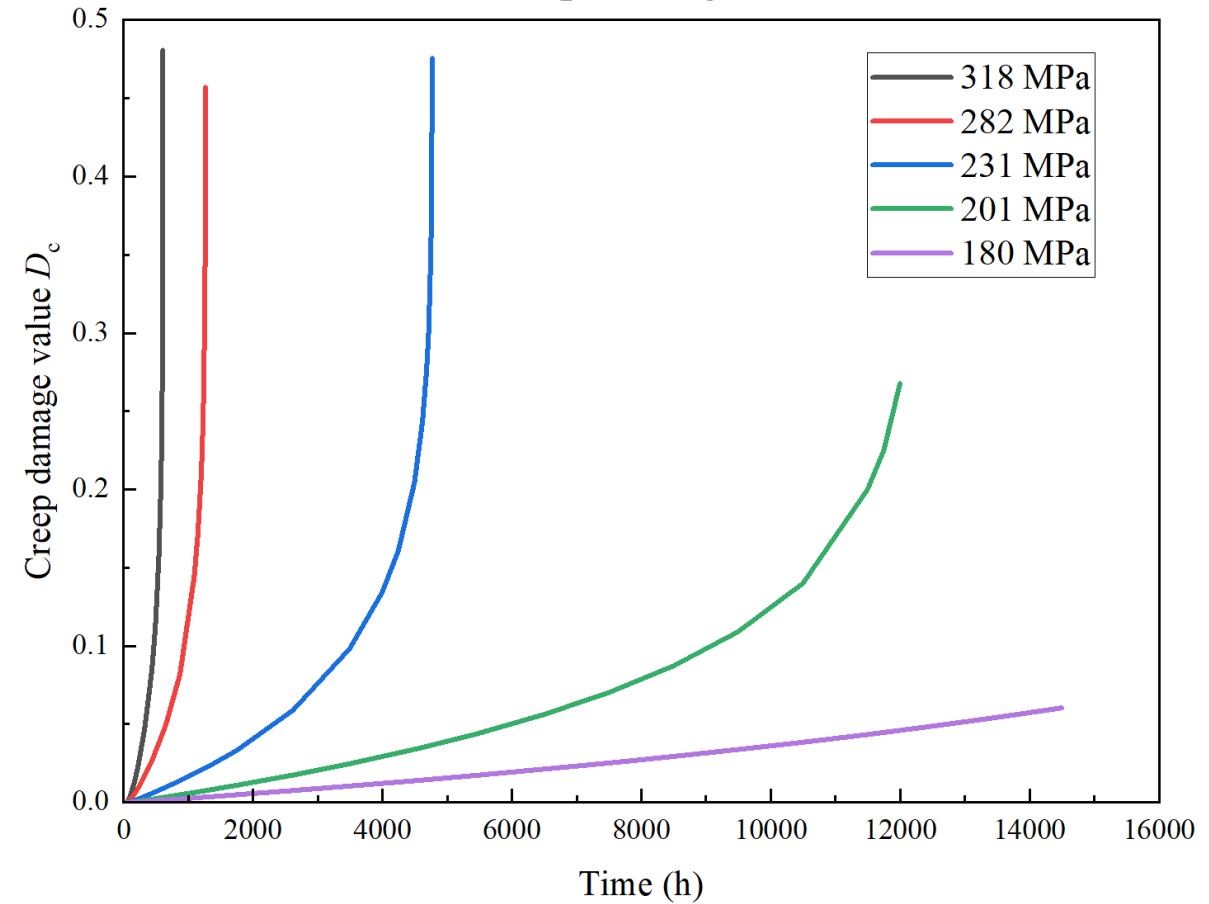
Single element test (Creep strain rate & Damage value-time)

Creep strain rate



(performed by ULiege Lagamine)

Creep damage value



$$\tilde{\sigma} = \frac{\sigma}{1 - hD}$$

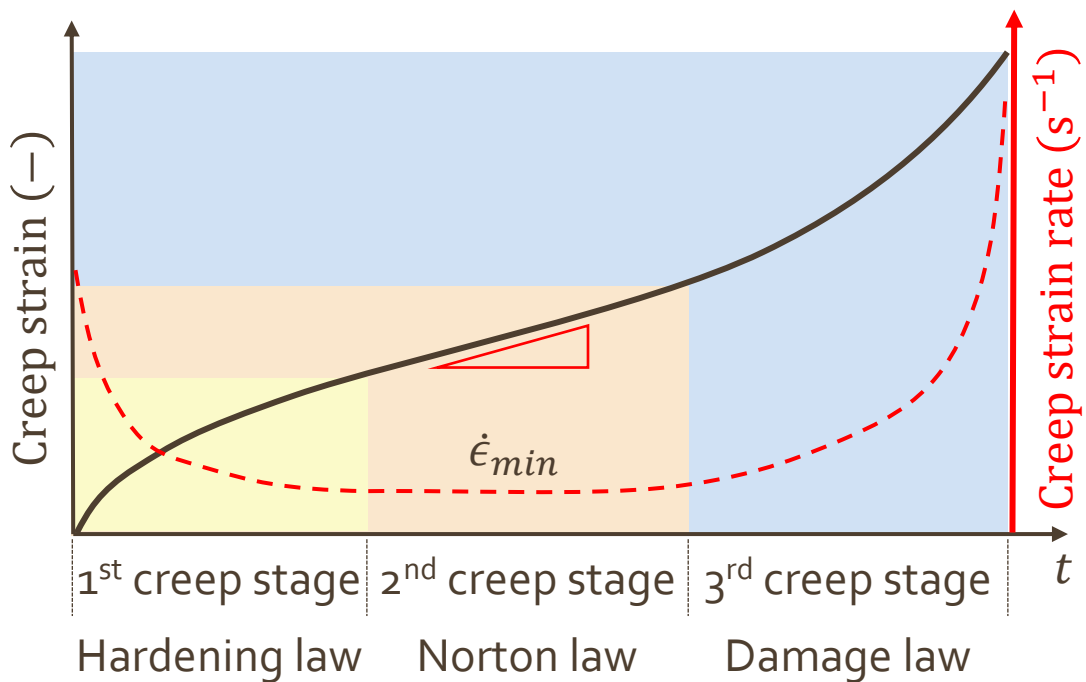
- Microdefects closure h
- Creep damage D

Creep modeling issues with Norton type law

Norton viscosity function

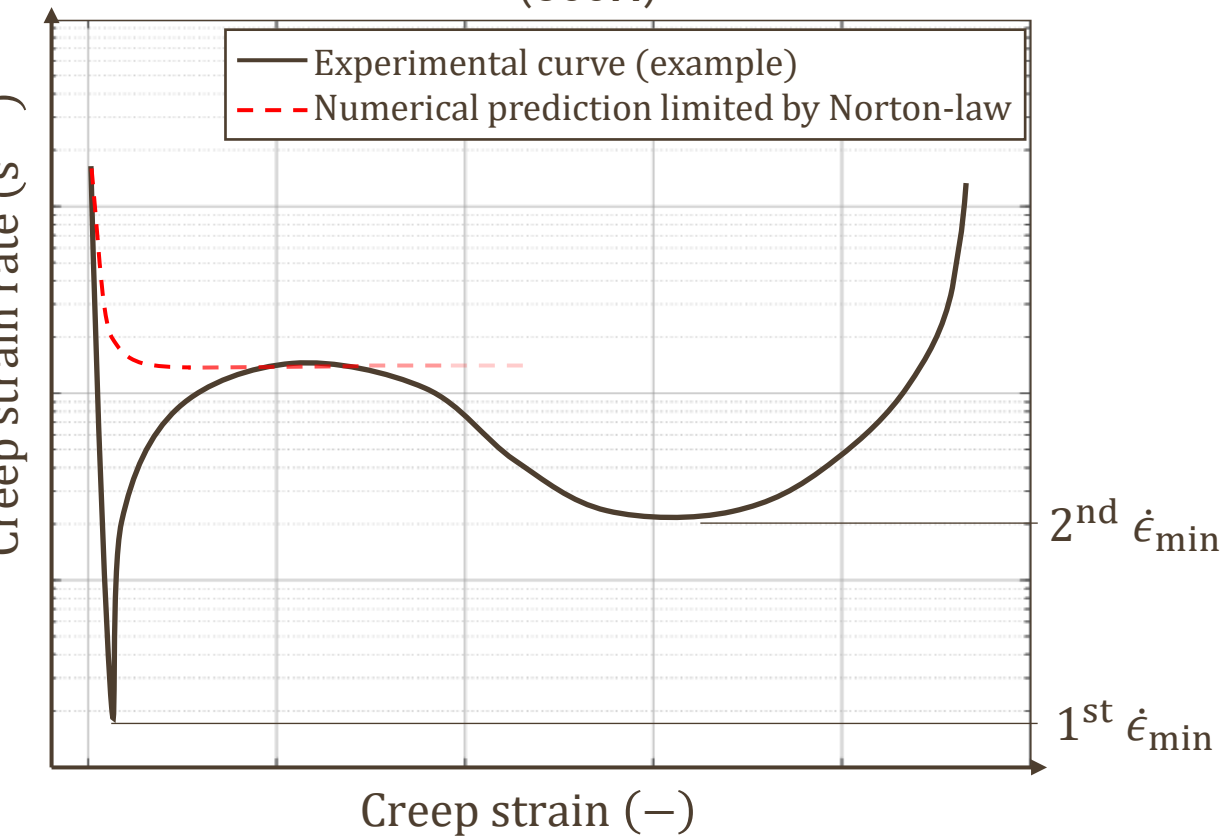
$$\dot{p} = \left(\frac{\sigma_v}{K} \right)^n$$

OK for classic creep behavior:



~~OK~~ for materials with non-classical creep

Non-classical creep response: 2-step creep rate minima (800H)



*: Experimental curves after (V. Gutmann & R. Bürgel, 1983)

Graham-Walles viscosity function

→ higher flexibility

Non-conventional approach, addition of i functions, implemented in Lagamine FE code

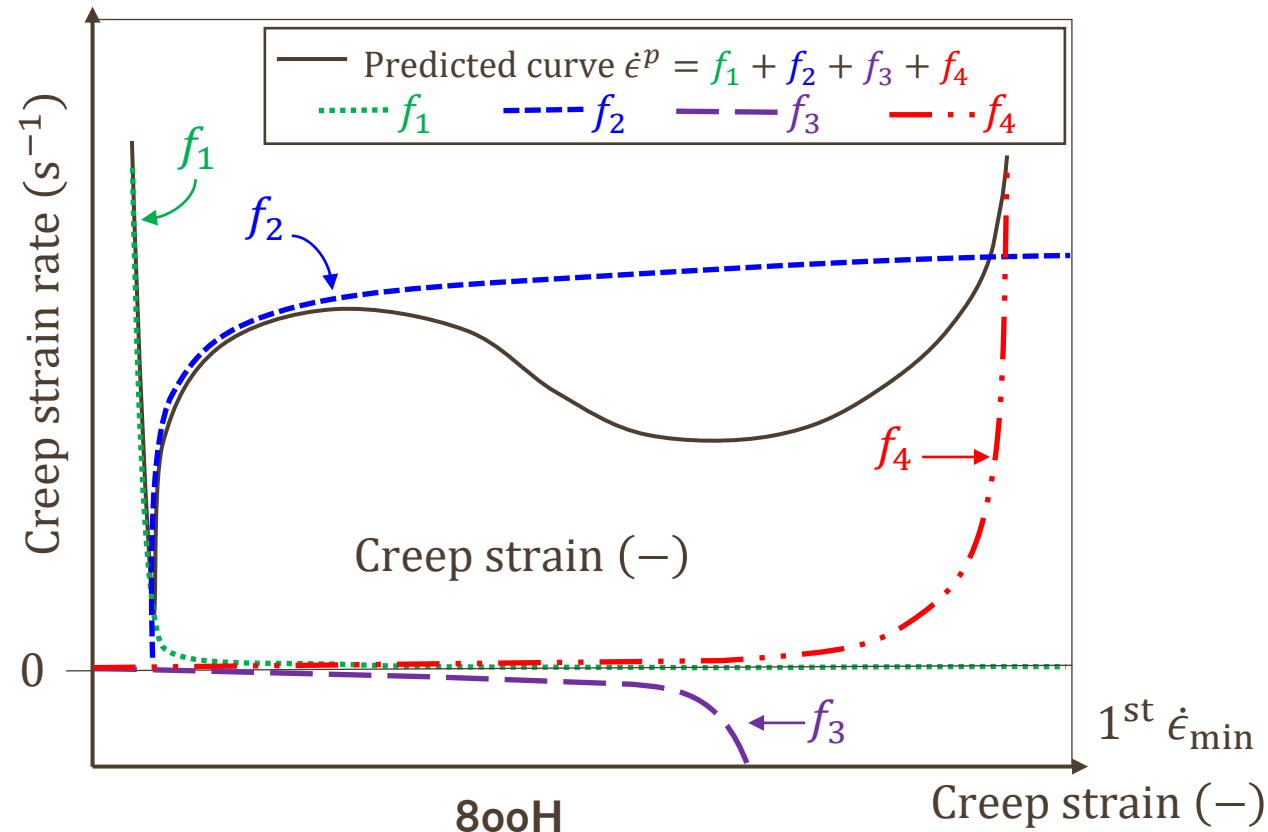
$$\dot{\epsilon}^p = \sum_{i=1}^{vp_i} K_i \exp\left(\frac{T}{C}\right) [\bar{\sigma}]^{n_i} (\epsilon^p)^{m_i}$$

→ $f(\bar{\sigma}, T, \epsilon^p)$ → non-linear!

Parameters: C ($^{\circ}\text{C}$) + 3 per equation (vp_i)

$\bar{\sigma}$	Eq. stress	(MPa)
T	Temperature	($^{\circ}\text{C}$)
ϵ^p	Eq. plastic strain	(-)

Possible to model non-classical creep response:
2-step creep rate minima



Graham-Walles viscosity function

$$\dot{\epsilon}^p = \sum_{i=1}^{vp_i} K_i \exp\left(\frac{T}{C}\right) (\bar{\sigma})^{n_i} (\epsilon^p)^{m_i}$$

→ $f(\bar{\sigma}, T, \epsilon^p)$

$\bar{\sigma}$	Eq. stress	(MPa)
T	Temperature	(°C)
ϵ^p	Eq. plastic strain	(-)

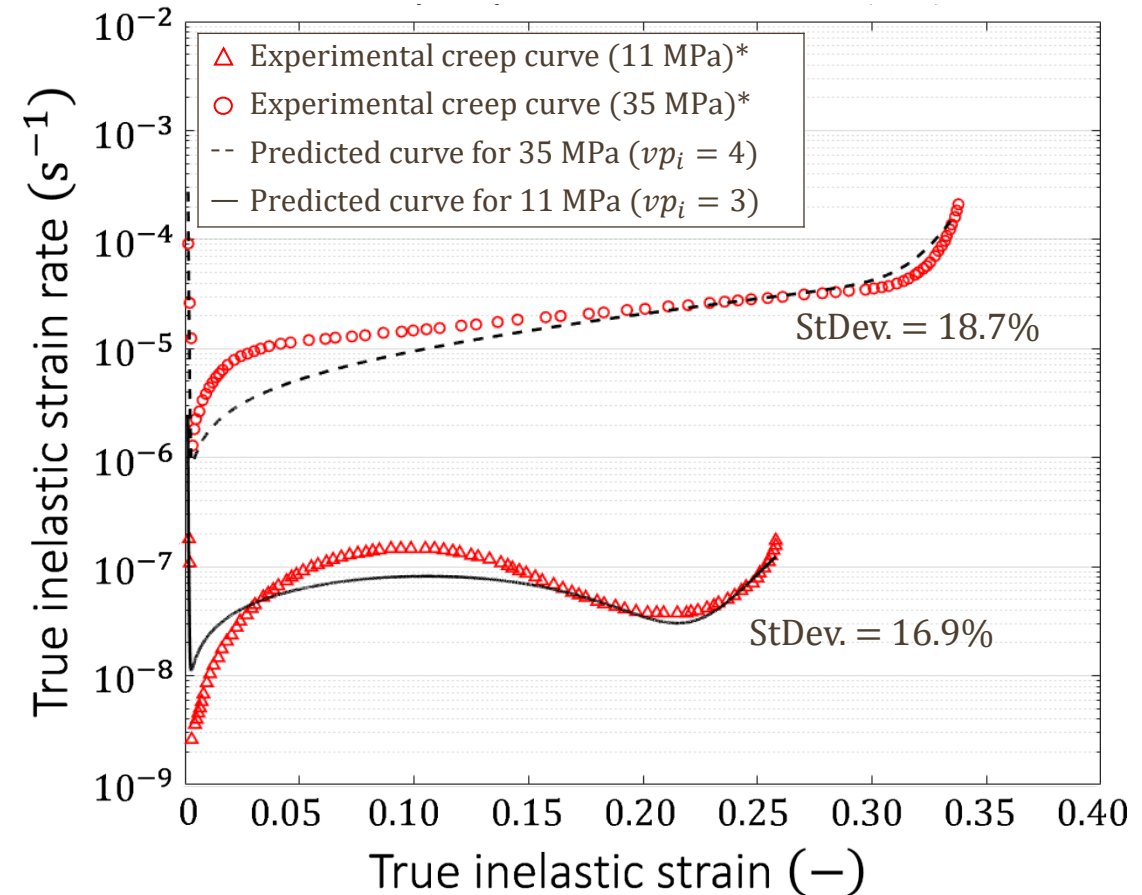
non-linear!

Parameters:

C	(°C)
K_i	(s^{-1})
n_i	(-)
m_i	(-)

+ 3 per equation (vp_i)

Case study: creep response of 800H alloy at 1000°C

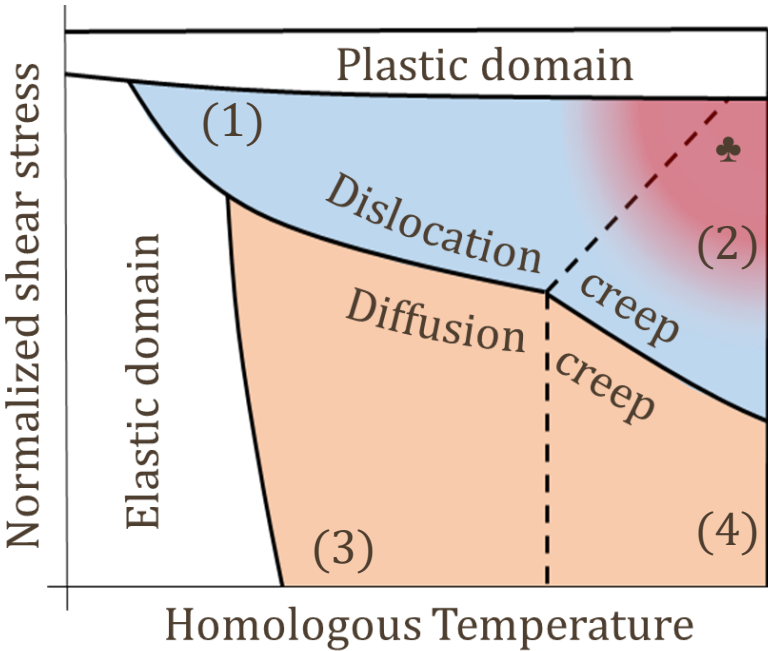
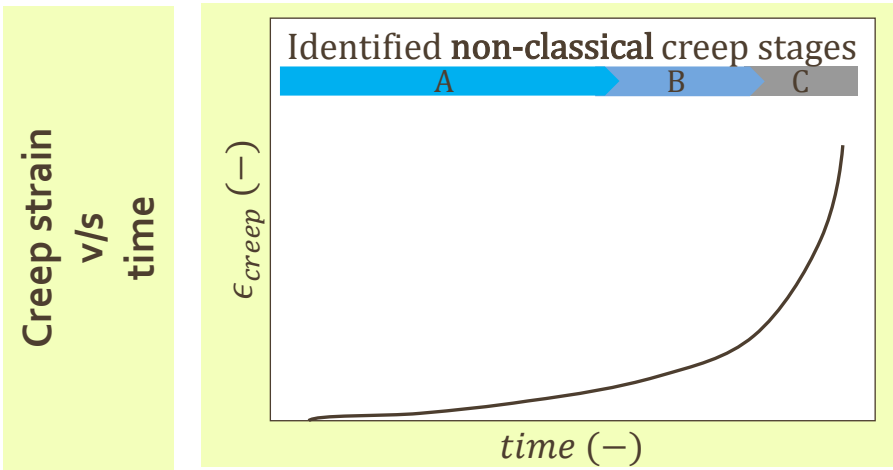


*: Experimental curves after (V. Gutmann & R. Bürgel, 1983)

Contents

- Introduction
- **Phenomenological approaches**
 - Scalars
 - Larson Miller etc...
 - Curves and constitutive laws FE
 - Norton
 - Graham Wales
- **Micro physical based approach**
 - The basis
 - Incoloy 718 application
- **Fatigue-Creep, Dwell effect and FE Morch constitutive macro law**
- **Nitriding effect**
- **AID4Greenest EU project ...**

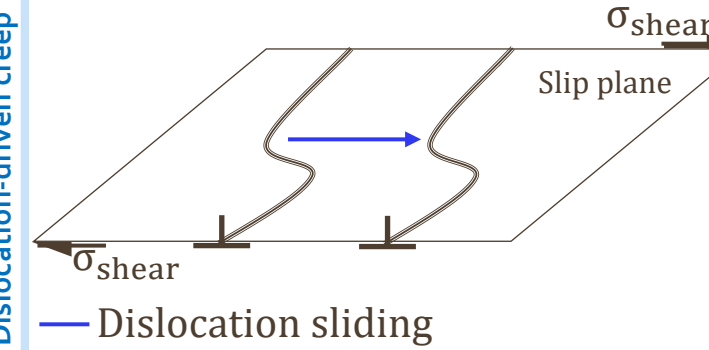
Classical curve (low microstructure evolution)



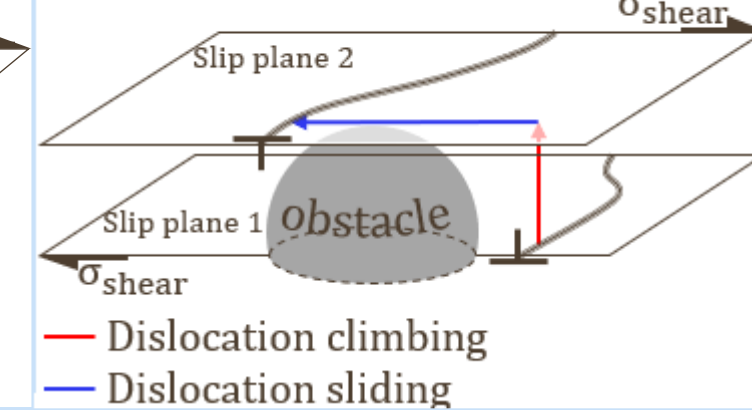
Creep mechanisms

Time effect

Low tp° and high stress (1)

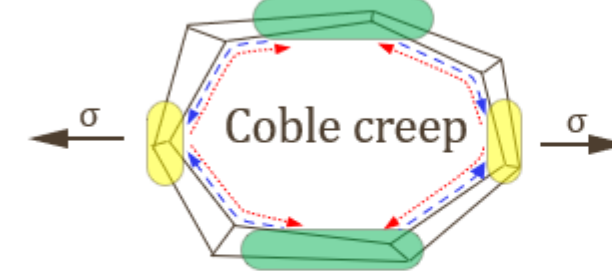


High tp° high stress (2)

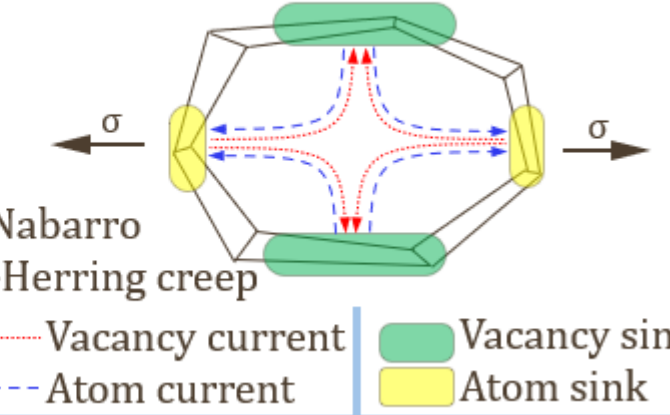


Diffusion-driven creep

Low tp° low stress (3)



High Tp° Low stress (4)



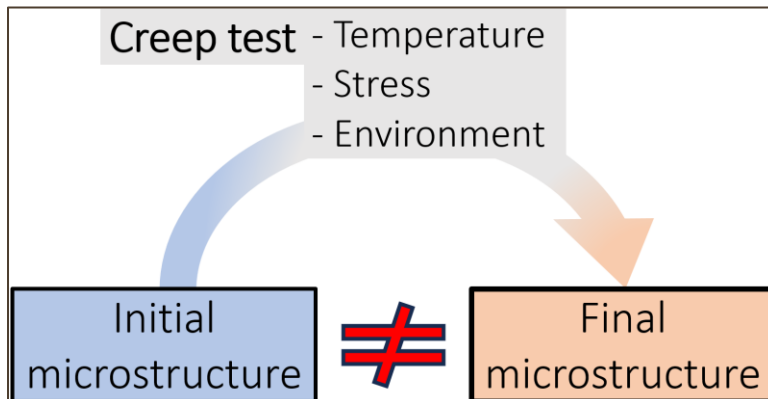
Diffusion : along GB

inside the grain → GB sliding

Semi-physical creep model → macro FE Coupled approach ?

Creep properties of materials depend on:

- Permanent microstructural features
- Evolving microstructural features



(S. Mesarovic et al., Springer, 2019)

	Semi-physical	Phenomenological
• Deterministic	• Statistical	• Empirical
• Nano-scale	• Meso-scale	• Macro-scale
• Complex	• Moderate	• Simplified

A Macro law (used in macro FE simulations)

T, \dot{T}, σ or ϵ loading, q state variables
→ $\dot{\epsilon}$ or $\dot{\sigma}$, updated q state variables

→ Macro law identified through predicted creep curves computed by a creep Meso-scale model

OR

→ Macro law sequentially or continuously updated based on state variable(s) kinetic of reflecting microstructure state computed
-from a set of equations
-from interpolation within in a data base
-from a meso or nano model (phase-field...)

OR

-multi scale ...

$$\dot{\epsilon} = \frac{\rho b v_g}{M}$$

$\dot{\epsilon}$	Creep rate	(s^{-1})
ρ	Dislocation density	(m^{-2})
b	Burger's vector	(m)
v_g	Dislocation glide velocity	(ms^{-1})
M	Taylor factor	(-)

Semi-physical creep modeling approach

N.M. Ghoniem et al., 1990 → a comprehensive mean-field model

5 co-dependent non-linear equations.

Each = specific microstructural feature involved in the creep mechanism.

$$\dot{\epsilon} = \frac{\rho_m b v_g}{M}$$

Creep strain rate

$$\dot{\rho}_m = v_g \left[\rho_m^{3/2} + \frac{\beta \rho_s R_{sb}}{h_b^2} - \frac{\rho_m}{2R_{sb}} - \delta_a (\rho_m^2 - \rho_m \rho_s) \right] - 8 \rho_m^{3/2} v_{cm}$$

Mobile dislocation density

$$\dot{\rho}_s = v_g \left[\frac{\rho_m}{2R_{sb}} - \delta_a \rho_m \rho_s \right] - 8 \frac{\rho_s}{h_b} v_c$$

Static (dipole) dislocation density

$$\dot{\rho}_b = 8(1 - 2\zeta) \frac{\rho_s}{h_b} v_c - \frac{\rho_b}{R_{sb}} M_{sb} \left[P_{sb} - 2\pi \left(\sum_i r_p^2 \cdot N_{p_i} \right) \gamma_{sb} \right]$$

Boundary dislocation density

$$\dot{R}_{sb} = M_{sb} \left[P_{sb} - 2\pi \left(\sum_i r_p^2 \cdot N_{p_i} \right) \gamma_{sb} \right] - \mu \eta_v K_c R_{sb} \left[(\rho_m + \rho_s)^{1/2} - \frac{K_c}{2R_{sb}} \right] \frac{\Omega D_s}{KT}$$

Subgrain radius

Semi-physical creep modeling approach

N.M. Ghoniem et al., 1990 → a comprehensive mean-field model

5 co-dependent non-linear equations.

Each = specific microstructural feature involved in the creep mechanism.

$$\dot{\epsilon} = \frac{\rho_m b v_g}{M}$$

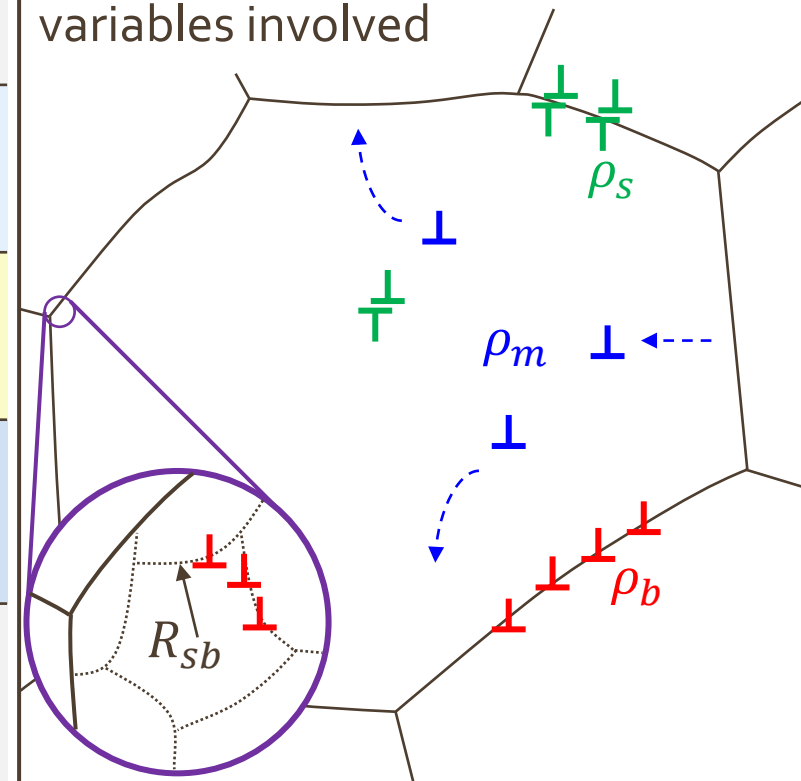
$$\dot{\rho}_m = v_g \left[\rho_m^{3/2} + \frac{\beta \rho_s R_{sb}}{h_b^2} - \frac{\rho_m}{2R_{sb}} - \delta_a (\rho_m^2 - \rho_m \rho_s) \right] - 8 \rho_m^{3/2} v_{cm}$$

$$\dot{\rho}_s = v_g \left[\frac{\rho_m}{2R_{sb}} - \delta_a \rho_m \rho_s \right] - 8 \frac{\rho_s}{h_b} v_c$$

$$\dot{\rho}_b = 8(1 - 2\zeta) \frac{\rho_s}{h_b} v_c - \frac{\rho_b}{R_{sb}} M_{sb} \left[P_{sb} - 2\pi \left(\sum_i r_p^2 i \cdot N_{pi} \right) \gamma_{sb} \right]$$

$$\dot{R}_{sb} = M_{sb} \left[P_{sb} - 2\pi \left(\sum_i r_p^2 i \cdot N_{pi} \right) \gamma_{sb} \right] - \mu \eta_v K_c R_{sb} \left[(\rho_m + \rho_s)^{1/2} - \frac{K_c}{2R_{sb}} \right] \frac{\Omega D_s}{KT}$$

Illustration of the different state variables involved



C. Rojas ULiege

Semi-physical creep modeling approach

N.M. Ghoniem et al., 1990 → a comprehensive mean-field model

5 co-dependent non-linear equations.

Each = specific microstructural feature involved in the creep mechanism.

$$\dot{\epsilon} = \frac{\rho_m b v_g}{M}$$

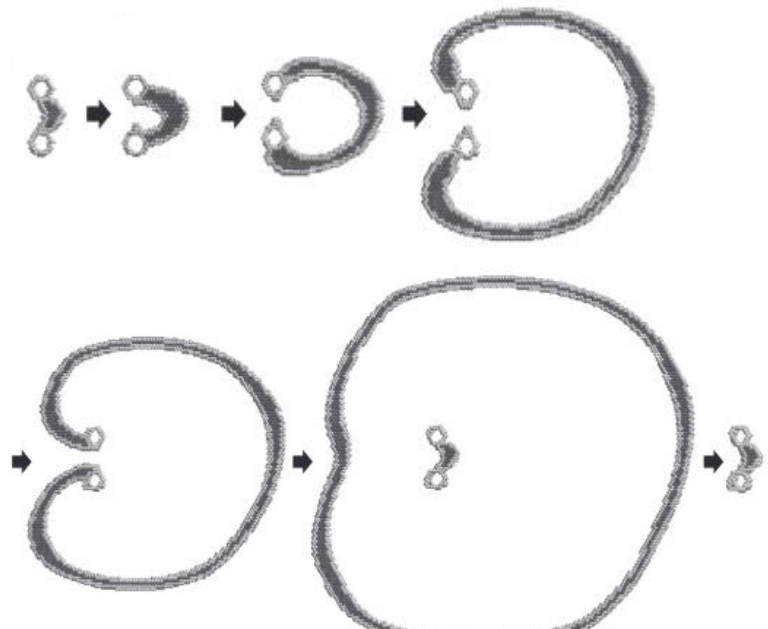
$$\dot{\rho}_m = v_g \left[\rho_m^{3/2} + \frac{\beta \rho_s R_{sb}}{h_b^2} - \frac{\rho_m}{2R_{sb}} - \delta_a (\rho_m^2 - \rho_m \rho_s) \right] - 8 \rho_m^{3/2} v_{cm}$$

$$\dot{\rho}_s = v_g \left[\frac{\rho_m}{2R_{sb}} - \delta_a \rho_m \rho_s \right] - 8 \frac{\rho_s}{h_b} v_c$$

$$\dot{\rho}_b = 8(1 - 2\zeta) \frac{\rho_s}{h_b} v_c - \frac{\rho_b}{R_{sb}} M_{sb} \left[P_{sb} - 2\pi \left(\sum_i r_p^2 i \cdot N_{p_i} \right) \gamma_{sb} \right]$$

$$\dot{R}_{sb} = M_{sb} \left[P_{sb} - 2\pi \left(\sum_i r_p^2 i \cdot N_{p_i} \right) \gamma_{sb} \right] - \mu \eta_v K_c R_{sb} \left[(\rho_m + \rho_s)^{1/2} - \frac{K_c}{2R_{sb}} \right] \frac{\Omega D_s}{KT}$$

Frank-Read dislocation source



(T. Shimokawa & S. Kitada, 2014)

Semi-physical creep modeling approach

N.M. Ghoniem et al., 1990 → a comprehensive mean-field model

5 co-dependent non-linear equations.

Each = specific microstructural feature involved in the creep mechanism.

$$\dot{\epsilon} = \frac{\rho_m b v_g}{M}$$

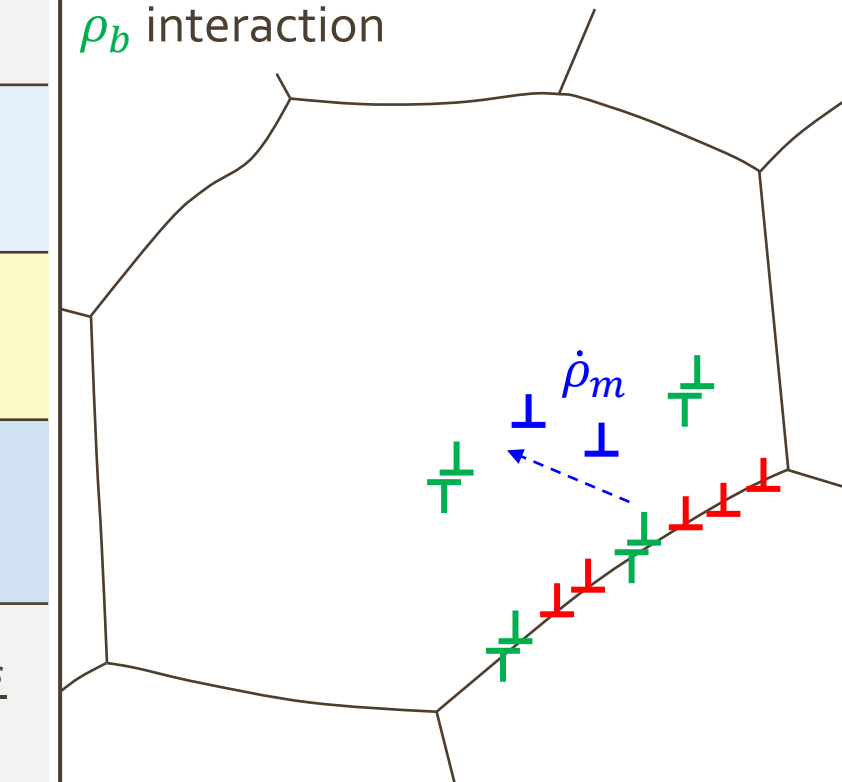
$$\dot{\rho}_m = v_g \left[\rho_m^{3/2} + \frac{\beta \rho_s R_{sb}}{h_b^2} - \frac{\rho_m}{2R_{sb}} - \delta_a (\rho_m^2 - \rho_m \rho_s) \right] - 8 \rho_m^{3/2} v_{cm}$$

$$\dot{\rho}_s = v_g \left[\frac{\rho_m}{2R_{sb}} - \delta_a \rho_m \rho_s \right] - 8 \frac{\rho_s}{h_b} v_c$$

$$\dot{\rho}_b = 8(1 - 2\zeta) \frac{\rho_s}{h_b} v_c - \frac{\rho_b}{R_{sb}} M_{sb} \left[P_{sb} - 2\pi \left(\sum_i r_p^2 \cdot N_{p_i} \right) \gamma_{sb} \right]$$

$$\dot{R}_{sb} = M_{sb} \left[P_{sb} - 2\pi \left(\sum_i r_p^2 \cdot N_{p_i} \right) \gamma_{sb} \right] - \mu \eta_v K_c R_{sb} \left[(\rho_m + \rho_s)^{1/2} - \frac{K_c}{2R_{sb}} \right] \frac{\Omega D_s}{KT}$$

Dislocations generated after ρ_s & ρ_b interaction



C. Rojas ULiege

Semi-physical creep modeling approach

N.M. Ghoniem et al., 1990 → a comprehensive mean-field model

5 co-dependent non-linear equations.

Each = specific microstructural feature involved in the creep mechanism.

$$\dot{\epsilon} = \frac{\rho_m b v_g}{M}$$

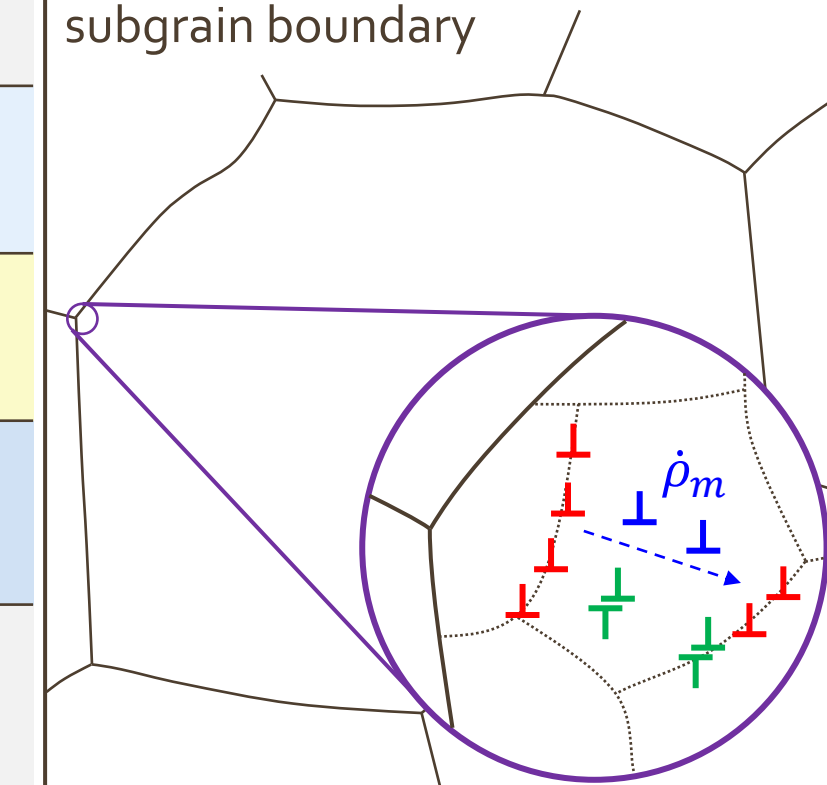
$$\dot{\rho}_m = v_g \left[\rho_m^{3/2} + \frac{\beta \rho_s R_{sb}}{h_b^2} - \frac{\rho_m}{2R_{sb}} - \delta_a (\rho_m^2 - \rho_m \rho_s) \right] - 8 \rho_m^{3/2} v_{cm}$$

$$\dot{\rho}_s = v_g \left[\frac{\rho_m}{2R_{sb}} - \delta_a \rho_m \rho_s \right] - 8 \frac{\rho_s}{h_b} v_c$$

$$\dot{\rho}_b = 8(1 - 2\zeta) \frac{\rho_s}{h_b} v_c - \frac{\rho_b}{R_{sb}} M_{sb} \left[P_{sb} - 2\pi \left(\sum_i r_p^2 \cdot N_{p_i} \right) \gamma_{sb} \right]$$

$$\dot{R}_{sb} = M_{sb} \left[P_{sb} - 2\pi \left(\sum_i r_p^2 \cdot N_{p_i} \right) \gamma_{sb} \right] - \mu \eta_v K_c R_{sb} \left[(\rho_m + \rho_s)^{1/2} - \frac{K_c}{2R_{sb}} \right] \frac{\Omega D_s}{KT}$$

Dislocations absorbed at the subgrain boundary



C. Rojas ULiege

Semi-physical creep modeling approach

N.M. Ghoniem et al., 1990 → a comprehensive mean-field model

5 co-dependent non-linear equations.

Each = specific microstructural feature involved in the creep mechanism.

$$\dot{\epsilon} = \frac{\rho_m b v_g}{M}$$

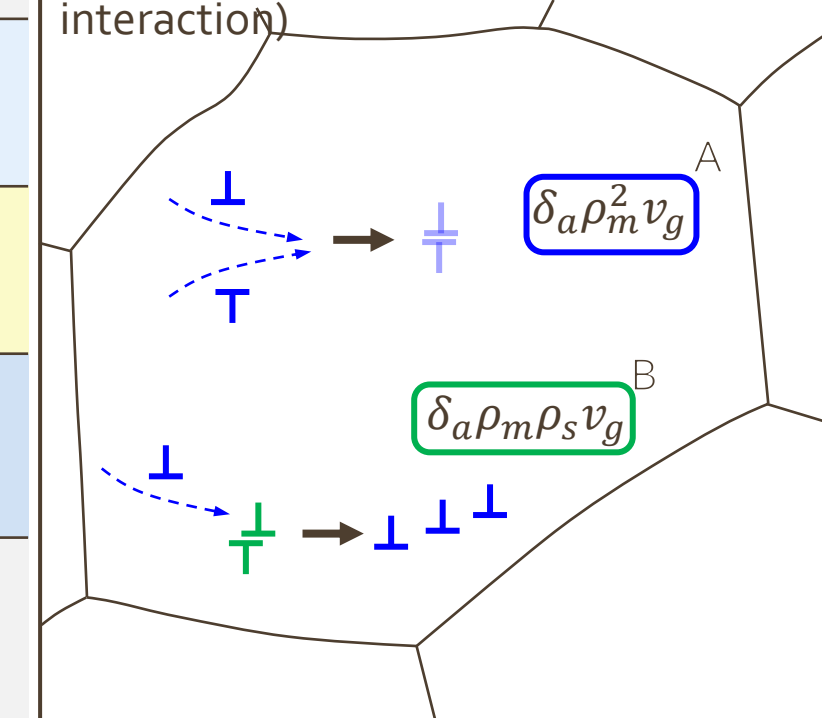
$$\dot{\rho}_m = v_g \left[\rho_m^{3/2} + \frac{\beta \rho_s R_{sb}}{h_b^2} - \frac{\rho_m}{2R_{sb}} - \boxed{\delta_a(\rho_m^2)}^A + \boxed{\delta_a \rho_m \rho_s}^B \right] - 8 \rho_m^{3/2} v_{cm}$$

$$\dot{\rho}_s = v_g \left[\frac{\rho_m}{2R_{sb}} - \boxed{\delta_a \rho_m \rho_s}^B \right] - 8 \frac{\rho_s}{h_b} v_c$$

$$\dot{\rho}_b = 8(1 - 2\zeta) \frac{\rho_s}{h_b} v_c - \frac{\rho_b}{R_{sb}} M_{sb} \left[P_{sb} - 2\pi \left(\sum_i r_p^2 i \cdot N_{p_i} \right) \gamma_{sb} \right]$$

$$\dot{R}_{sb} = M_{sb} \left[P_{sb} - 2\pi \left(\sum_i r_p^2 i \cdot N_{p_i} \right) \gamma_{sb} \right] - \mu \eta_v K_c R_{sb} \left[(\rho_m + \rho_s)^{1/2} - \frac{K_c}{2R_{sb}} \right] \frac{\Omega D_s}{KT}$$

Dynamic recovery: Annihilation by glide (ρ_m - ρ_m and ρ_m - ρ_s interaction)



C. Rojas ULiege

Semi-physical creep modeling approach

N.M. Ghoniem et al., 1990 → a comprehensive mean-field model

5 co-dependent non-linear equations.

Each = specific microstructural feature involved in the creep mechanism.

$$\dot{\epsilon} = \frac{\rho_m b v_g}{M}$$

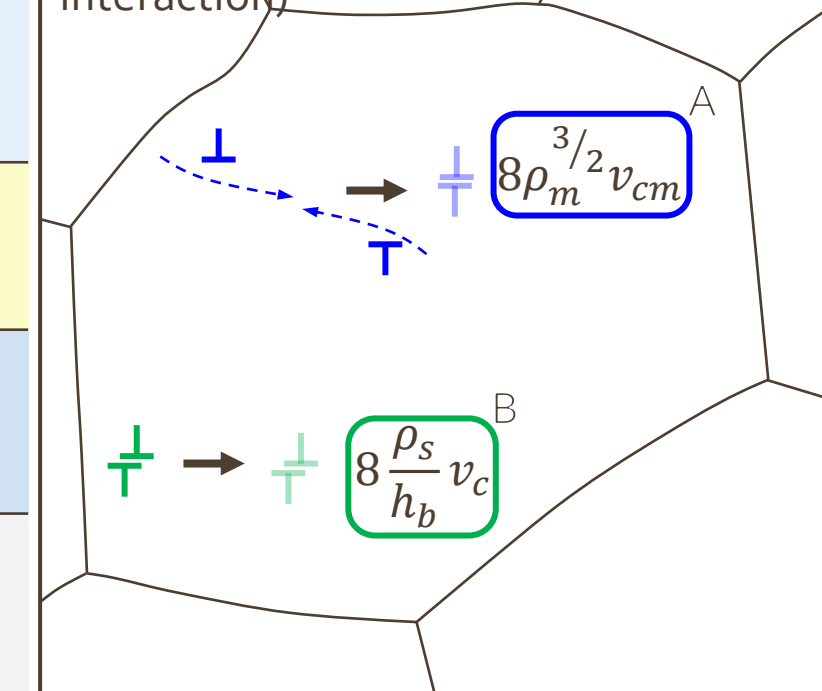
$$\dot{\rho}_m = v_g \left[\rho_m^{3/2} + \frac{\beta \rho_s R_{sb}}{h_b^2} - \frac{\rho_m}{2R_{sb}} - \delta_a (\rho_m^2 - \rho_m \rho_s) \right] - 8 \rho_m^{3/2} v_{cm}$$

$$\dot{\rho}_s = v_g \left[\frac{\rho_m}{2R_{sb}} - \delta_a \rho_m \rho_s \right] - 8 \frac{\rho_s}{h_b} v_c$$

$$\dot{\rho}_b = 8(1 - 2\zeta) \frac{\rho_s}{h_b} v_c - \frac{\rho_b}{R_{sb}} M_{sb} \left[P_{sb} - 2\pi \left(\sum_i r_p^2 i \cdot N_{p_i} \right) \gamma_{sb} \right]$$

$$\dot{R}_{sb} = M_{sb} \left[P_{sb} - 2\pi \left(\sum_i r_p^2 i \cdot N_{p_i} \right) \gamma_{sb} \right] - \mu \eta_v K_c R_{sb} \left[(\rho_m + \rho_s)^{1/2} - \frac{K_c}{2R_{sb}} \right] \frac{\Omega D_s}{KT}$$

Dynamic recovery: Annihilation by **climb** (ρ_m - ρ_m and ρ_s - ρ_s interaction)



C. Rojas ULiege

Semi-physical creep modeling approach

N.M. Ghoniem et al., 1990 → a comprehensive mean-field model

5 co-dependent non-linear equations.

Each = specific microstructural feature involved in the creep mechanism.

$$\dot{\epsilon} = \frac{\rho_m b v_g}{M}$$

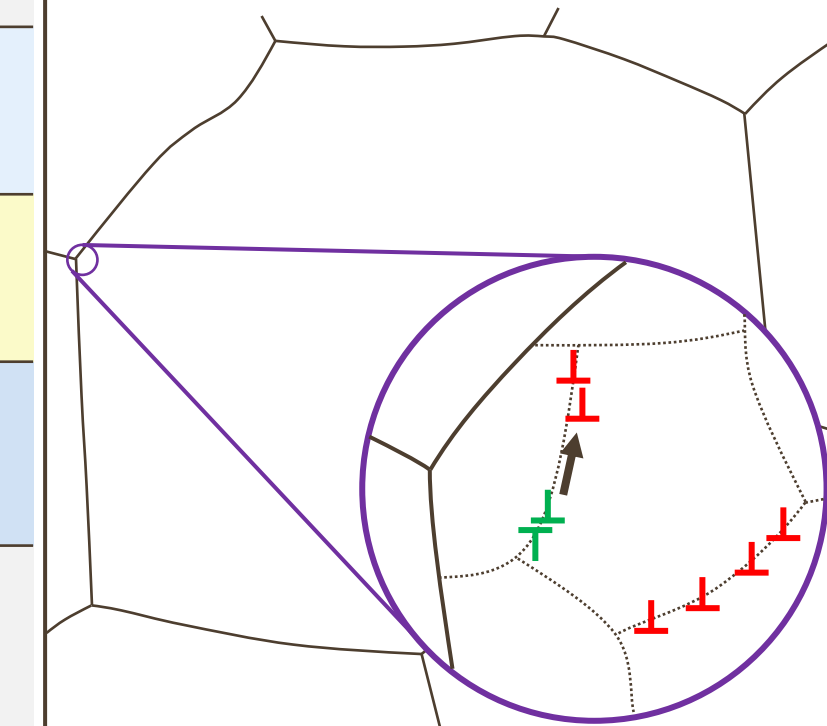
$$\dot{\rho}_m = v_g \left[\rho_m^{3/2} + \frac{\beta \rho_s R_{sb}}{h_b^2} - \frac{\rho_m}{2R_{sb}} - \delta_a (\rho_m^2 - \rho_m \rho_s) \right] - 8 \rho_m^{3/2} v_{cm}$$

$$\dot{\rho}_s = v_g \left[\frac{\rho_m}{2R_{sb}} - \delta_a \rho_m \rho_s \right] - 8 \frac{\rho_s}{h_b} v_c$$

$$\dot{\rho}_b = 8(1 - 2\zeta) \frac{\rho_s}{h_b} v_c - \frac{\rho_b}{R_{sb}} M_{sb} \left[P_{sb} - 2\pi \left(\sum_i r_p^2 \cdot N_{p_i} \right) \gamma_{sb} \right]$$

$$\dot{R}_{sb} = M_{sb} \left[P_{sb} - 2\pi \left(\sum_i r_p^2 \cdot N_{p_i} \right) \gamma_{sb} \right] - \mu \eta_v K_c R_{sb} \left[(\rho_m + \rho_s)^{1/2} - \frac{K_c}{2R_{sb}} \right] \frac{\Omega D_s}{KT}$$

Share of boundary dislocations produced after ρ_s



Semi-physical creep modeling approach

N.M. Ghoniem et al., 1990 → a comprehensive mean-field model

5 co-dependent non-linear equations.

Each = specific microstructural feature involved in the creep mechanism.

$$\dot{\epsilon} = \frac{\rho_m b v_g}{M}$$

$$\dot{\rho}_m = v_g \left[\rho_m^{3/2} + \frac{\beta \rho_s R_{sb}}{h_b^2} - \frac{\rho_m}{2R_{sb}} - \delta_a (\rho_m^2 - \rho_m \rho_s) \right] - 8 \rho_m^{3/2} v_{cm}$$

$$\dot{\rho}_s = v_g \left[\frac{\rho_m}{2R_{sb}} - \delta_a \rho_m \rho_s \right] - 8 \frac{\rho_s}{h_b} v_c$$

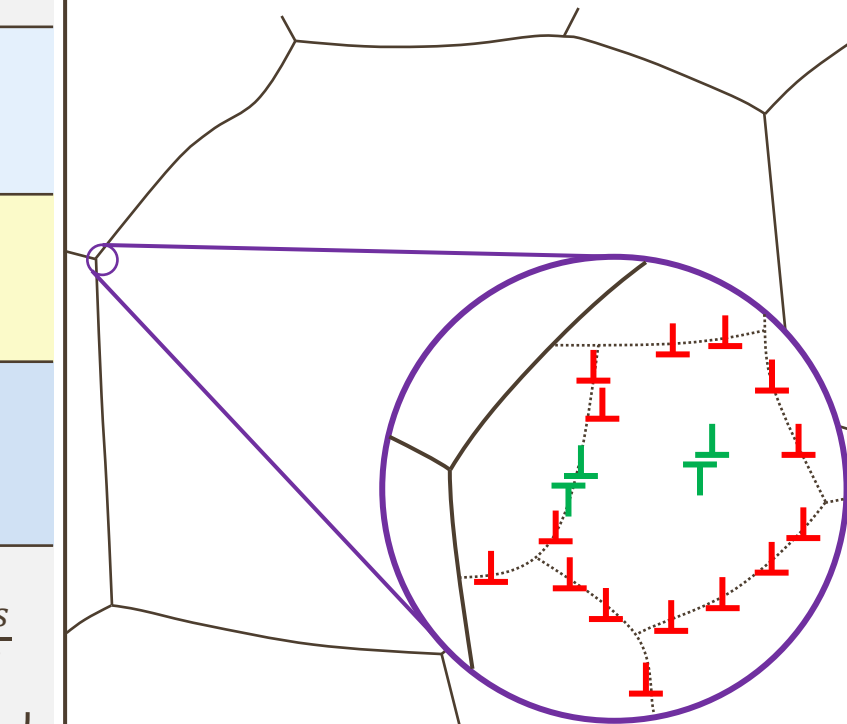
$$\dot{\rho}_b = 8(1 - 2\zeta) \frac{\rho_s}{h_b} v_c - \frac{\rho_b}{R_{sb}} M_{sb} \left[P_{sb} - 2\pi \left(\sum_i r_p^2 i \cdot N_{pi} \right) \gamma_{sb} \right]$$

$$\dot{R}_{sb} = M_{sb} \left[P_{sb} - 2\pi \left(\sum_i r_p^2 i \cdot N_{pi} \right) \gamma_{sb} \right] - \mu \eta_v K_c R_{sb} \left[(\rho_m + \rho_s)^{1/2} - \frac{K_c}{2R_{sb}} \right] \frac{\Omega D_s}{KT}$$

Subgrain growth

Subgrain nucleation

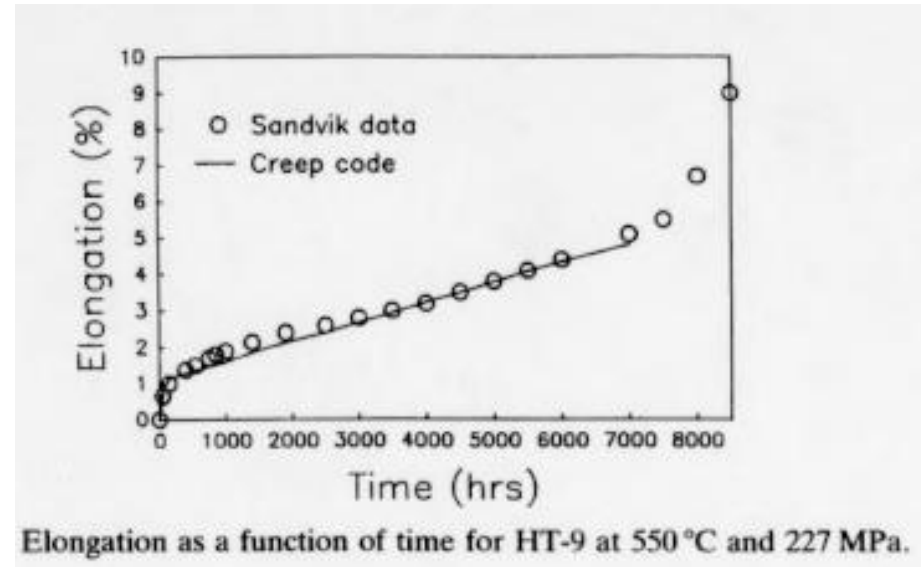
Evolution of subgrains: growth and nucleation terms



Martensitic steel HT9 - Ghoniem model application

Creep curve predictions : validated

- Earlier stade I \rightarrow II transition point if $T \nearrow$
- $\dot{\epsilon}_m \propto \sigma^5$ (steel type forming dislocation cells)
- $T \nearrow \rightarrow \dot{\epsilon} \nearrow$ (recovery and glide velocity \nearrow)
- $\rho \nearrow$ with $\dot{\epsilon}$ until saturation

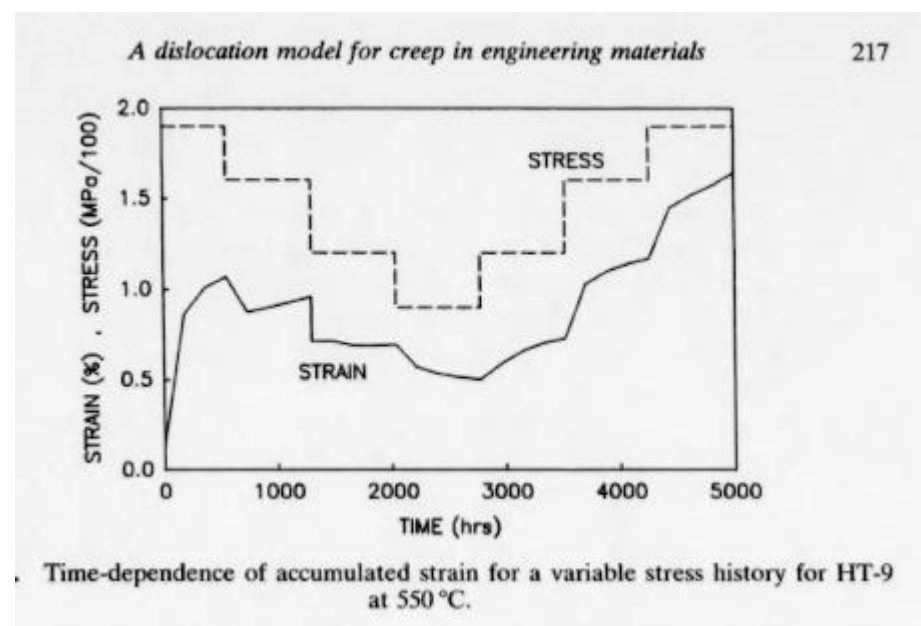


Strain related to stress history is logic

1st stress $\searrow \dot{\epsilon} \searrow$ than \nearrow

Effective stress applied on dislocation $\searrow \dot{\epsilon} \searrow$

ρ , internal stress readjust, threshold is again reached $\dot{\epsilon} \nearrow$



Semi-physical creep modeling approach

Accommodation of more particles (MX and M₂₃C₆) phase effects,
New functions for Cavitation damage (D_{cav}) and precipitate coarsening (D_{ppt})

$$\dot{\epsilon} = \frac{\rho_m b v_g}{M(1 - D_{ppt})(1 - D_{cav})}$$

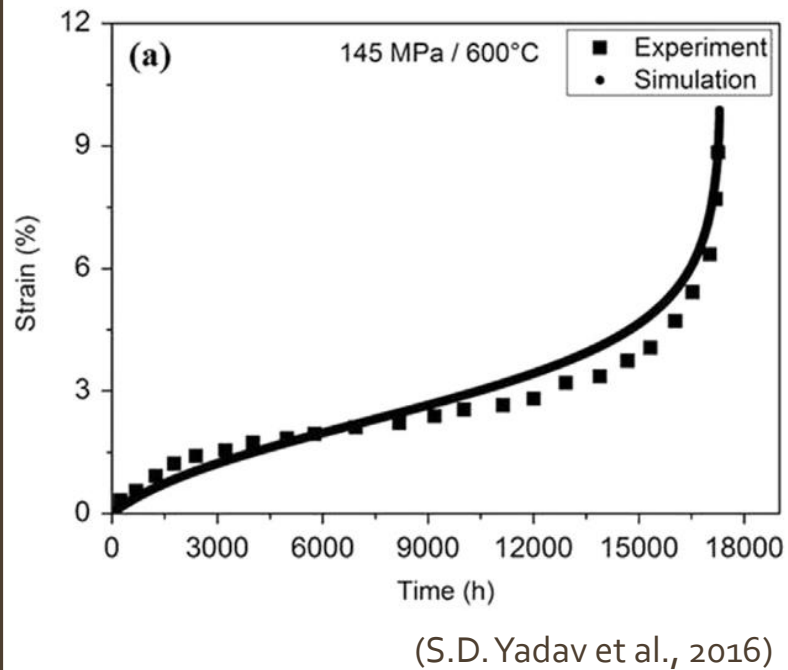
$$\dot{\rho}_m = v_g \left[\rho_m^{3/2} + \frac{\beta \rho_s R_{sb}}{h_b^2} - \frac{\rho_m}{2R_{sb}} - \delta_a (\rho_m^2 - \rho_m \rho_s) \right] - 8 \rho_m^{3/2} v_{cm}$$

$$\dot{\rho}_s = v_g \left[\frac{\rho_m}{2R_{sb}} - \delta_a \rho_m \rho_s \right] - 8 \frac{\rho_s}{h_b} v_c$$

$$\dot{\rho}_b = 8(1 - 2\zeta) \frac{\rho_s}{h_b} v_c - \frac{\rho_b}{R_{sb}} M_{sb} \left[P_{sb} - 2\pi \left(\sum_i r_p^2 i \cdot N_{p_i} \right) \gamma_{sb} \right]$$

$$\dot{R}_{sb} = M_{sb} \left[P_{sb} - 2\pi \left(\sum_i r_p^2 i \cdot N_{p_i} \right) \gamma_{sb} \right] - \mu \eta_v K_c R_{sb} \left[(\rho_m + \rho_s)^{1/2} - \frac{K_c}{2R_{sb}} \right] \frac{\Omega D_s}{KT}$$

Application on P92 tempered martensitic steel



Semi-physical creep modeling approach

Addition of effective velocity (v_{eff}) calculated as the sum of glide + climb velocity contributions

$$\dot{\epsilon} = \frac{\rho_m b v_{eff}}{M(1 - D_{ppt})(1 - D_{cav})}$$

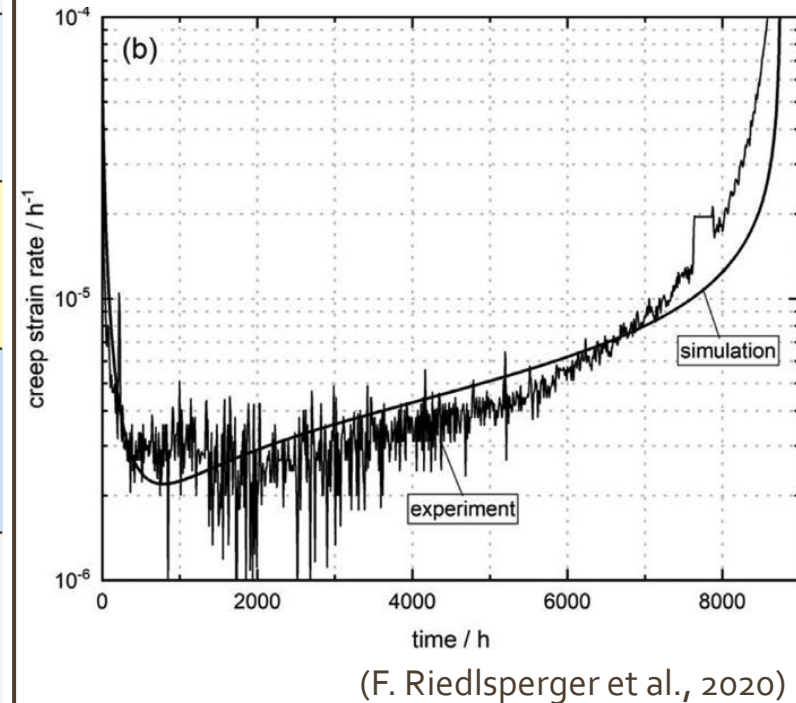
$$\dot{\rho}_m = v_g \left[\rho_m^{3/2} + \frac{\beta \rho_s R_{sb}}{h_b^2} - \frac{\rho_m}{2R_{sb}} - \delta_a (\rho_m^2 - \rho_m \rho_s) \right] - 8 \rho_m^{3/2} v_{cm}$$

$$\dot{\rho}_s = v_g \left[\frac{\rho_m}{2R_{sb}} - \delta_a \rho_m \rho_s \right] - 8 \frac{\rho_s}{h_b} v_c$$

$$\dot{\rho}_b = 8(1 - 2\zeta) \frac{\rho_s}{h_b} v_c - \frac{\rho_b}{R_{sb}} M_{sb} \left[P_{sb} - 2\pi \left(\sum_i r_p^2 i \cdot N_{p_i} \right) \gamma_{sb} \right]$$

$$\dot{R}_{sb} = M_{sb} \left[P_{sb} - 2\pi \left(\sum_i r_p^2 i \cdot N_{p_i} \right) \gamma_{sb} \right] - \mu \eta_v K_c^2 \left[(\rho_m + \rho_s)^{1/2} - \frac{K_c}{2R_{sb}} \right] \frac{\Omega D_s}{2KT}$$

Application on P91 austenitic-martensitic steel



Semi-physical creep modeling approach

The base model is modified to include more complex intragranular precipitate-dislocation interaction terms, and a **diffusional creep rate term**

$$\dot{\epsilon}_{disl} = \frac{\rho_m b v_g}{M(1 - D_{cav})}$$

$$\dot{\epsilon}_{diff} = A_c \frac{D_{gb} \delta_{gb} \sigma_{app} \Omega}{8R_{sb}^3 K_B T}$$

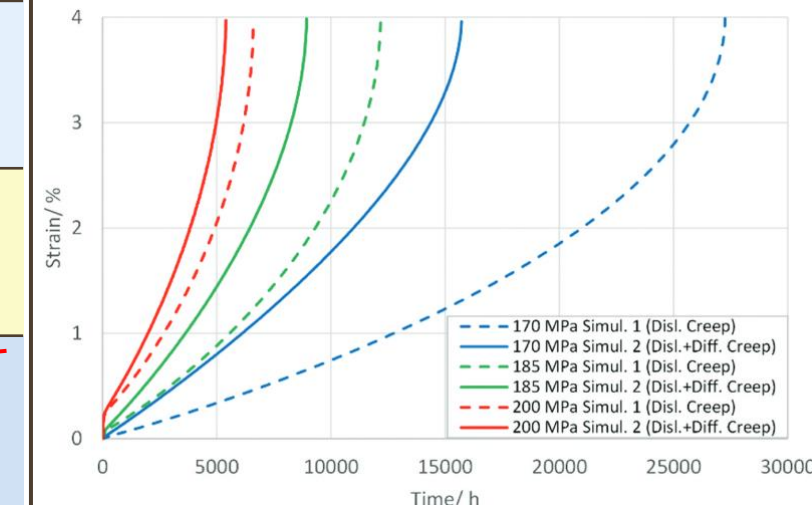
$$\dot{\rho}_m = v_g \left[\rho_m^{3/2} + \frac{\beta \rho_s R_{sb}}{h_b^2} - \frac{\rho_m}{2R_{sb}} - \delta_a (\rho_m^2 - \rho_m \rho_s) \right] - 8 \rho_m^{3/2} v_{cm}$$

$$\dot{\rho}_s = v_g \left[\frac{\rho_m}{2R_{sb}} - \delta_a \rho_m \rho_s \right] - 8 \frac{\rho_s}{h_b} v_c$$

$$\dot{\rho}_b = 8(1 - 2\zeta) \frac{\rho_s}{h_b} v_c - \frac{\rho_b}{R_{sb}} M_{sb} \left[P_{sb} - 2\pi \left(\sum_i r_p^2 i \cdot N_{p_i} \right) \gamma_{sb} \right]$$

$$\dot{R}_{sb} = M_{sb} \left[P_{sb} - 2\pi \left(\sum_i r_p^2 i \cdot N_{p_i} \right) \gamma_{sb} \right] - \mu \eta_v K_c^2 \left[(\rho_m + \rho_s)^{1/2} - \frac{K_c}{2R_{sb}} \right] \frac{\Omega D_s}{2KT}$$

Application on A617 Ni-based alloy



(F. Riedlsperger et al., 2023)

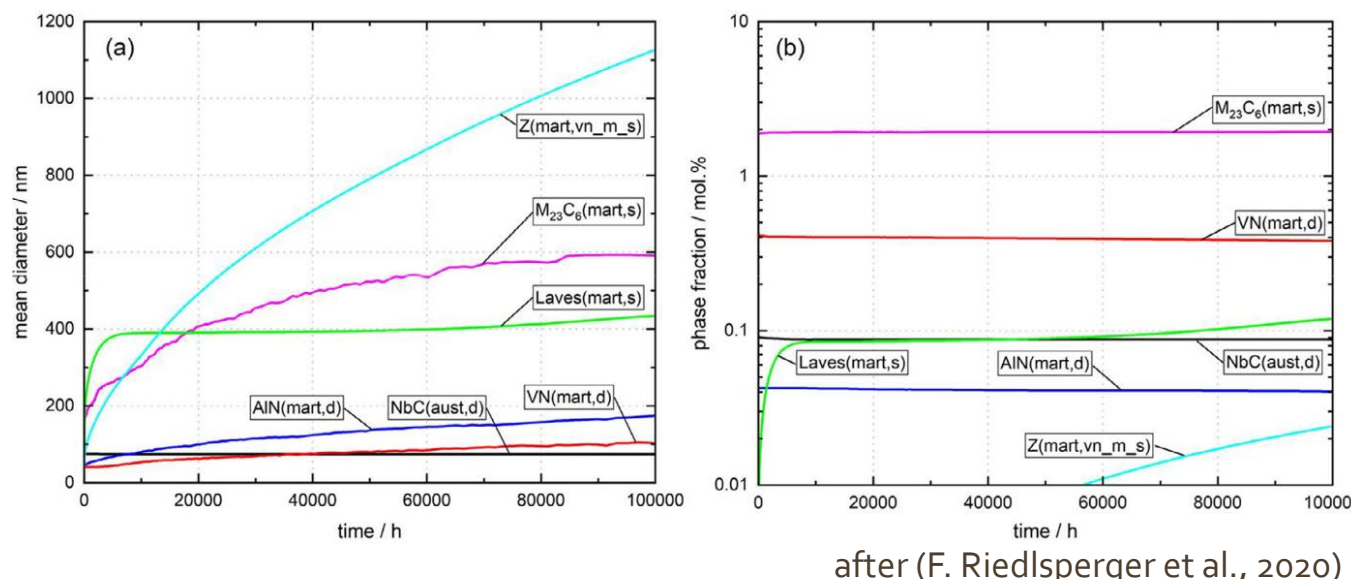
Semi-physical creep modeling approach

Knowledge on the microstructure evolution is mandatory

- Thermodynamic simulations
- Microstructure characterization after (interrupted) tests to validate **precipitate state and kinetic**

- Phase fraction (mol. %)
- Mean diameter (m)
- Nucleation site (dislocation paths, intra- or intergranular,...)?

MatCalc simulations performed for P91 steel



microstructure evolution by 4 physical variables:

ρ_m	Mobile dislocation density	(m ⁻²)
ρ_s	Static dislocation density	(m ⁻²)
ρ_b	Dynamic dislocation density	(m ⁻²)
R_{sgb}	Sub-grain radius	(m)

creep behavior ($\dot{\epsilon}$) is conditioned by their:

- Growth
- Production
- Annihilation
- Transformation

X. Wu law (Grain Boundary + Intragrain events)

Based on strain decomposition
1 D approach

Plasticity law
for instance

$$\varepsilon_p = K \left(\frac{\sigma}{E} \right)^n$$

β microstructure param

D diffusion constant

b Burgers vector

μ shear modulus

r grain boundary precipitate size,

q GB precipitate distribution (1 none,
2 discrete, 3 continuous)

p stress exponent for GB sliding
 Φ shape factor of GB

Elasticity

$$\varepsilon = \left(\frac{\sigma}{E} + \varepsilon_p \right) + \boxed{\varepsilon_{gbs}} + \boxed{\varepsilon_v}$$

Creep

GB sliding , dislocation slip
and climb in presence of precipitates in GB
Creep stage I and II

$$\varepsilon_{gbs} = \varepsilon_0 + \phi \dot{\varepsilon}_{ss} t + \frac{\sigma}{\beta^2 H_{obs}} \left[1 - \exp \left(- \frac{\beta^2 \phi H_{gbs} \dot{\varepsilon}_{ss} t}{\sigma (\beta - 1)} \right) \right]$$

$$\dot{\varepsilon}_{ss} = \varphi (1 - \beta^{-1}) \frac{D \mu b}{kT} \left(\frac{b}{d} \right)^q \left(\frac{l+r}{b} \right)^{q-1} \frac{\sigma (\sigma - \sigma_{ic})}{\mu^2}$$

σ_{ic} threshold value

σ

d grain size

k Boltzman constant

H_{gbs} GB hardening coeff

l grain boundary precipitate spacing

effective stress introduced

Dislocation climb and multiplication, intragranular deformation

Creep State III

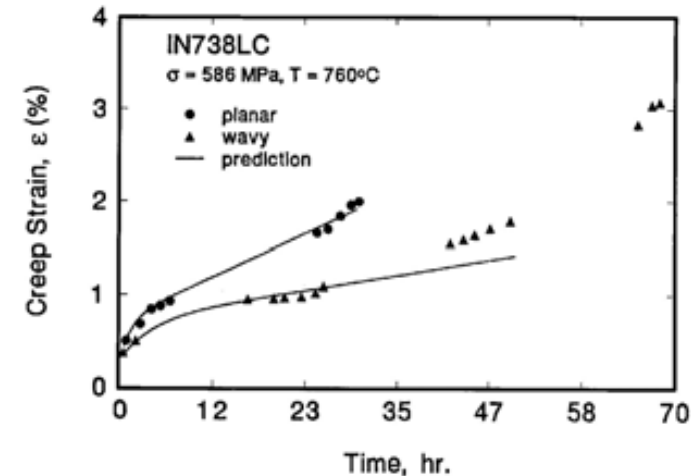
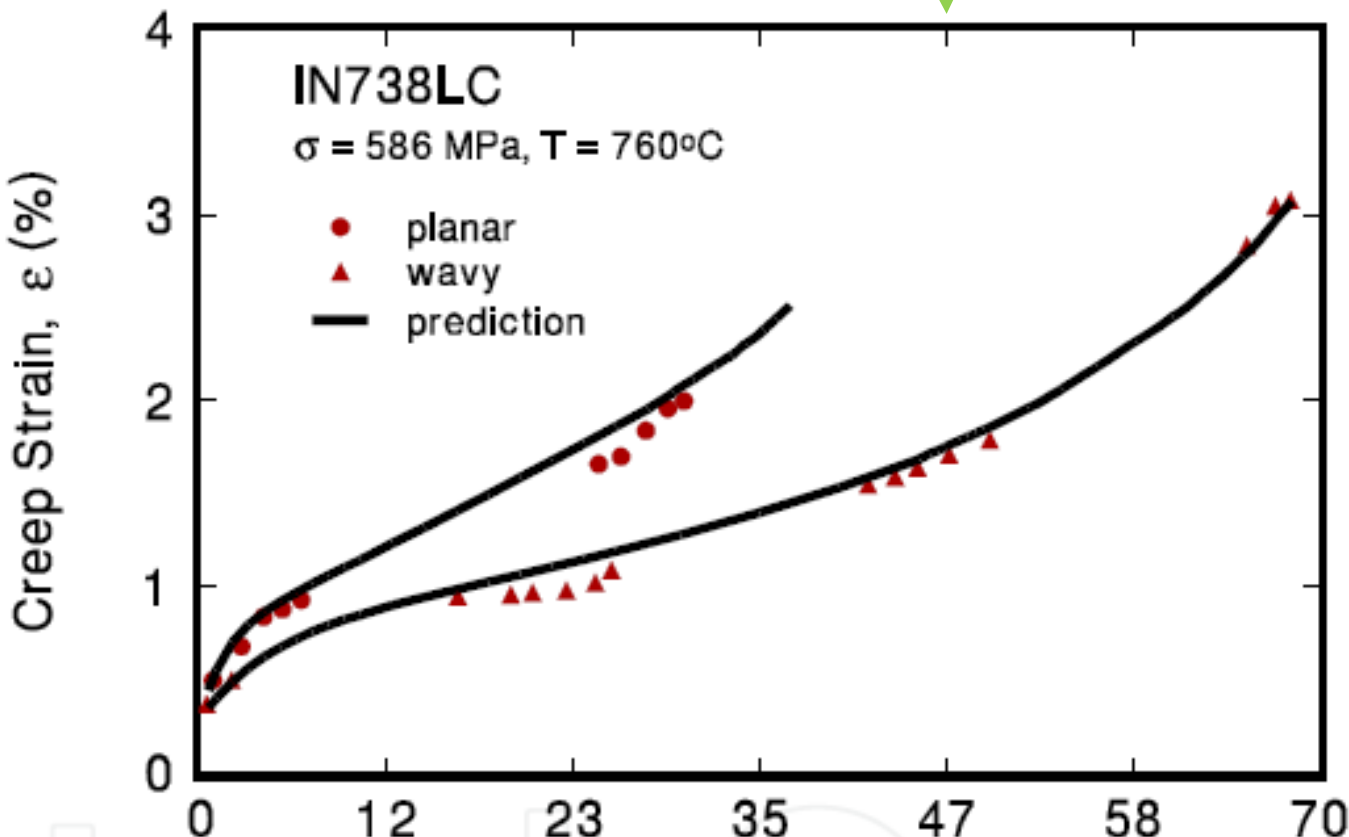
$$\varepsilon_v = \frac{1}{M} [\exp(M \dot{\varepsilon}_v t) - 1]$$

"M dislocation multiplicator factor?"
→ Taylor factor

Each eq. is related to dislocation genesis and movement

Application of X.Wu creep law

$$\dot{\epsilon} = \left(\frac{\sigma}{E} + \dot{\epsilon}_p \right) + \dot{\epsilon}_{gbs} + \dot{\epsilon}_v$$



1. Only GB effect

Wu, X.J. & Koul, A.K.
(1996). Modelling creep
in complex engineering
alloys. In: *Creep and
Stress Relaxation in
Miniature Structures
and Components*, pp. 3-
19. The Metallurgical
Society, Warrendale, PA.

2. GB effect
+ precipitate
dislocation
interaction intra
granular

A lack according S. Wu:
contribution of creep cavitation (Acta Mat 2022)

→ Deeper in creep mechanism understanding

Additive or Cast & Wrought Incoly 718 → ≠ creep behavior

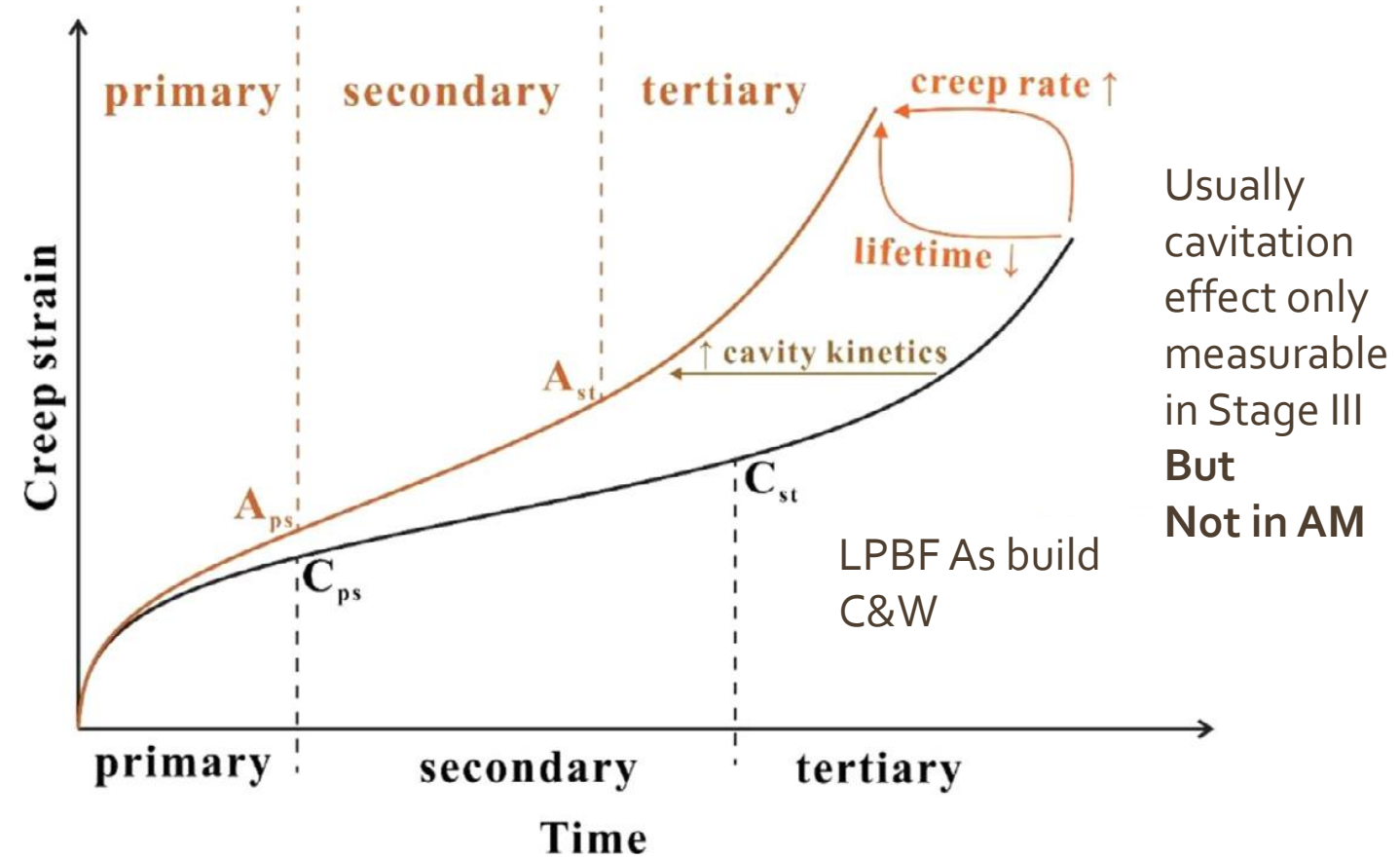
X. Wu, Kock-Mecking-Estrin...

OK for dislocation motion or grain boundary sliding
(if the cavitation kinetics slow)

If cavity density or formation is high,
→ + cavitation creep strain contribution

In AM materials

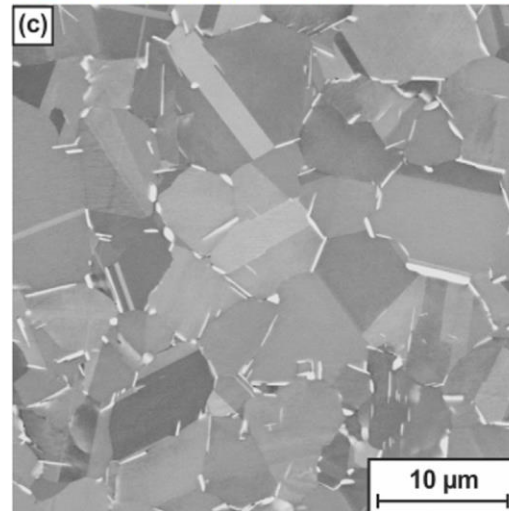
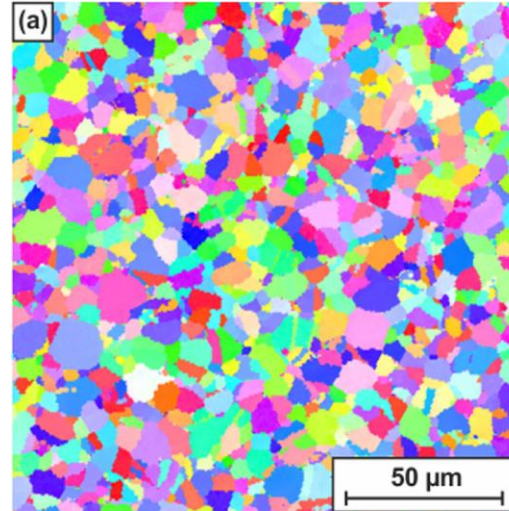
- High density of vacancies, high porosity
- Compositional inhomogeneity
- Grain anisotropy
- Out of equilibrium microstructure, so evolving with T and t



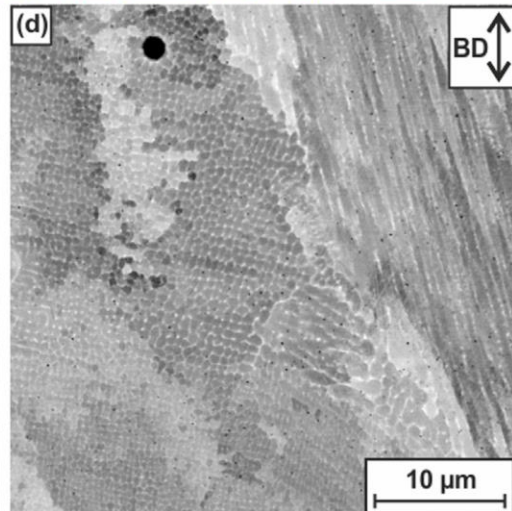
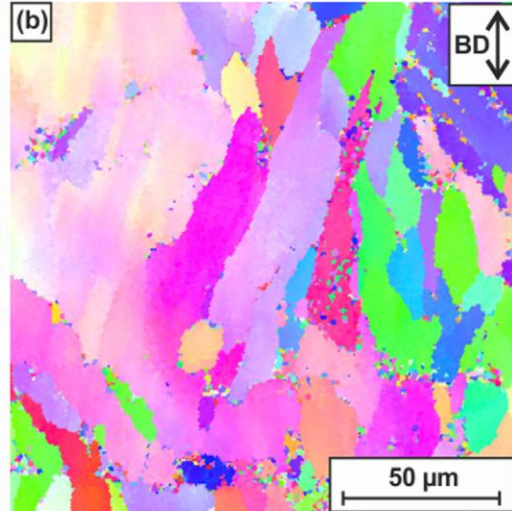
Creep behavior of heat treated Inconel 718 ? Which microstructure ?

Completely
recrystallized
Average
grain $7 \mu\text{m}$

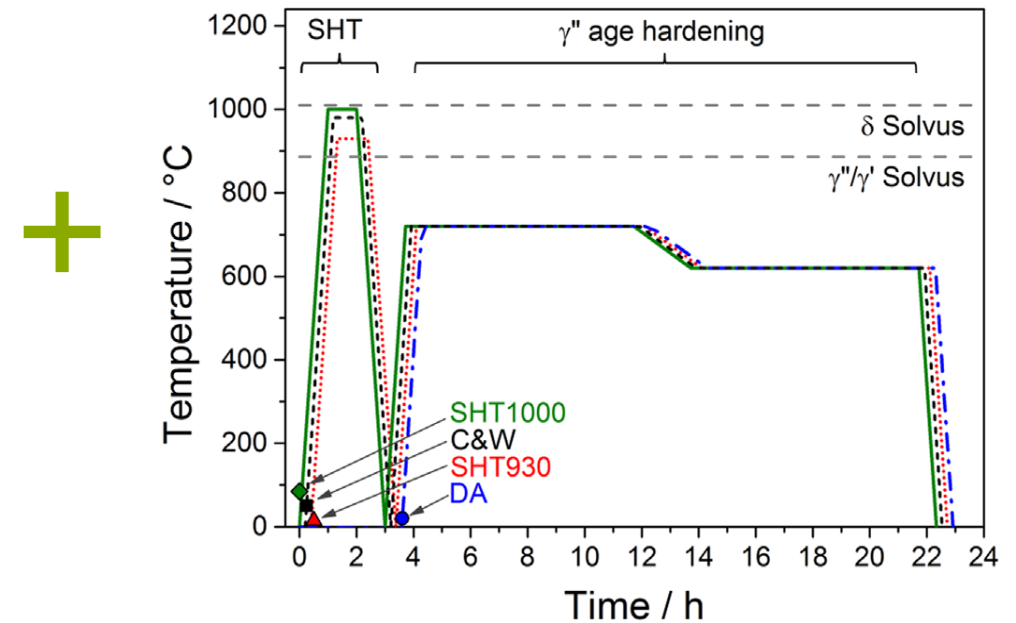
Cast & Forged (C&W)
+ 1.5h 980°C + Aging



As built LPBF



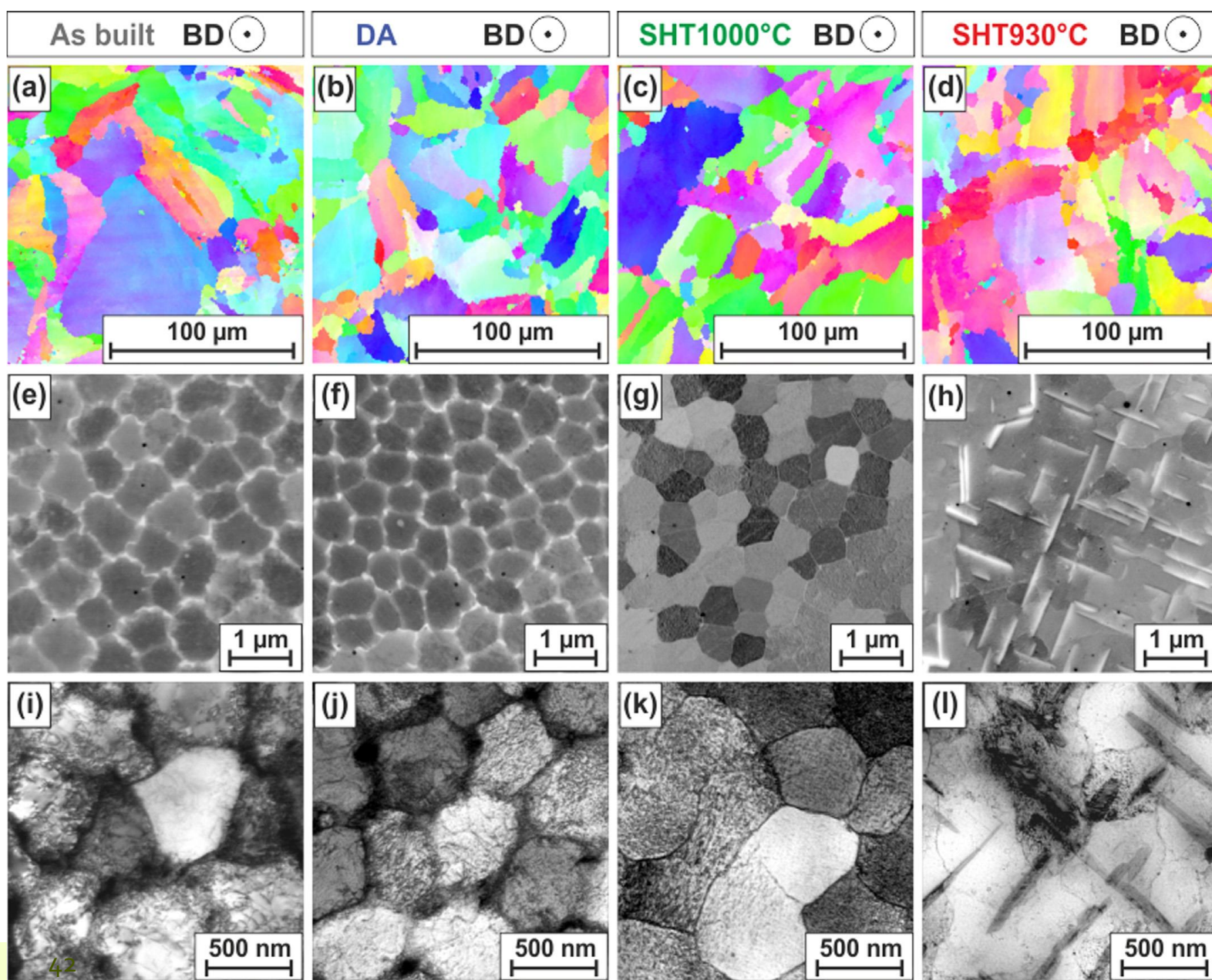
1st example



Fine dendrites
with spacing $< 1 \mu\text{m}$

(SHT Solution Heat Treatment)

Inconel 718: Microstructures LPBF + heat treatment



No γ' γ''

AS built

Aged

γ' a lot
 $\gamma'' \neq$ amount

SHT 1000°C
+ Aged

SHT 930°C
+ Aged

A lot of δ
Intra granular (fine)
+ in High Angle GB (thicker)

Interdendritic region
(rich in Nb) + Lave 14
+ High dislocation
density around subgrain
No δ

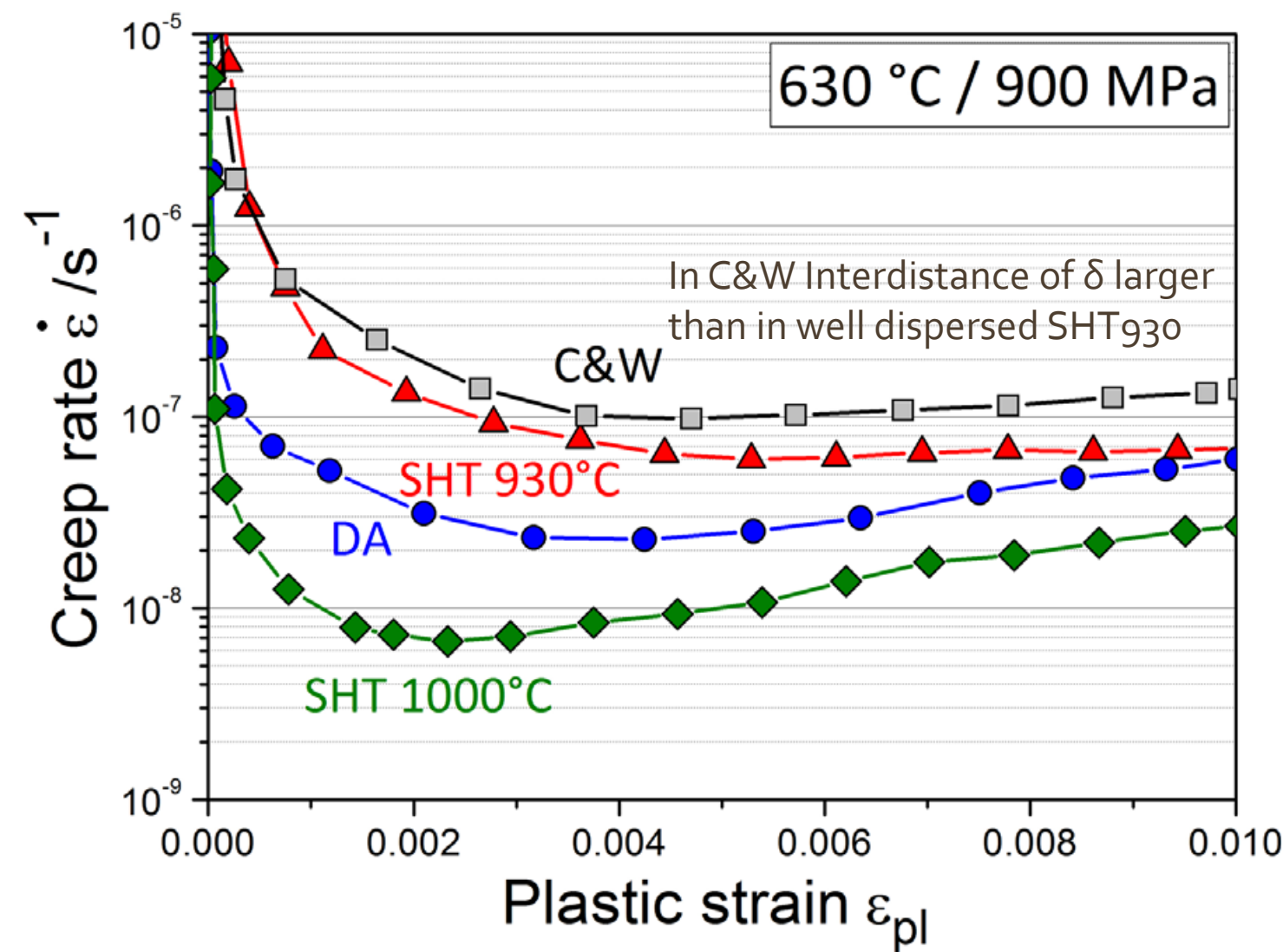
Nearly no δ

Subgrain size \simeq ct 0.6 µm

Pröbstle et al MSEA 2016

Creep behavior of Inconel 718 LPBF + heat treatment

Experiments: compression 630°C
(TP such that no over aging and strong
micro. evolution like recrystallisation)



γ'' --> creep strength
different amount and length

δ (high Nb) \rightarrow less γ' γ''
+ Thick $\delta \rightarrow$ vacancy nucleation
 \rightarrow SHT 930 not optimal

Laves (high Nb)
 \rightarrow less γ' γ'' but higher than SHT 930
 \rightarrow Aged state better

No δ , no Laves, low dislocations
Larger γ'' size in addition to higher volume
But sub grains less stable

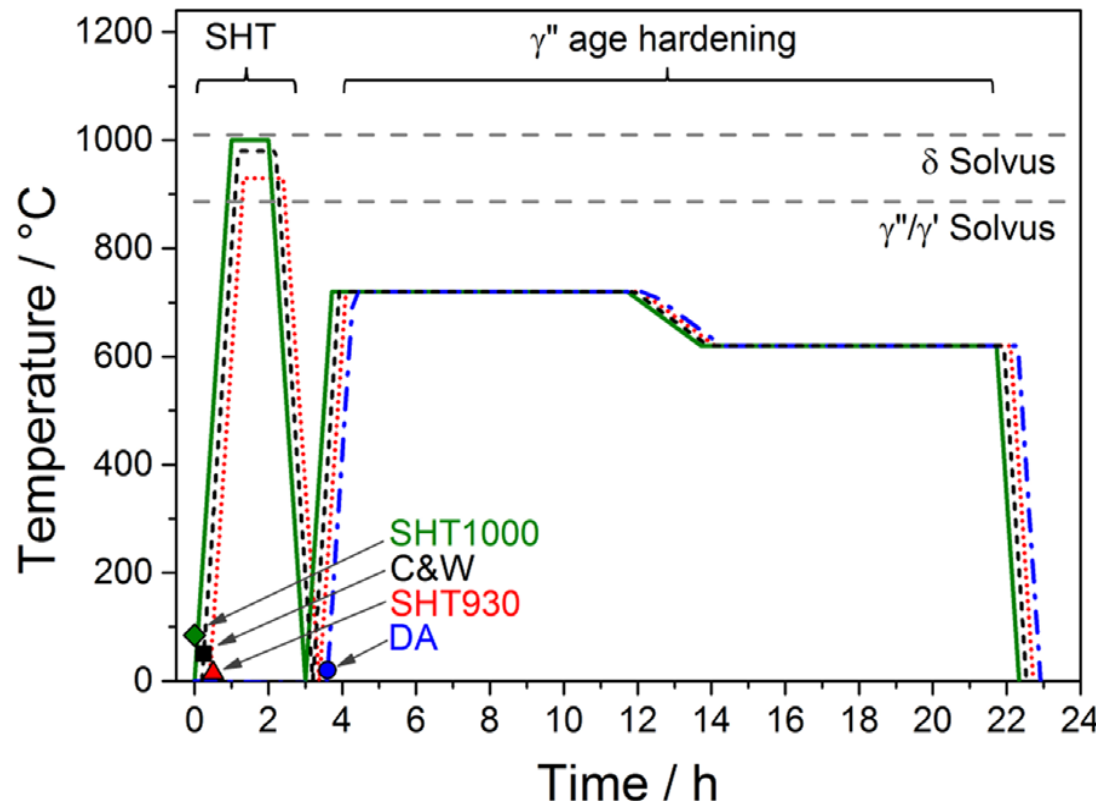
LPBF Subgrain size \simeq ct at 630°C

Sub grain generated by high creep stress
will be smaller

Creep behavior of Inconel 718 LPBF + Post Heat treatments

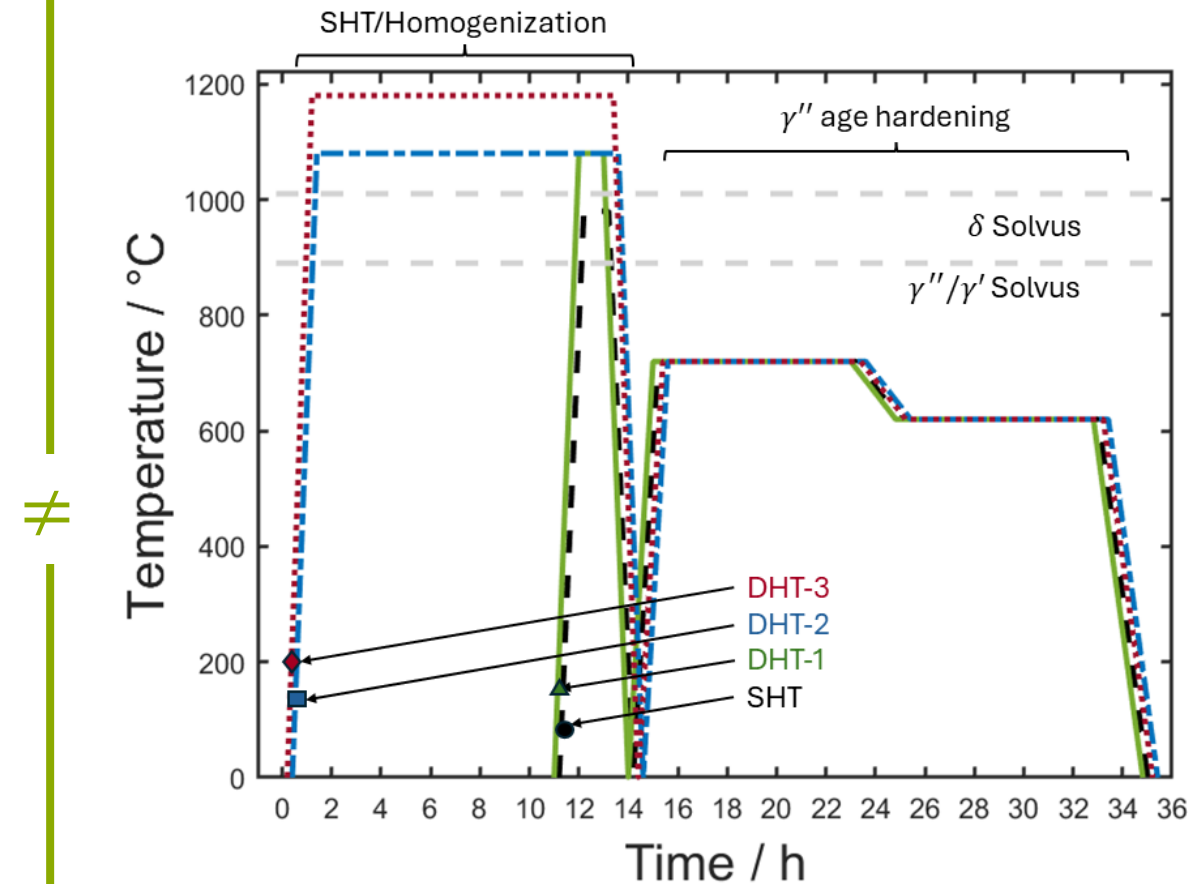
2nd example

Experiments: tension 630°C
(strong micro. evolution like recrystallisation)



Creep tests
Compression

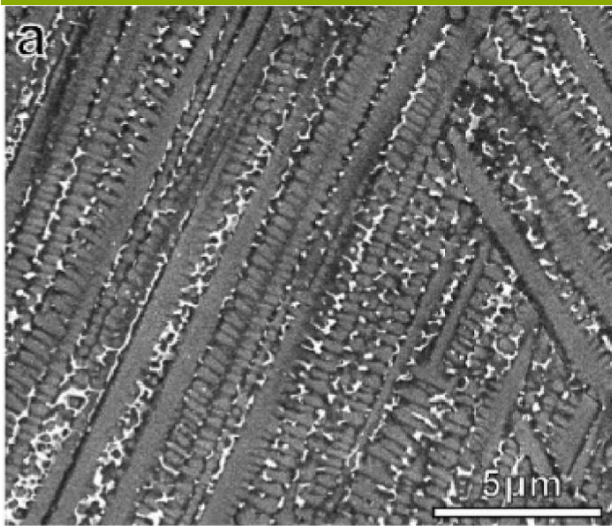
Pröbstle et al. MSEA 2016
LPBF 175W 620mm/s



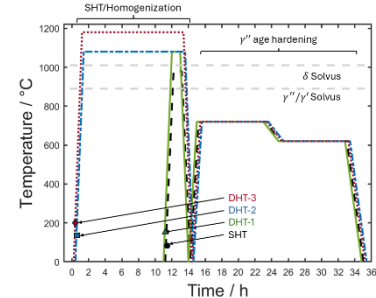
All DHT are performed $> 1050^\circ$
→ recrystallisation and no more subgrains
according. Zhang MSEA 2015

DHT
designed heat
treatment

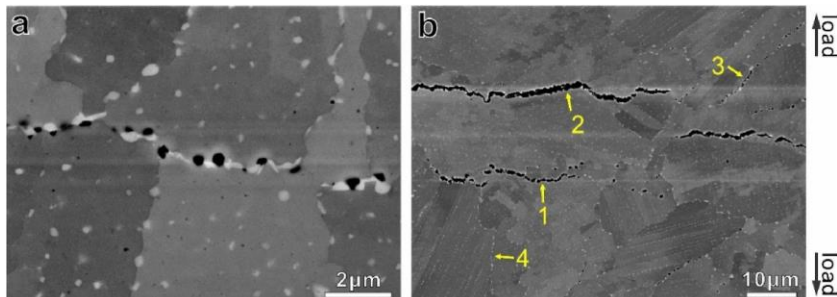
Inconel 718: Microstructures LPBF+ Heat Treatment



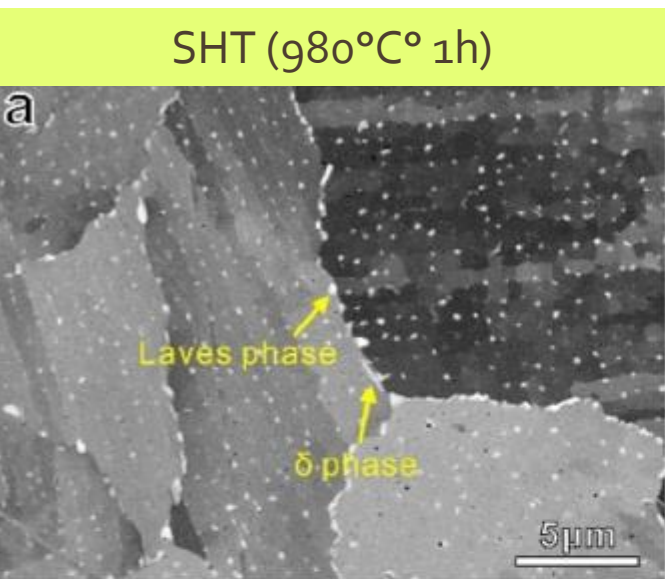
Dendritic structure and
inter-dendritic Laves phase
LPBF manufacturing param: 285 W
laser power, 960mm/s scan speed



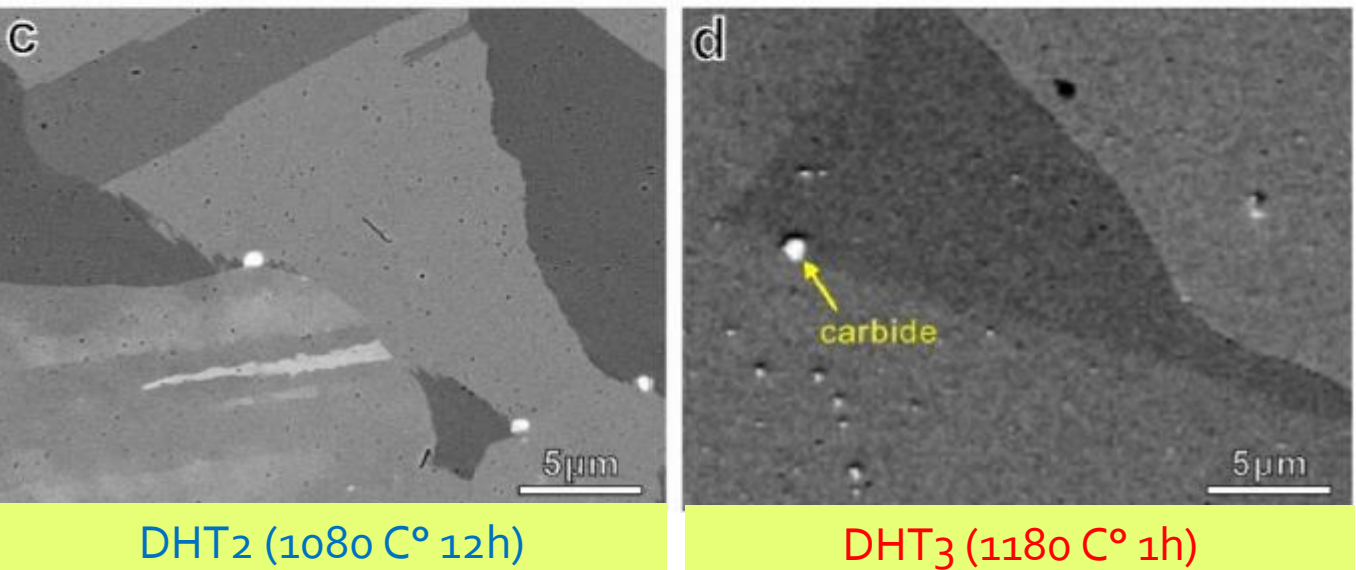
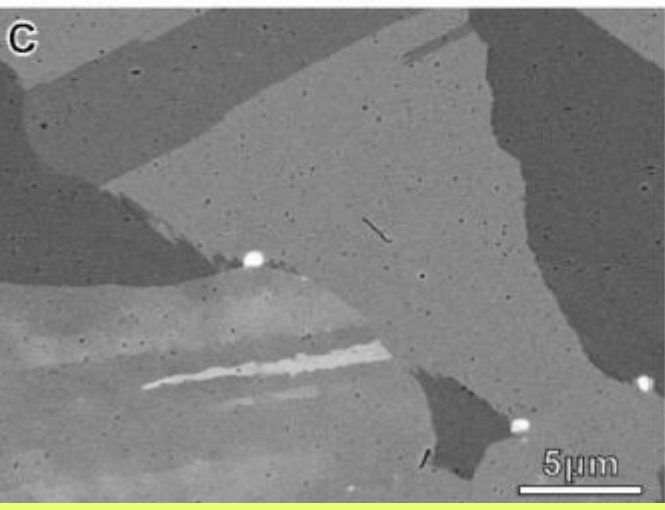
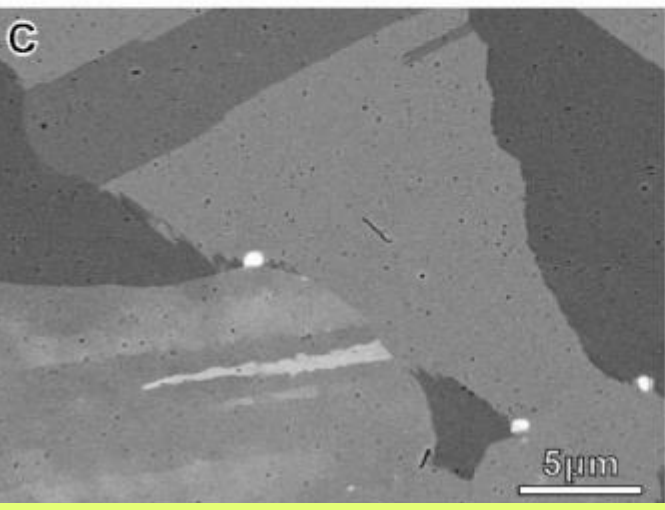
GB particles dissolution → cavity nucleation
(mostly in GB \perp building dir.)



Laves + δ in GB



Laves + δ in GB \downarrow , NbC present,



Laves + δ disappear GB, NbC present

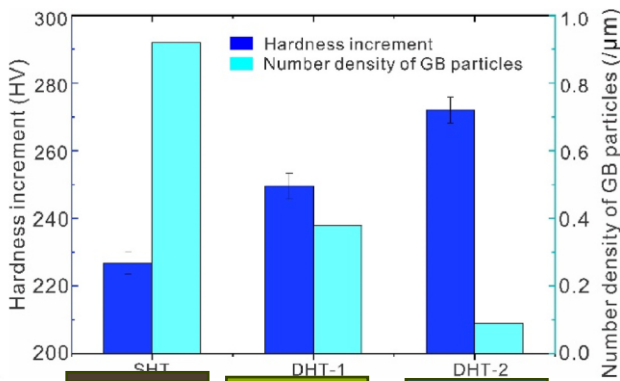
Inconel 718: Microstructures LPBF+ Heat Treatment

SHT, **DHT₁**: columnar grain structure
low angle GBs
Grain aspect ratio ≈ 3.26

DHT₂ and **DHT₃**:
recrystallized equiaxed grains
high angle GBs
Grain aspect ratio ≈ 1
high fraction of annealing twins
(effect higher for **DHT₂**
grain growth decreases them)

DHT₂: average grain size $80\mu\text{m}$

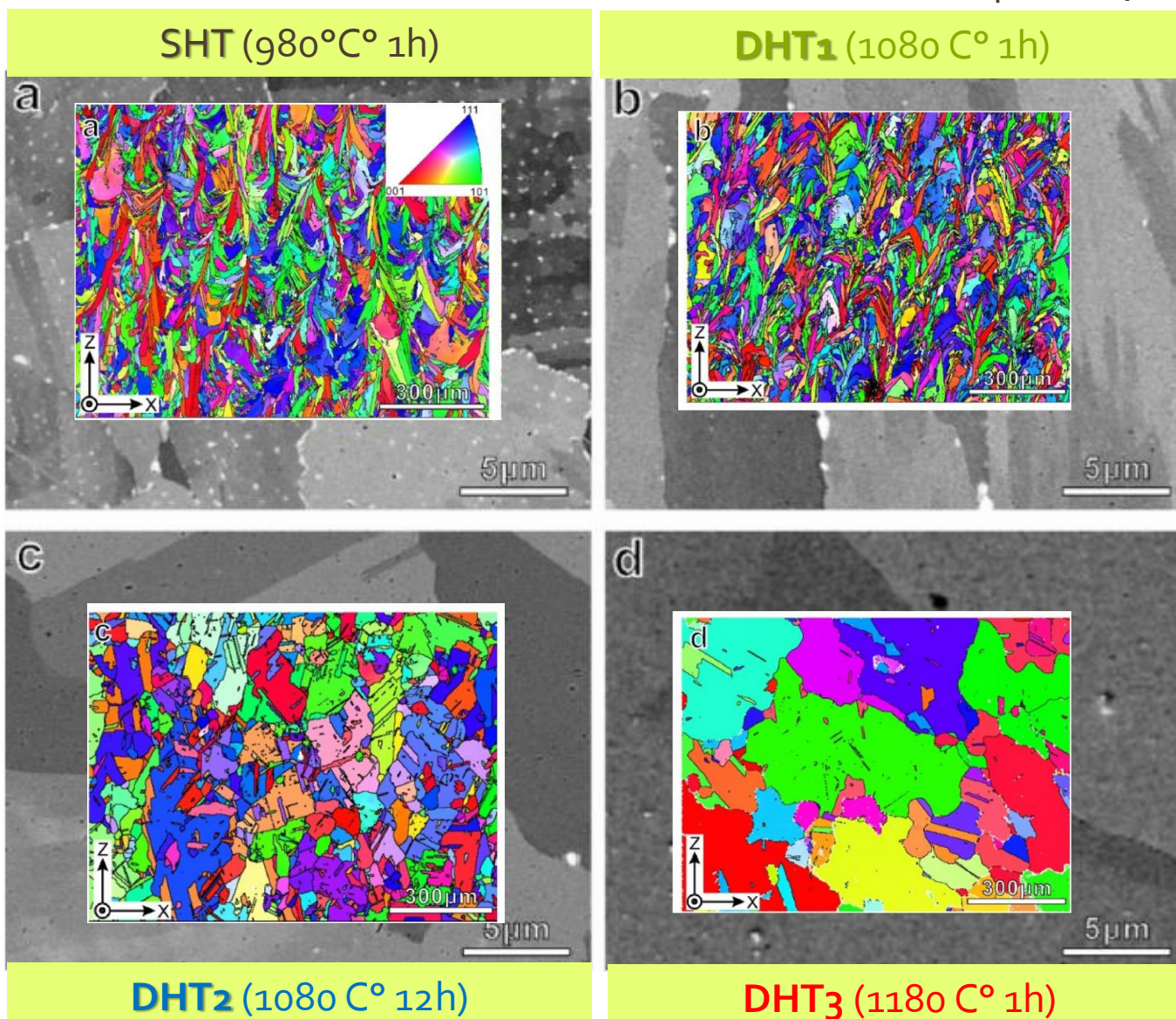
DHT₃: average grain size $\approx 80\mu\text{m}$



$$\gamma'' \propto \text{hardness}$$

Related to
dissolution of GB
particles

Laves + δ in GB



Creep behavior of Inconel 718 : S. Wu model

$$t_r \propto 1/(N_p + N_{gb})$$

N_p potential nucleation site density \approx GB particle density well oriented
→ grain shape effect !!!

N_{gb} triple points and GB ledge density
(identified from difference between SHT and DHT1)

$$\dot{\epsilon}_m^c \propto \frac{\emptyset_m \lambda_m}{h} \sinh\left(\frac{\sigma b^2 \lambda_m}{MkT}\right)$$

\emptyset_m Volume fraction precipitate

λ_m Average dislocation glide distance

h Dislocation climb distance against precipitates

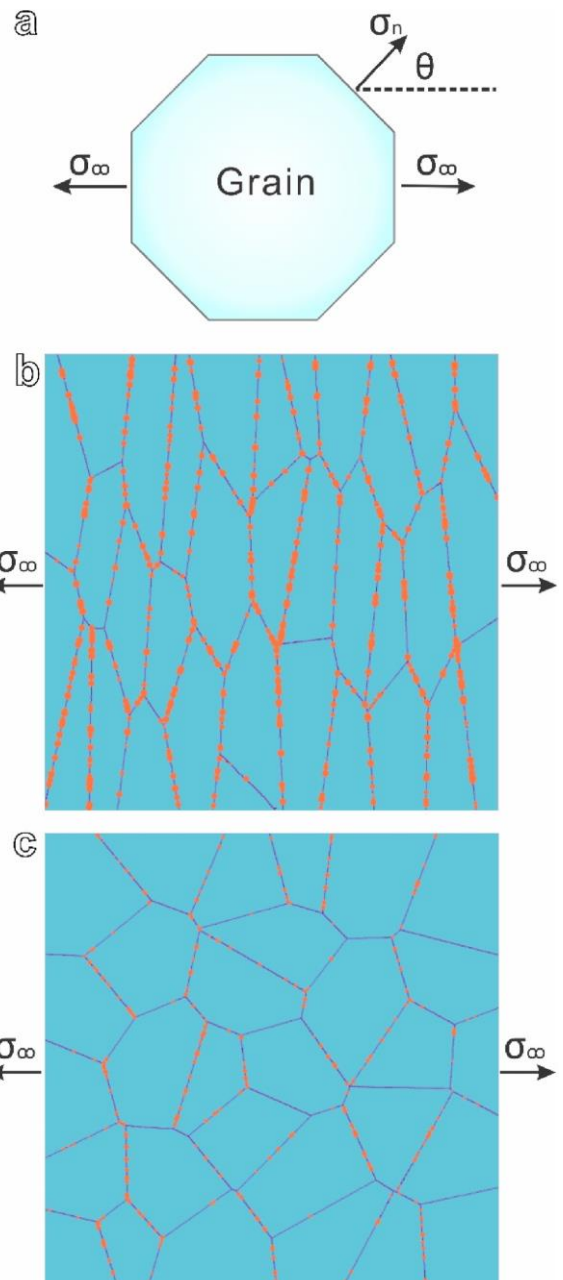
b Burgers vector

M Taylor factor

effect of GB particles (SHT>DHT₁>DHT₂ & DHT₃)

γ'' density - intra granular effect (larger in DHT₂ & DHT₃>DHT₁>SHT)

Grain shape (Larger in SHT and DHT₁ + anisotropy) as cavitation if orientation of GB OK

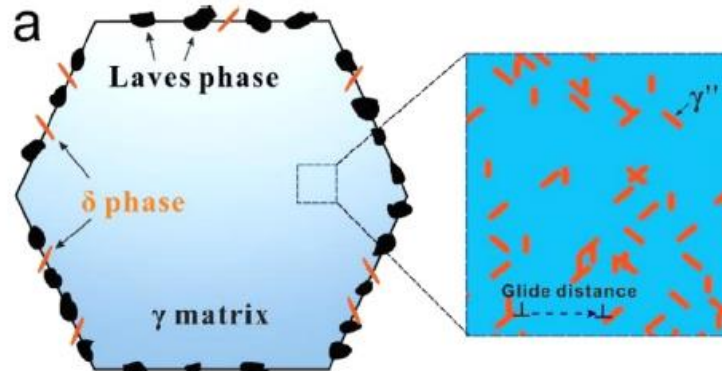


Creep behavior of Inconel 718 : S. Wu model

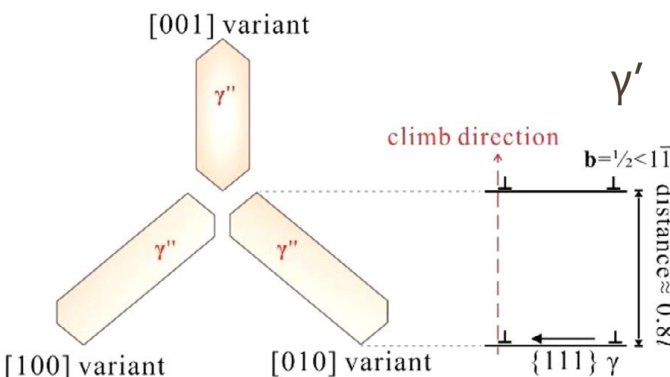
Total set of equations to model

- Dislocation motion (glide + climb) and GB sliding
- Cavitation kinetics

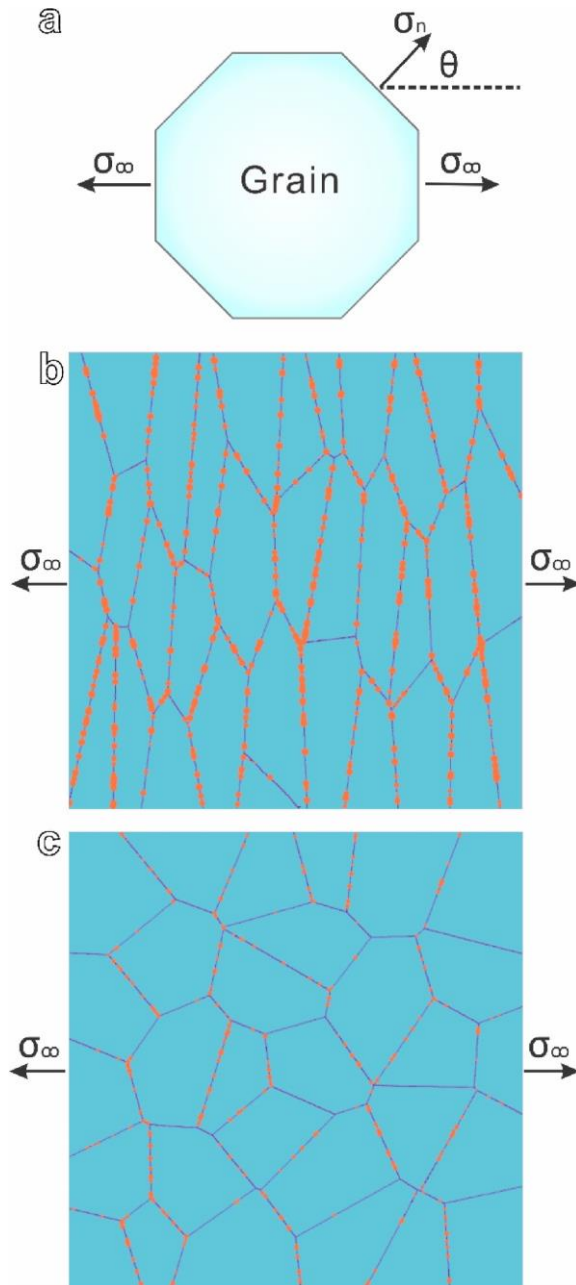
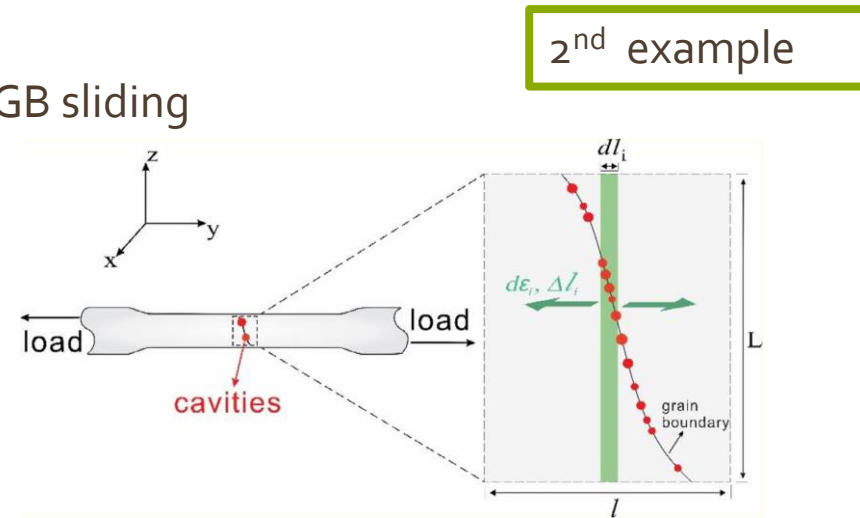
Concept of effective stress due to damage
Idealized Microstructure



3 Variants of γ''



Estimation of climb distance for dislocation



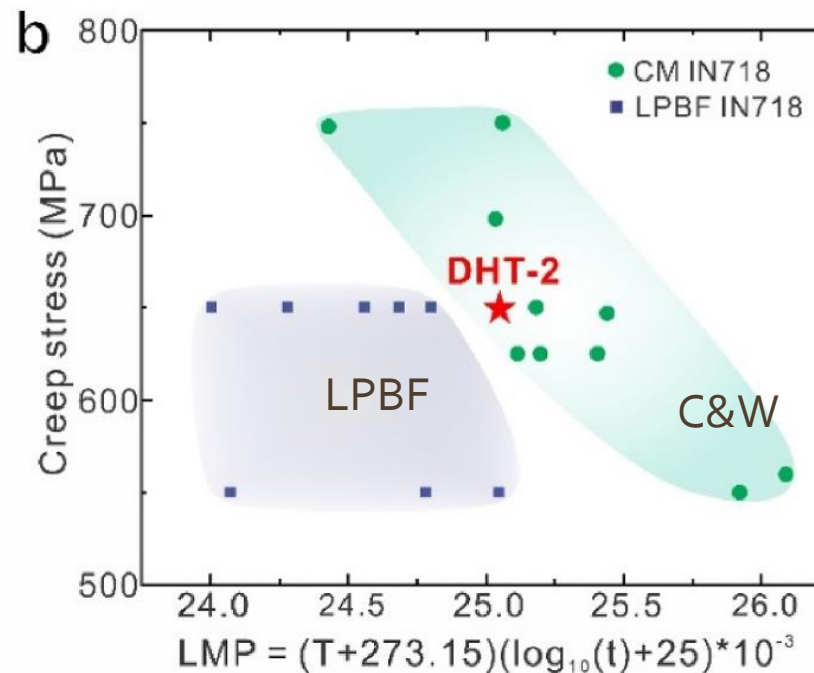
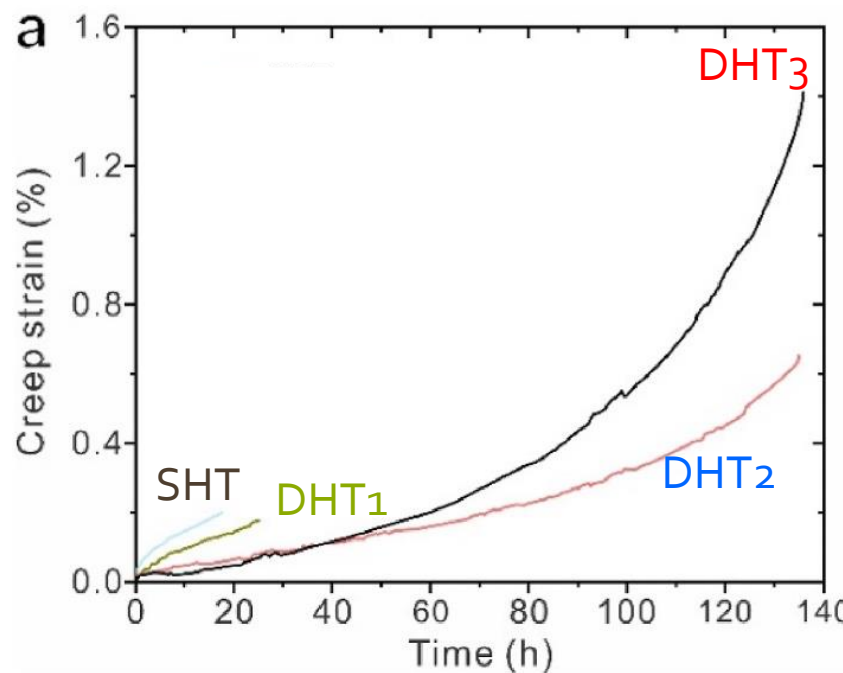
Creep behavior of Inconel 718 LPBF + heat treatment

Experiments: tension 630°C
(strong micro. evolution like recrystallisation)

Which dominant mechanism ?

GB sliding dominant creep mechanism (cavity formation at triple junction points)

Dislocation dominant creep mechanism (cavity formation due to dislo pile up at GB or GB ledge or at subgrains boundary)



T_r of DHT₂ = DHT₃
→ GB non dominant mechanism
as strong different grain size
 $80 \rightarrow 280 \mu\text{m}$

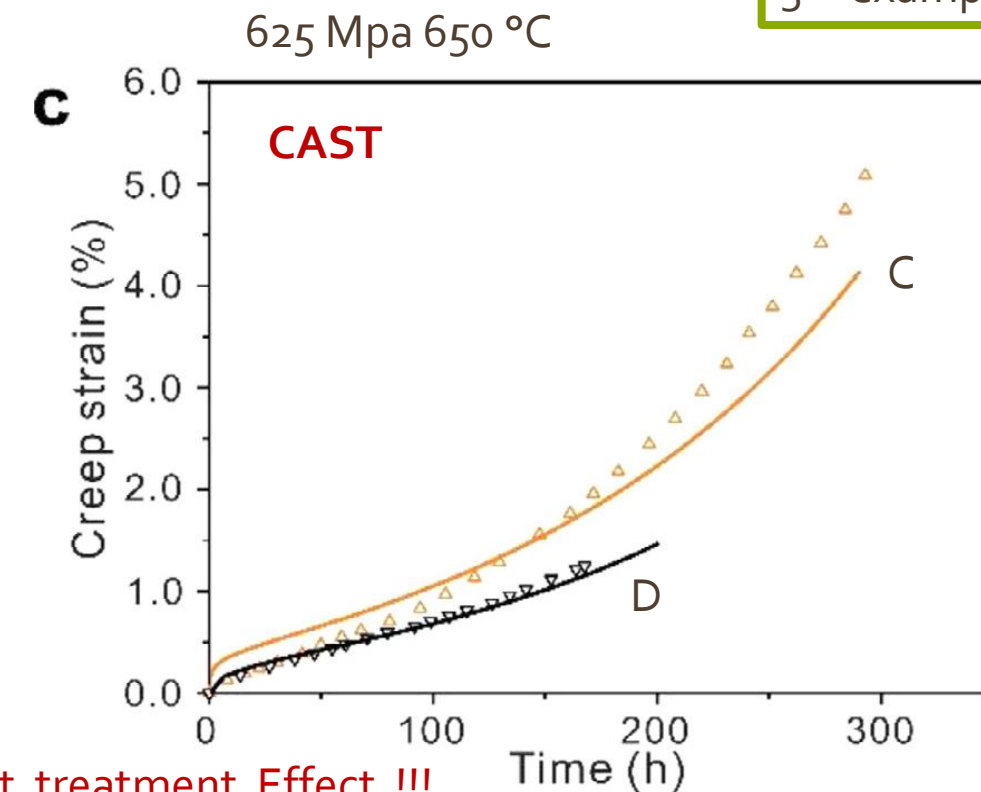
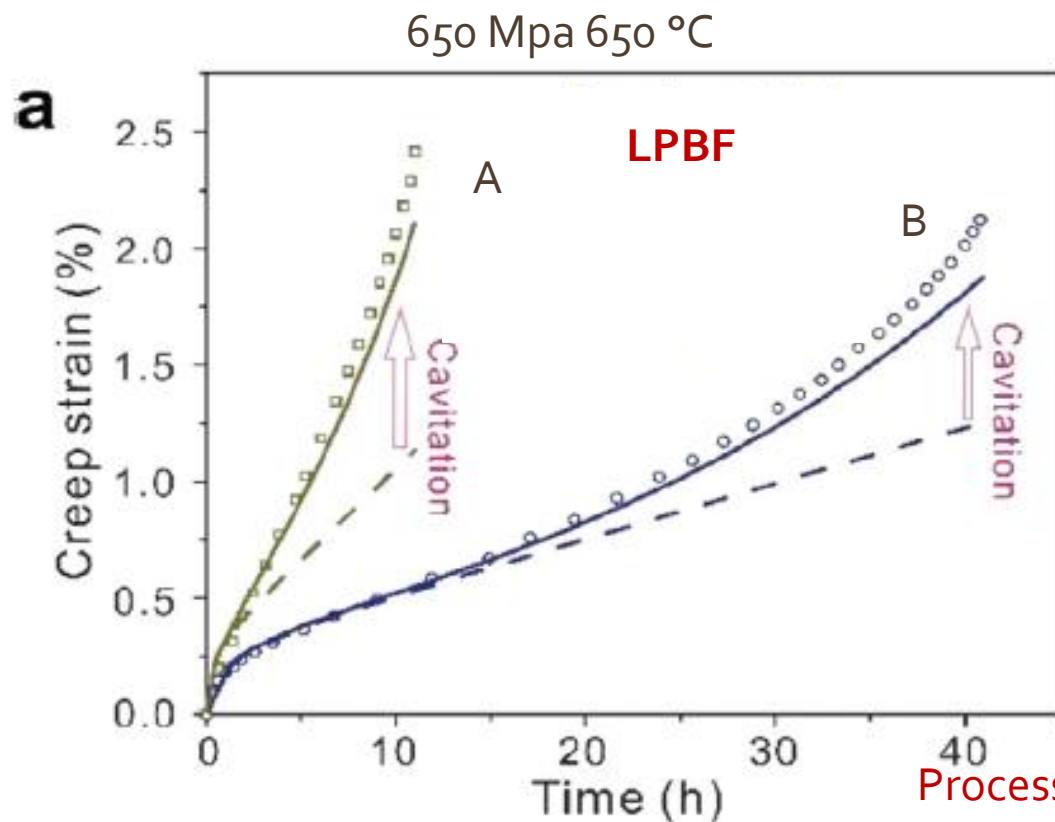
Dislocation glide-climb
=main mechanism

Cavitation \propto GB particle number

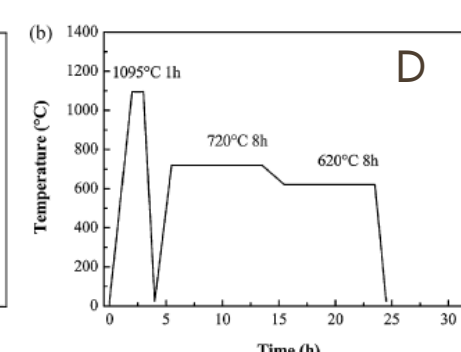
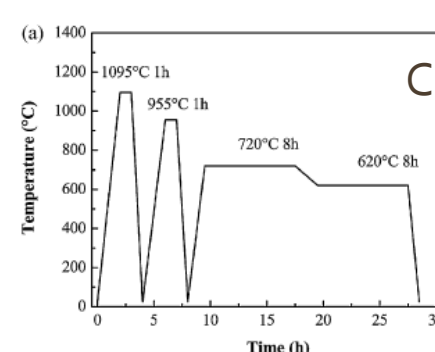
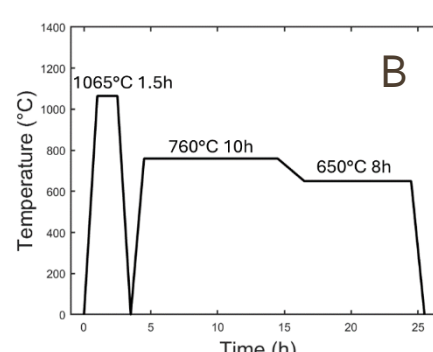
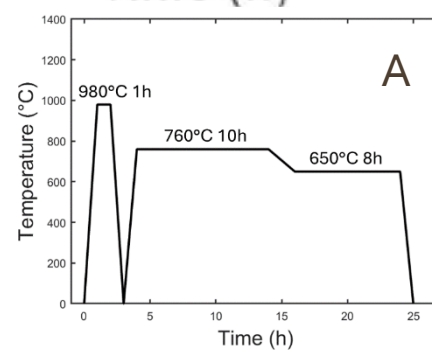
SHT > DHT₁ > DHT₂

Creep behavior of Inconel 718: S. Wu model's result

3rd example



Prediction
--- without cavitation
— with cavitation
Experiment 0 0 0 0 0



Contents

- Introduction
- **Phenomenological approaches**
 - Scalars
 - Larson Miller etc...
 - Curves and constitutive laws FE
 - Norton
 - Graham Wales
- **Micro physical based approach**
 - The basis
 - Incoloy 718 application
- **Fatigue-Creep, Dwell effect and FE Morch constitutive macro law**
- Nitriding effect
- AID4Greenest EU project ...

Solar receivers - Walloon Region projects (Experiments + Modeling)



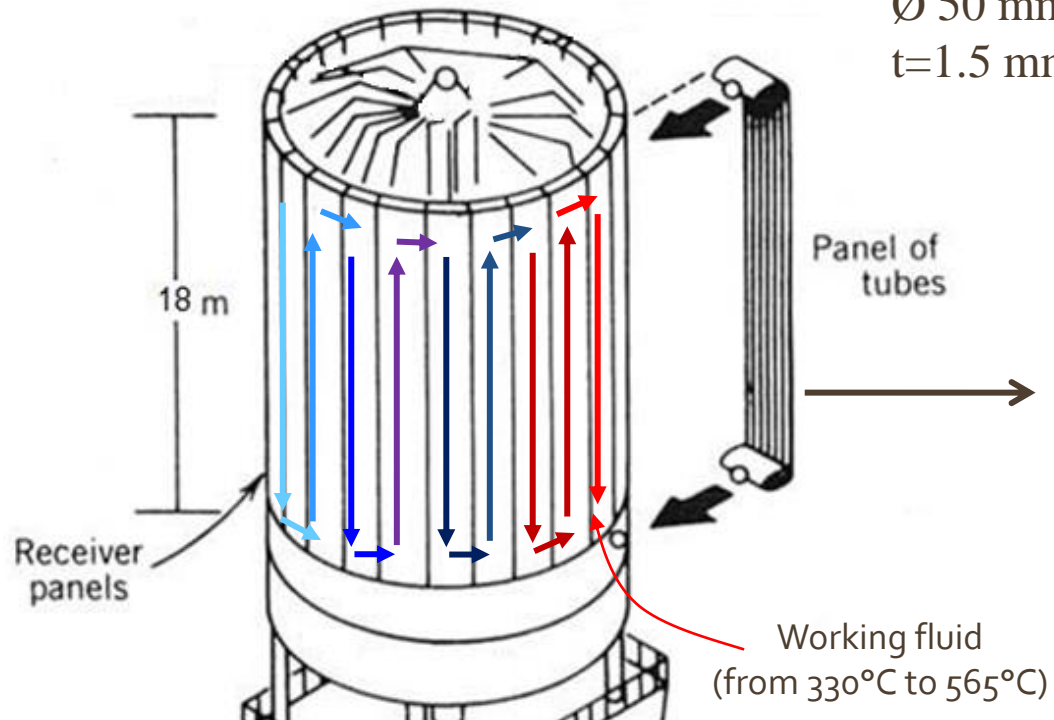
LIÈGE université
Sciences Appliquées



LITHCOTE



RÉGION WALLONNE
DE BELGIQUE



Solar receiver
(source : W.B.Stine, R.W.Harrigan,
Solar Energy Systems Design)

Tube:
 $\varnothing 50 \text{ mm}$
 $t=1.5 \text{ mm}$



Panel of tubes manufactured from nickel
alloy sheet (Haynes 230)
(source : CMI Solar)

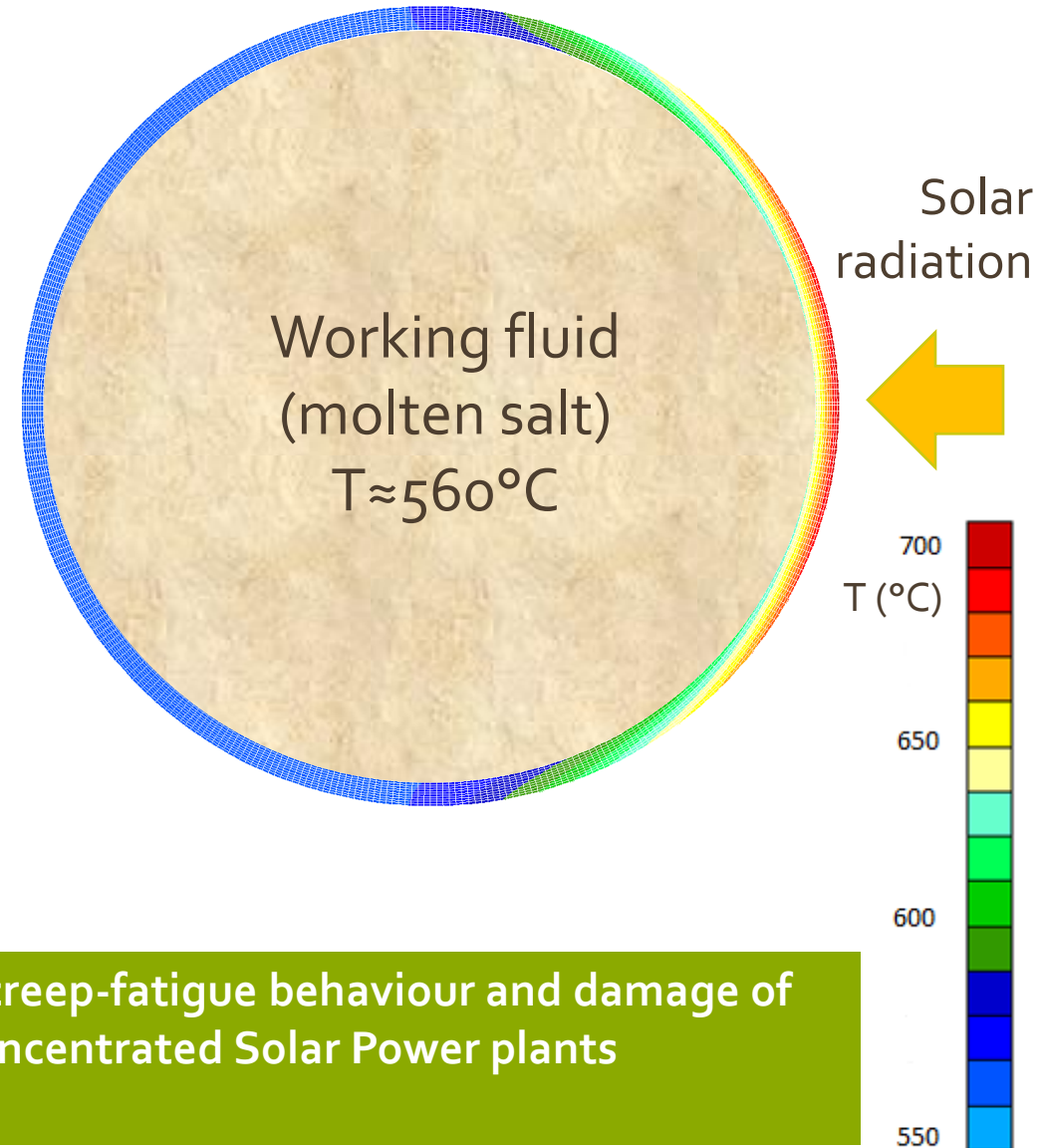


The tubes

Temperature distribution in a tube
(Lagamine FE code)

- Fatigue + creep
- Extreme Thermo-mechanical loading
(Haynes 230)
- Advanced model

Thermomechanical modelling of the creep-fatigue behaviour and damage of Nickel-alloy receiver tubes used in Concentrated Solar Power plants
Morch, Hélène PhD Uliege 2022

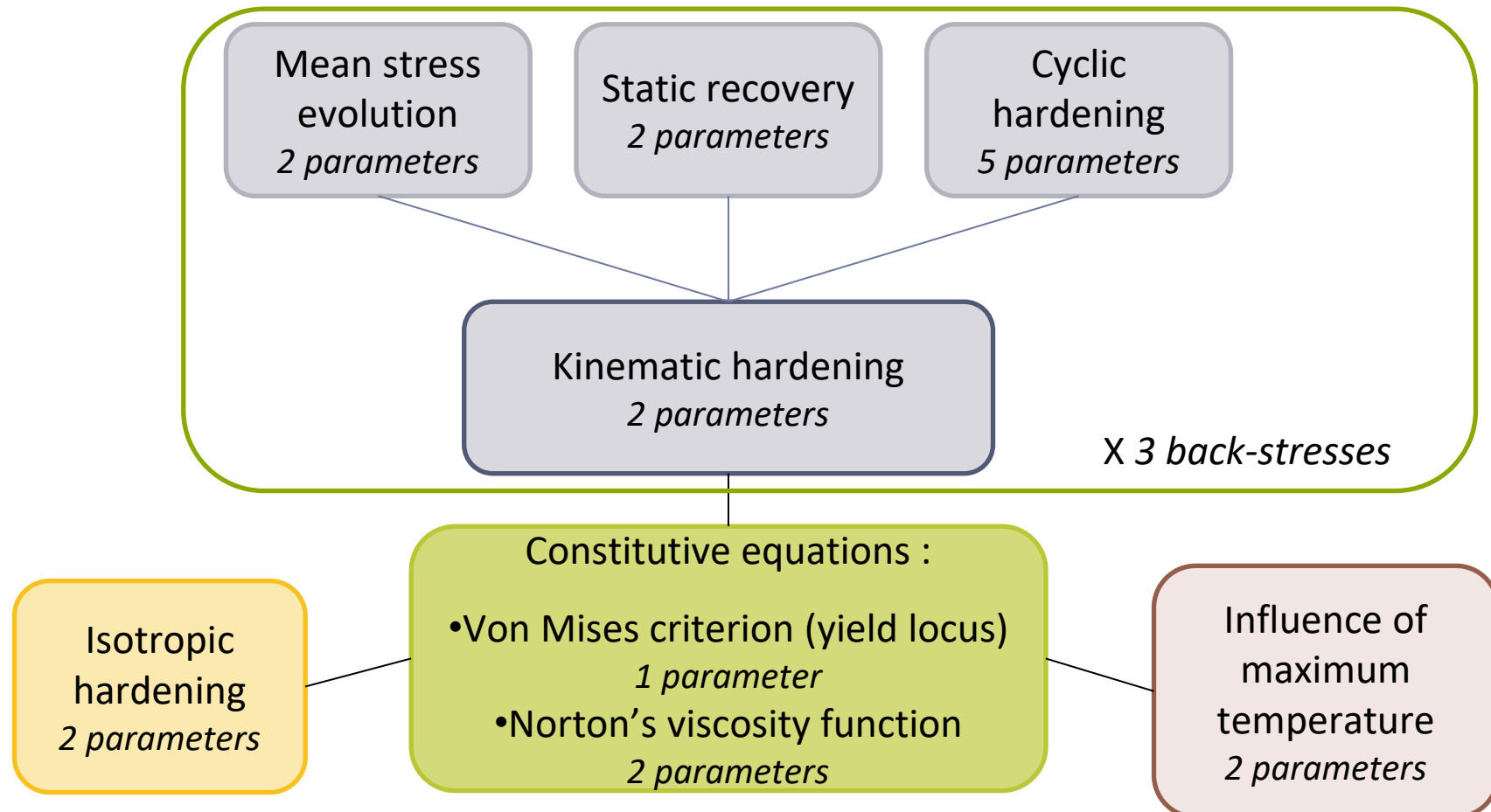


“Morch law”

Advanced damage Chaboche coupled model

Effect of tensile and compressive hold times on the rupture behavior of nickel-based alloy 230 at 700°C submitted... Mørch et al.

31 Equations
to solve...



²⁸
→ 40 parameters → Efficient temperature dependence of parameters for thermo-mechanical finite element modeling of alloy 230 Mørch et al. European Journal of Mechanics – A/Solids, 85, p. 104-116

Morch law: 1st version uncoupled , 2nd coupled... D_{creep} + D_{fatigue}

Isotropic EVP model

$$\underline{\varepsilon} = \underline{\varepsilon}^{\dot{\varepsilon}l} + \underline{\varepsilon}^{vp} + \underline{\varepsilon}^{th}$$

$$\underline{\sigma} = \underline{\underline{E}} : \underline{\varepsilon}^{\dot{\varepsilon}l}$$

$$\underline{\dot{\sigma}} = \underline{\underline{E}} : \underline{\dot{\varepsilon}}^{\dot{\varepsilon}l} + \dot{\underline{\underline{E}}} : \underline{\varepsilon}^{\dot{\varepsilon}l}$$

$$f = \|\underline{\sigma} - \underline{X}\| - \sigma_0 - R \leq 0$$

Viscous stress

$$\sigma_v = f > 0$$

Viscosity Norton

$$\dot{p} = \left\langle \frac{\sigma}{K} \right\rangle^*$$

$$A vec : \dot{p} = \sqrt{\frac{2}{3}} \underline{\varepsilon}^{vp} : \underline{\varepsilon}^{vp}$$

Or Graham Wales

Kinematic hardening

$$\hat{\underline{X}} = \sum_{i=1}^{nAF} \hat{\underline{X}}_i$$

$$\dot{\hat{\underline{X}}}_i = \frac{2}{3} C_i \underline{\varepsilon}^{vp} - \gamma_i (\hat{\underline{X}}_i - Y_i) \dot{p}$$

Static recovery

$$\hat{\underline{X}}_i = \dots - b_i \|\underline{X}_i\|^{r_i-1} \hat{\underline{X}}_i$$

TP^o effect

$$\hat{\underline{X}}_i = \dots + \frac{1}{C_i} \frac{\partial C_i}{\partial T} T' \hat{\underline{X}}_i$$

Mean stress Effect

$$\dot{\underline{Y}}_i = -\alpha_{b,i} \left(\frac{3}{2} Y_{st,i} \frac{\hat{\underline{X}}_i}{\|\underline{X}_i\|} + \underline{Y}_i \right) \|\underline{X}_i\|^r$$

Cyclic Hardening

$$\dot{\gamma}_i = D_{\gamma i} (\gamma_i^0 - \gamma_i) \dot{p}$$

$$\gamma_i^0 = a_{\gamma i} + b_{\gamma i} e^{-c_{\gamma i} Q}$$

On cyclic hardening

$$\dot{D}_{\gamma i} = b_{D\gamma} (D_{\gamma i}^{T_{max}} - D_{\gamma i}) \dot{p}$$

Effect of Max tp^o

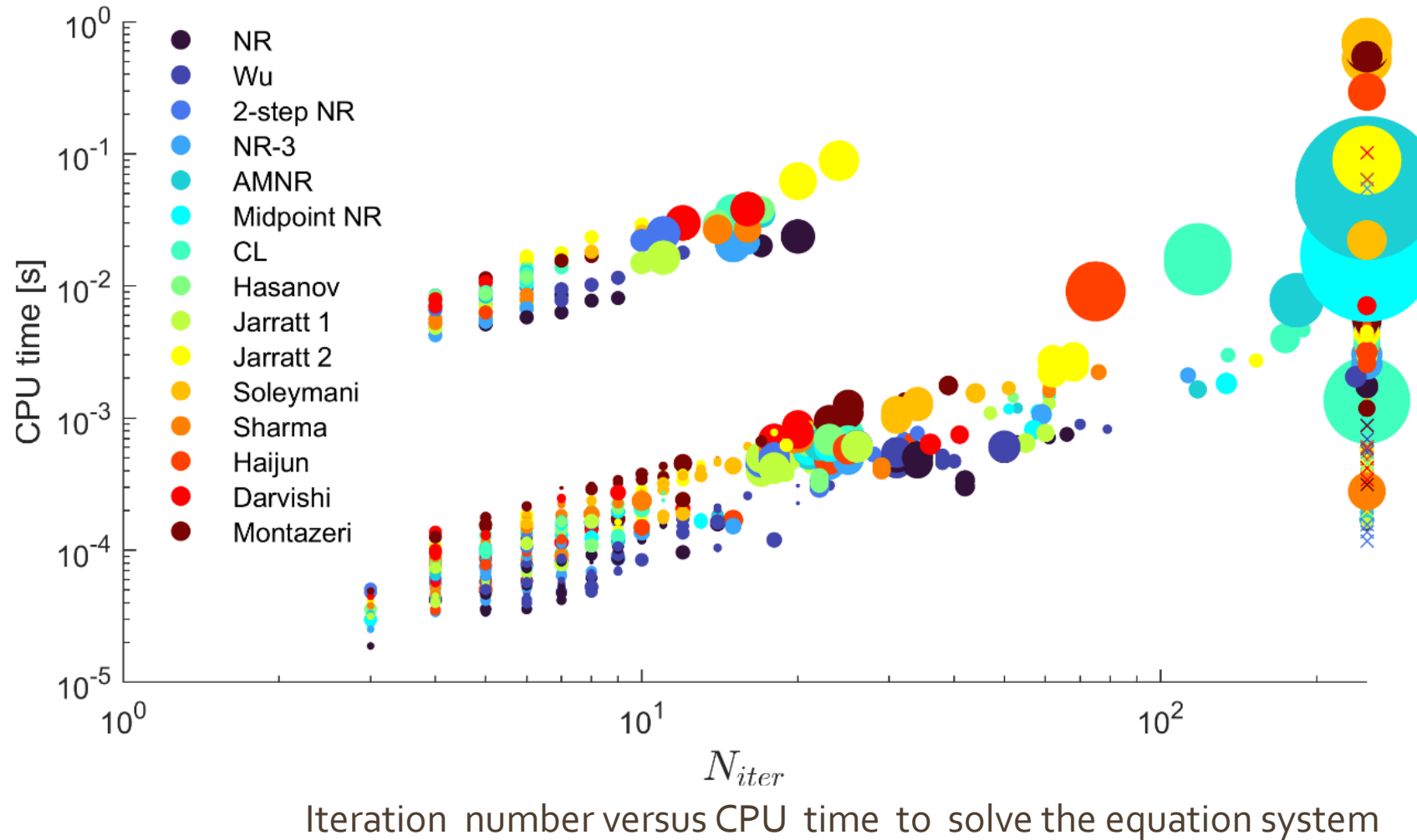
On cyclic hardening

$$E = f_E E + (1 - f_E) E_{T_{max}}$$

$$\dot{f}_E = b_E (f_E^S - f_E) \dot{p}$$

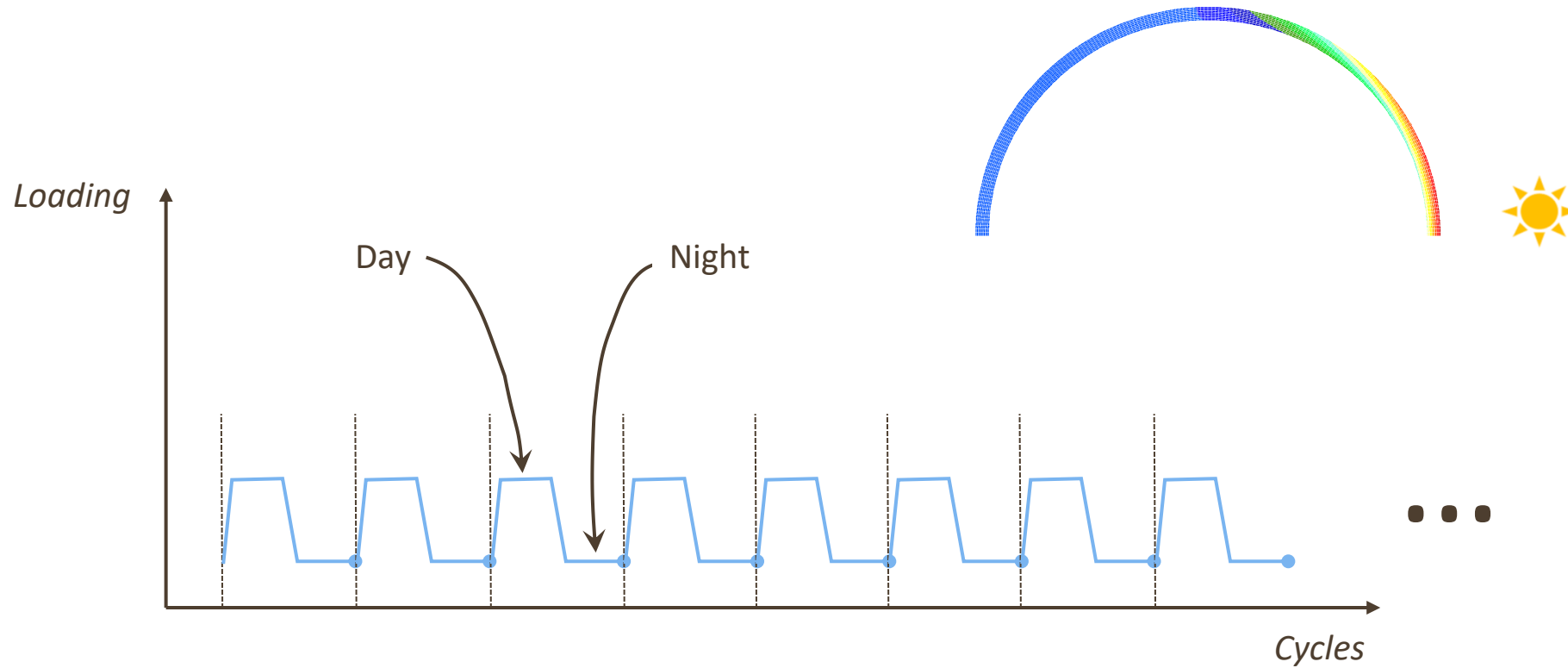
Study of optimal resolution → Newton Raphson !!!

Analysis of different resolution approach



A review of
higher order Newton type
methods and
the effect of numerical
damping
for the solution of
an advanced coupled
Lemaître damage model
Morch et al. *Finite Elements*
in Analysis and Design, 209,
p. 103801

Cycle jump approach

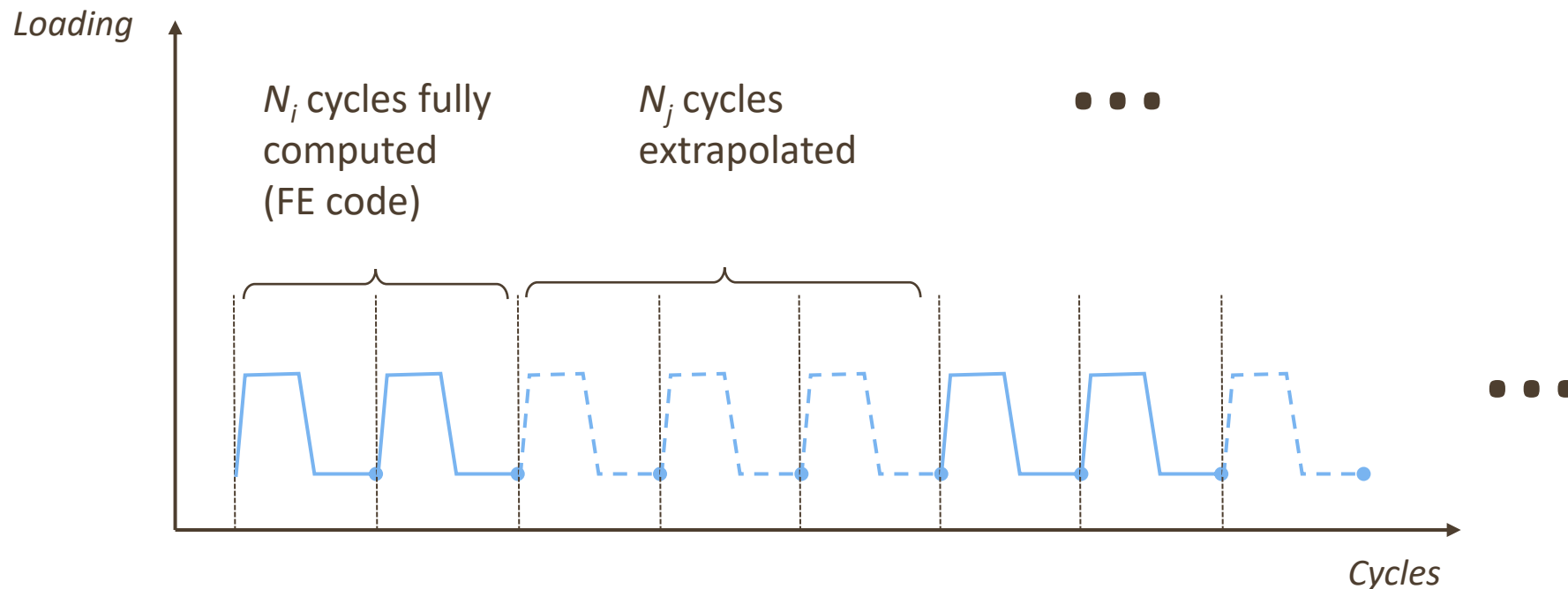


Target:

- 10 000 cycles
(~25 years)
- 18m long tube
(~200 000 FE, 10^6 DOFs)

Duchêne et al. ICTP 2023
Conf proc.

Cycle jump approach



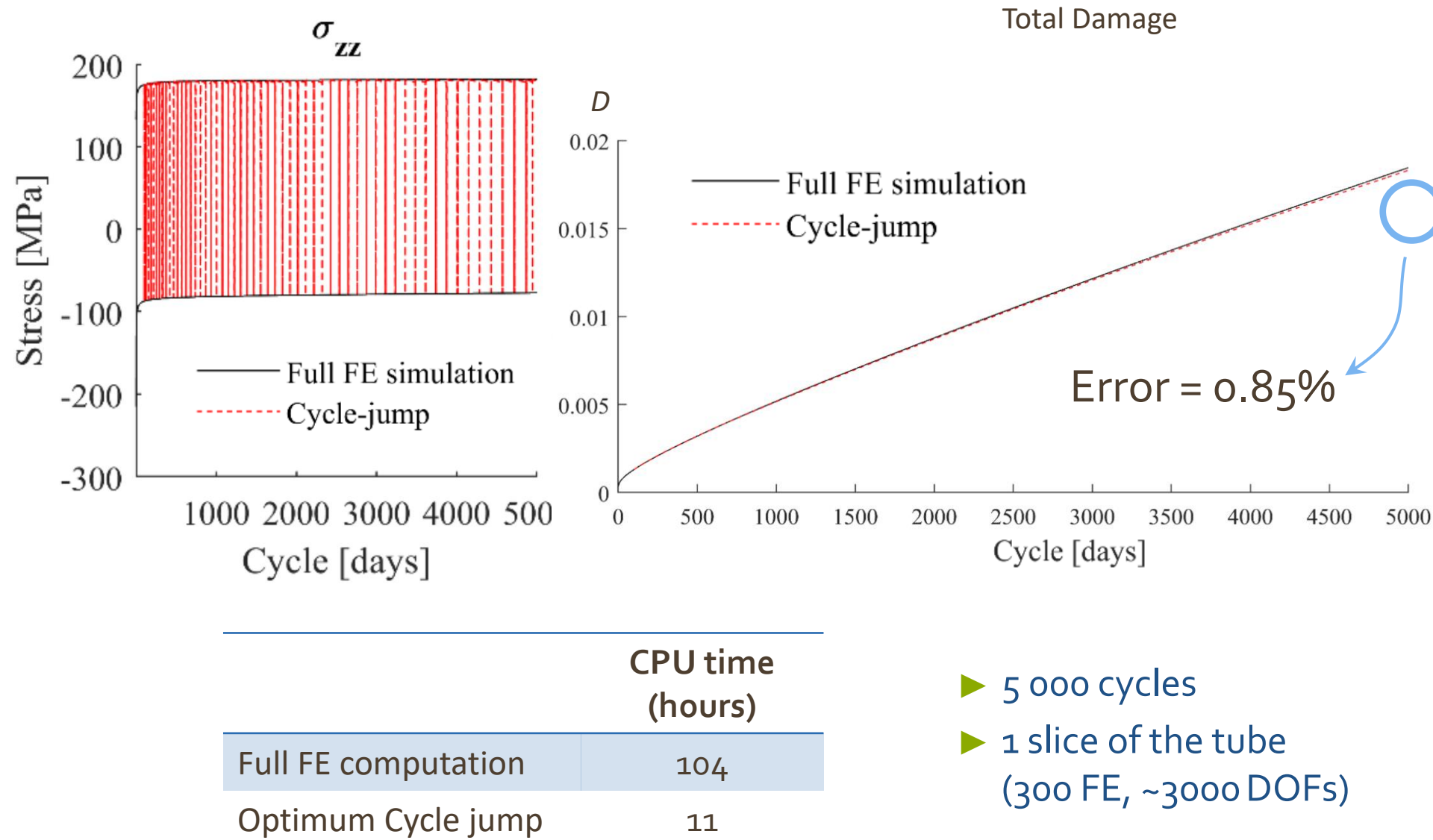
Target:

- 10 000 cycles (~25 years)
- 18m long tube (~200 000 FE, 10^6 DOFs)

This study:

- 5 000 cycles
- 1 slice of the tube (300 FE, ~3000 DOFs)

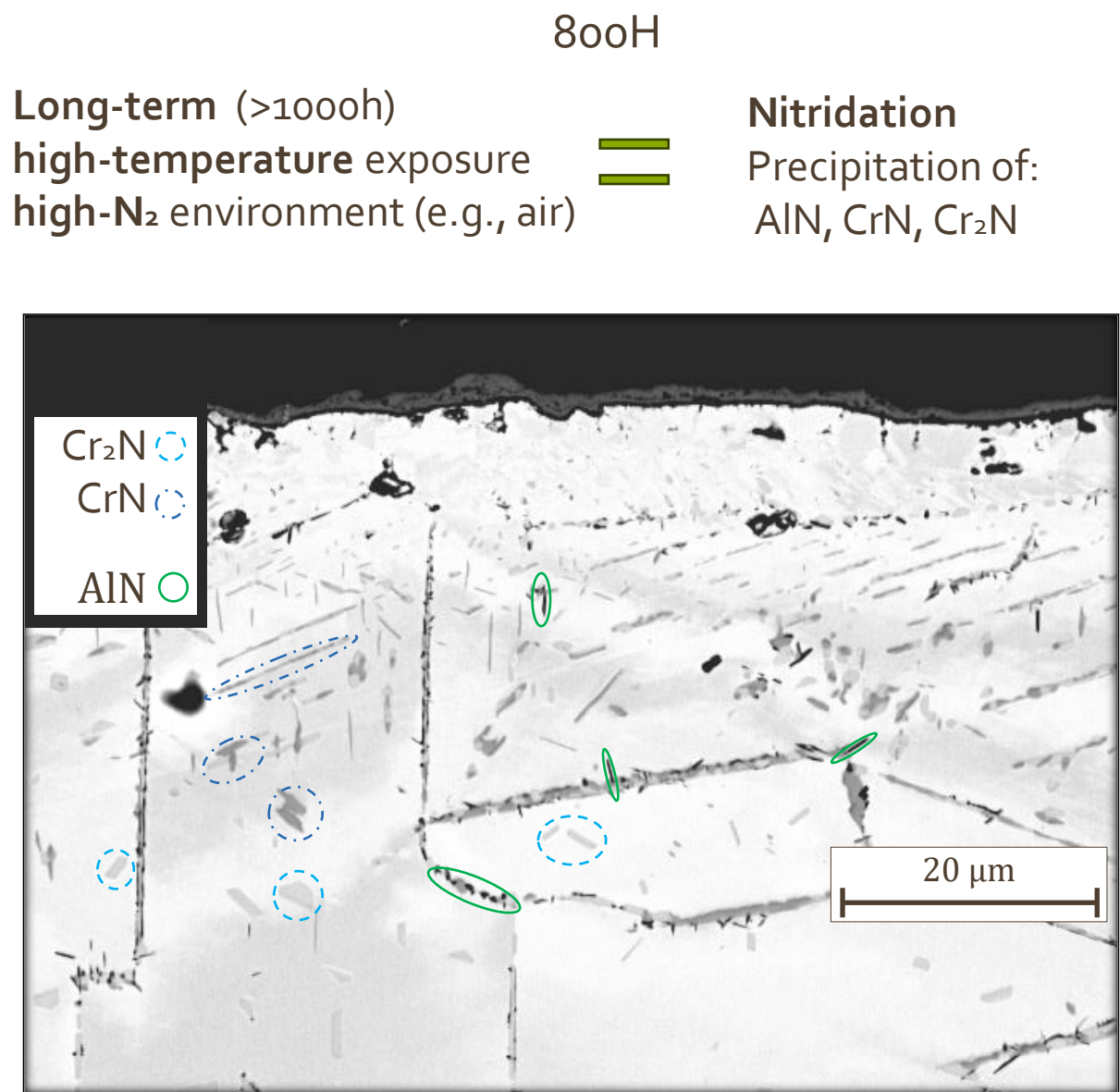
Cycle jump: optimum parameters



Contents

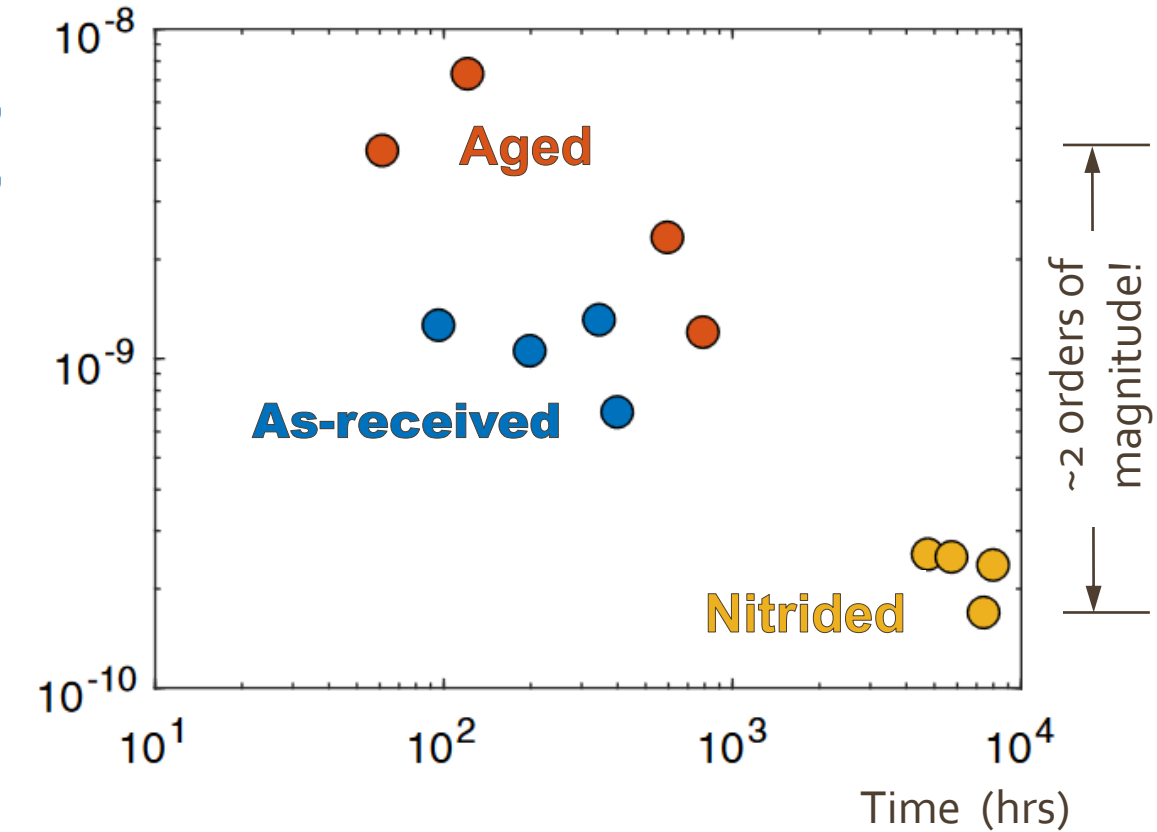
- Introduction
- **Phenomenological approaches**
 - Scalars
 - Larson Miller etc...
 - Curves and constitutive laws FE
 - Norton
 - Graham Wales
- **Micro physical based approach**
 - The basis
 - Incoloy 718 application
- **Fatigue-Creep, Dwell effect and FE Morch constitutive macro law**
- **Nitriding effect**
- **AID4Greenest EU project ...**

Environmental effects on creep: nitridation



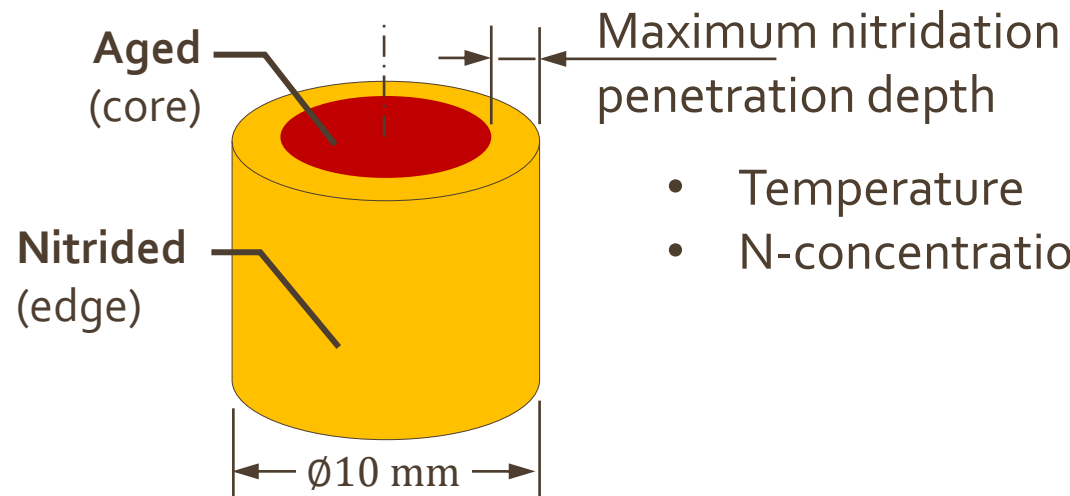
Nitridation → creep hardening

At 1000°C and 8 MPa



Environmental effects on creep: nitridation

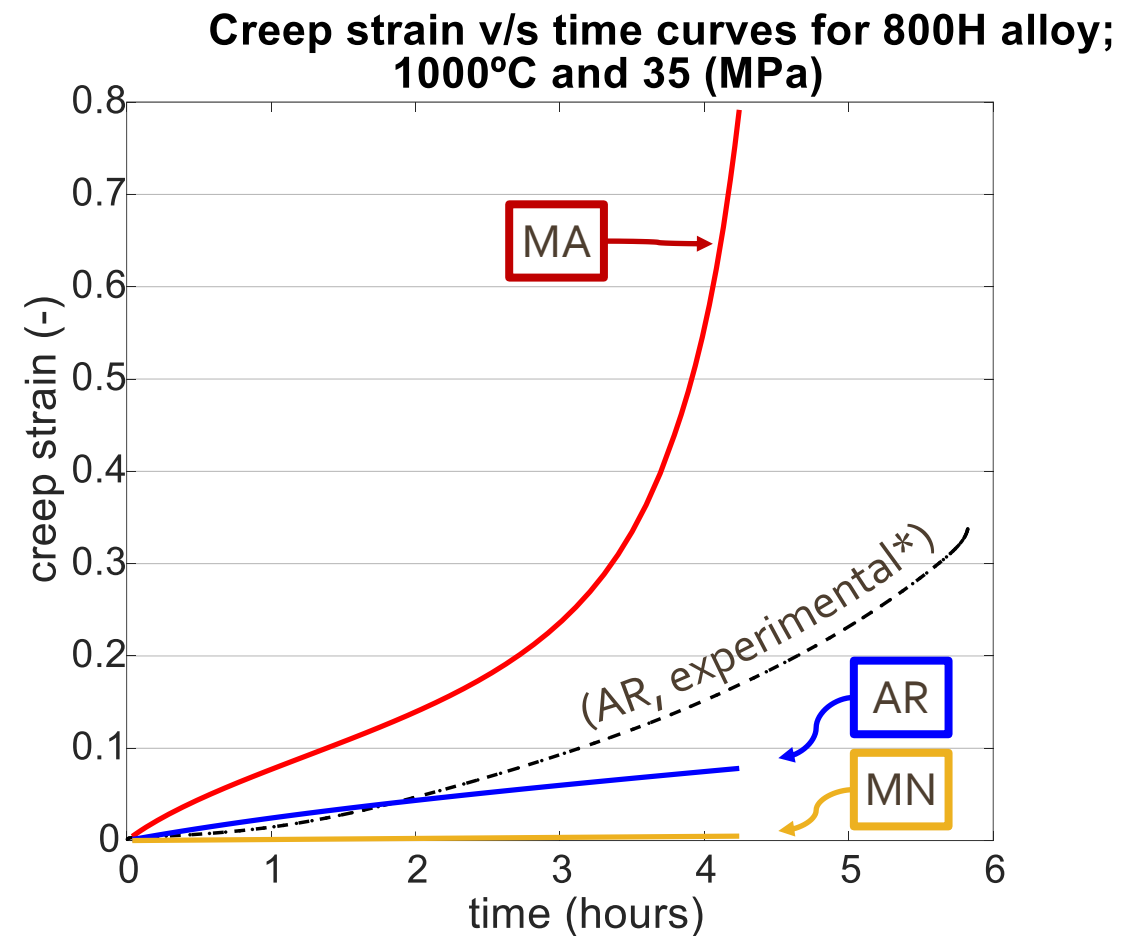
FE simulation of nitridation effect (Lagamine code Uliege)



Experiment for identification (A.M. Young et al., 2023):

Parameters	Aged (MA)	As-received (AR)	Nitrided (MN)
$\dot{p} = \left(\frac{\sigma_v}{K} \right)^n$	$k (\text{MPa})$	$3.10E + 04$	$7.50E + 04$
	$n (-)$	1.18	1.22

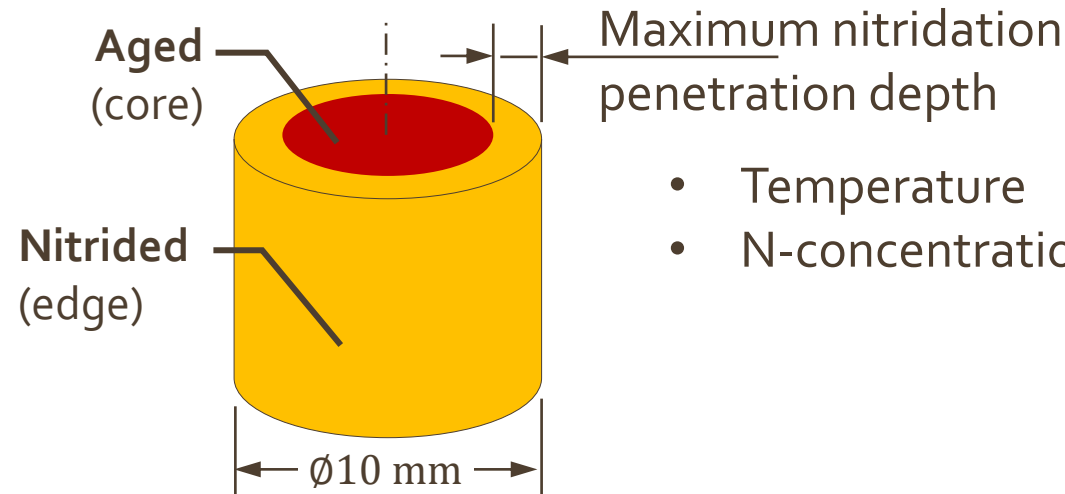
Prediction for homogeneous samples (Norton)



*: Experimental curve after (V. Gutmann & R. Bürgel, 1983)

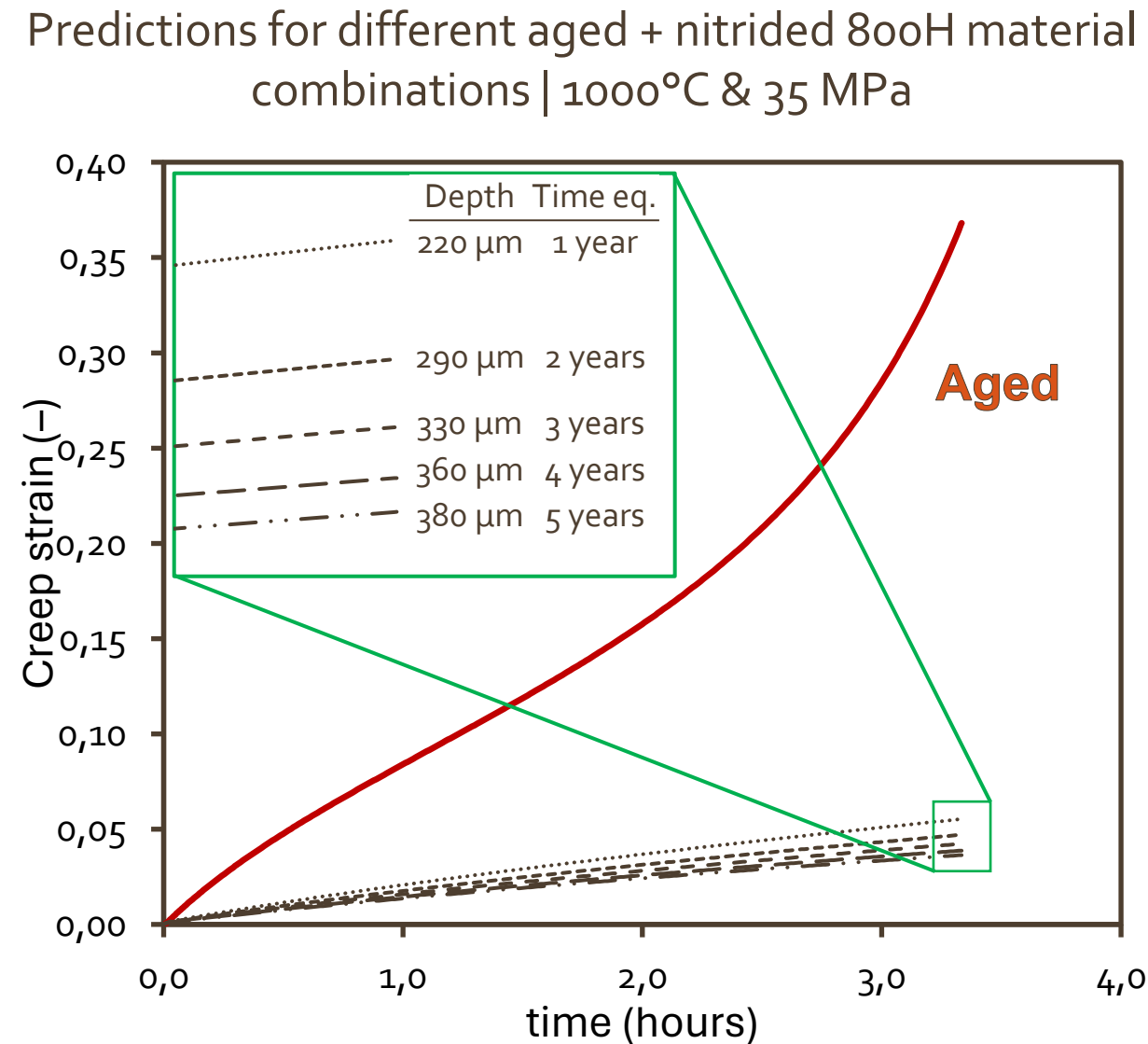
Environmental effects on creep: nitridation

FE simulation of nitridation effect (Lagamine code Uliege)



Using the information from (A.M. Young et al., 2023):

Parameters	Aged (MA)	As-received (AR)	Nitrided (MN)	
Norton law	$k \text{ (MPa)}$	3.10E + 04	7.50E + 04	5.35E + 05
$\dot{p} = \left(\frac{\sigma_v}{K} \right)^n$	$n \text{ (—)}$	1.18	1.22	1.29



Contents

- Introduction
- **Phenomenological approaches**
 - Scalars
 - Larson Miller etc...
 - Curves and constitutive laws FE
 - Norton
 - Graham Wales
- **Micro physical based approach**
 - The basis
 - Incoloy 718 application
- **Fatigue-Creep, Dwell effect and FE Morch constitutive macro law**
- **Nitriding effect**
- **AID4Greenest EU project ...**

AID4Greenest project WP3 30CrMoNiV5-11 ($\approx 1\%$ Cr)

- Manufacturing of a shaft *Reinosa*
- Characterization and prediction of microstructure *ULiege, Oulu, Fraunhofer, MDEA*
- Standard creep test *ULiege*
- 2 Types of Accelerated creep test *IMDEA - Fraunhofer*
- Forging + Cooling simulation *OULU*
- Creep Simulation:
 - Macro laws (Morch) *ULiege*
 - Micro law (under development) *ULiege*
 - Machine learning (under development) *Fraunhofer IMDEA*



Efficient way to predict shaft lifetime
→ Generic tool development

<https://aid4greenest.eu/>



AID4GREENEST Official



Thank you for your attention
Anne. Habraken@uliege.be



<https://aid4greenest.eu/>